UNIVERSITÀ DEGLI STUDI DI PADOVA

Department of Civil, Environmental and Architectural Engineering

UNIVERSITÀ
DEGLI STUDI
DI PADOVA

Master's degree in Environmental Engineering

Master Thesis

Academic year 2021-2022

NUMERICAL SIMULATION OF A PINNED DRAPERY MESH SYSTEM

Relatore
Dott. Ing. Gabrieli Fabio

Correlatore
Dott. Ing. Antonio Pol

Laureando: Marco Pellizzer
ID: 1238229

Alla mia famiglia,

Index

Abstract 7
Drapery mesh systems 9
1.1 Shallow rocky instabilities 10
1.2 Wire meshes 12
1.3 Simple drapery mesh systems 15
1.4 Secured drapery mesh systems 17
Pont Boset in situ test 23
2.1 Laboratory tests 23
2.2 Pont Boset on site application 25
2.3 Pont Boset testing phase 28
Discrete Element Model 31
3.1 The Discrete Element Method 32
3.1.1 DEM Cycle 32
3.1.2 DEM Contact Forces 34
3.1.3 DEM Integration time step 35
3.2 Wire mesh Modelling 36
3.2.1 Interaction law 36
3.2.2 Wire mesh discretization models 38
Numerical Simulation 43
4.1 Wire-mesh creation 43
4.2 Validation of the numerical model 48
4.3 Pont Boset Numerical Simulation 50
4.3.1 Force-Displacement curve analysis 52
Parametric analysis 61
5.1 Pont Boset Parametric Analysis 61
5.1.1 Anchor plate size influence 63
5.1.2 Panel aspect ratio influence 65
5.1.3 Anchor spacing influence 68
5.1.4 Punch direction influence 70
5.1.5 Punch dimension influence 73
5.1.6 Punch position influence 76
5.1.7 Wire diameter influence 79
5.1.8 Parametric analysis considerations 81
5.2 2nd Parametric Analysis 83

5.2.1 Anchor plate size influence 86
5.2.2 Panel aspect ratio influence 88
5.2.3 Anchor spacing influence 90
5.2.4 Punch direction influence 92
5.2.5 Punch dimension influence 96
5.2.6 Punch position influence 98
5.2.7 Wire diameter influence 100
5.2.8 Parametric analysis considerations 102
Conclusions 103
Bibliography 105

Abstract

Nowadays, secured drapery systems are commonly adopted in practice as a countermeasure to rockfalls and shallow unstable phenomena along slopes. These systems are composed of a steel wire mesh, which is pinned to stable outcrops or to firm layers by means of tie rods or bolts and anchor plates. Despite their wide application, the knowledge of the field mechanical behaviour of a secured drapery is limited and mostly based on practical experience. Furthermore, the laboratory tests used to characterize the wire mesh resistance are not representative of the field conditions. This may negatively reflect on the efficiency of these structures, leading to an over-dimensioning in some cases or to unsafe solutions in others. The thesis project aims to investigate the mechanical behaviour of a secured drapery system in rock-slope applications. A numerical approach based on the Discrete Element Method (DEM) for wire mesh reproduction is used. During the thesis work a large-scale model for analysing the punching behaviour of a secured drapery system when loaded by an unstable rock block has been implemented. Subsequently, a parametric analysis has been performed in order to understand the influence of the problem's different variables (e.g. block size and shape, block position, anchor size and spacing, etc) on the mechanical response of the system.

Chapter 1

Drapery mesh systems

Nowadays drapery mesh systems are commonly adopted in practice as a countermeasure to rockfalls and shallow instabilities along slopes. Casting debris and rockfalls of even limited proportions can obstruct an infrastructure and cause considerable economic damages. These systems (Fig 1.1) that consist in the application of a wire mesh adhering to the instable rocky/soil layer are relative economic solutions for railway, mines and road safety, preventing or only controlling the possible detachment of debris or rocky/soil masses from escarpment. In the field of drapery application no design guideline exists and very few in situ tests were performed, furthermore due to its infinite in situ circumstances it's very difficult to obtain a complete knowledge of their mechanical response. Moreover, all laboratory tests provide results that are not representative of the real in situ conditions. For these reasons the behaviour of these systems requires an in-depth analysis of the field boundary conditions and comparison with other case studies are very difficult.

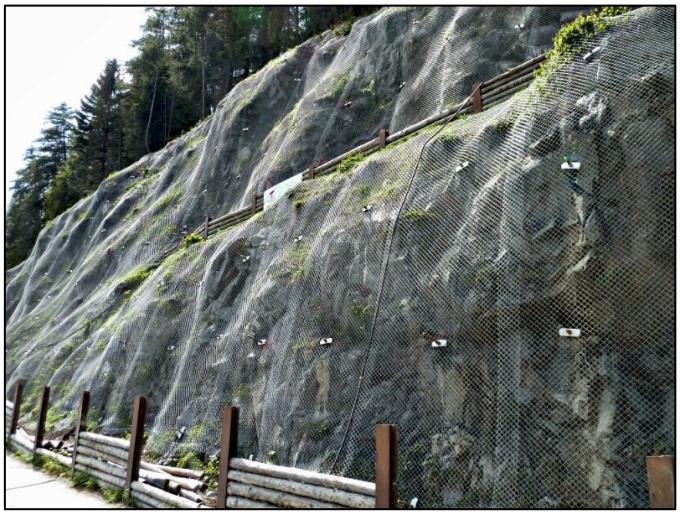

Fig 1.1: Drapery mesh system in a rocky slope

1.1 Shallow rocky instabilities

Drapery systems can be used both in rocky environments and in soil reinforcement applications with different purposes and installations. In this paper we will focus on applications in rock walls where these systems are used for the control of shallow rocky instabilities (Fig 1.2).

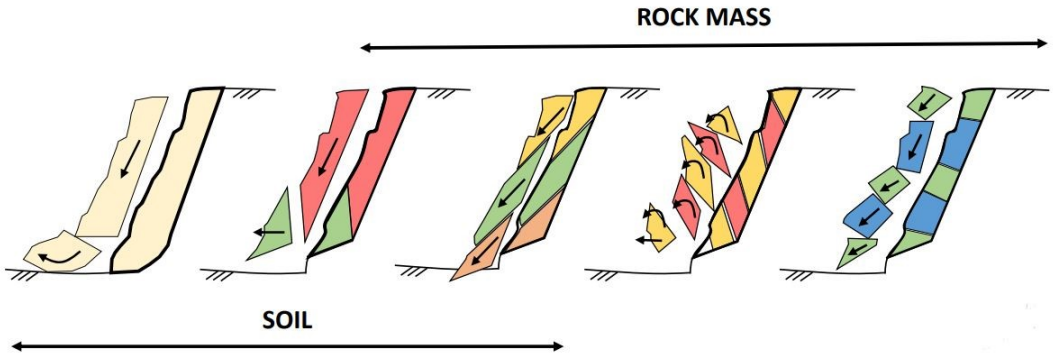

Fig 1.2: Rocky and soil field application

A shallow instability can be defined as a set of blocks of rocky matrix with geometry identified by discontinuities of different types. Generally it has a depth variable from 0.5m to 3m and does not affect the overall stability of the slope. A discontinuity is defined as a specific plane of mechanic or sedimentary origin that separates blocks. To investigate the cluster's capacity to oppose potential instability it is necessary to define the following resistance values:

- *Resistance of the rock material* -The resistance of the rock material is determined by investigating the behaviour of a rock specimen in the laboratory. The purpose of the tests is to determine the failure criterion (function of plasticity) of the rock material, i.e. the analytical expressions that allow to represent the resistance of the material as a function of the applied stresses and its intrinsic properties, to allow a prediction of when and how the break occurs.
- *Resistance of the rock mass* -When the rock mass is heavily fractured due to the presence of multiple systems of discontinuity, in terms of resistance a global behaviour of the cluster is evaluated. Due to the

dimensions and locations of the volume of the instable layer, it is obviously not possible to carry out tests in situ or in laboratory, which provide data representative of global behaviour. So, following approaches are used: indirect methods based on quality indices (geomechanical classifications); empirical methods with recourse to hypotheses on the role of discontinuities; mathematical models based on back analysis.

- *Resistance of discontinuities* -The planes of discontinuity present within a rock mass (see Fig 1.3) can substantially condition its properties and its resistance characteristics, to the point where, in the rock masses characterized by preferential planes of weakness, the resistance that governs behaviour is the intrinsic one of the planes of discontinuity. The shear strength of the discontinuities can be estimated with empirical methods that rely on geomechanical survey of the families of discontinuities present in a rock mass. The description of the different discontinuities is based on the following parameters: orientation, spacing, roughness, block size, humidity conditions and degree of alteration.

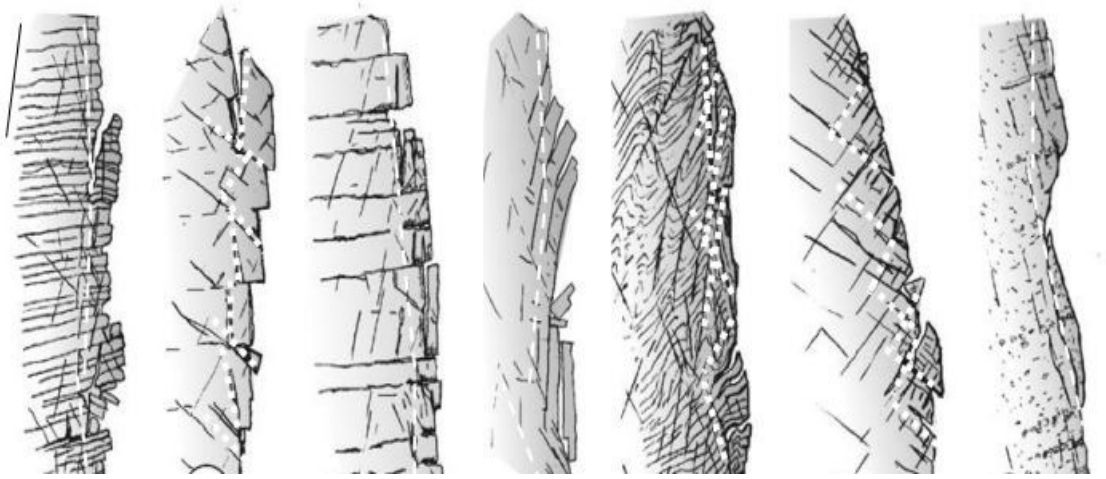

Fig 1.3: Examples of discontinuities

1.2 Wire meshes

In the commercial sphere there are currently many types of wire meshes employed in the field of drapery application which are chosen according to the particular in-situ morphological characteristics. The main wire mesh-features of choice are: wire diameter, net weaving structure, mesh opening degree, wire-mesh global deformability and steel properties. In particular focusing on the net mesh structure the following models can be identified:

Single-Twisted wire meshes

Characterized by a rhomboidal structure single-twisted wire meshes (Fig 1.4) are used as shock absorbers by virtue of their great deformation capacity, moreover they are used in drapery application where a very flexible structure is required. Their principal drawback is the possible net laceration following a single wire break.

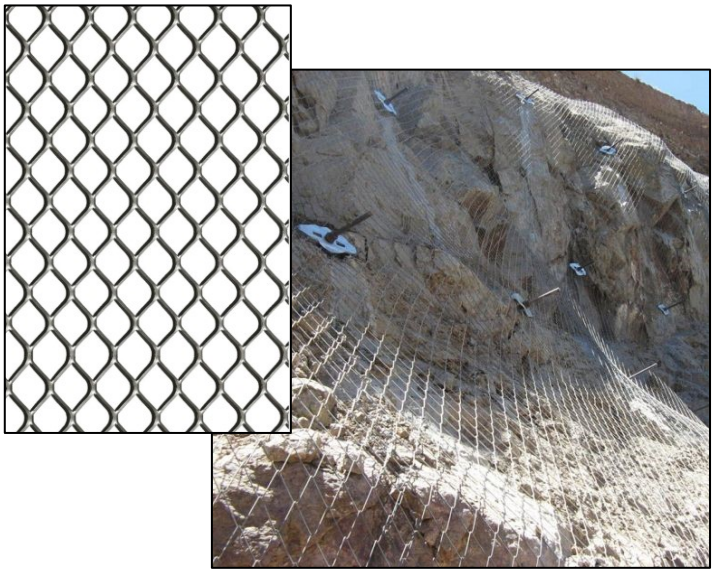

Fig 1.4: Single twisted wire mesh

Double-Twisted wire meshes

The system consists in a structure of multiple hexagons created with a double twisted steel woven wire and it is employed also in the field of cortical strengthening thanks to its moderate resistance and low deformability respect to the single-twisted one. This kind of metallic wire mesh is an ideal solution both for flexibility in every direction and for the ability to avoid great openings in case of accidental breakage of some wire. These are metallic structures that can be covered with a Galmac coating, a Zinc-Aluminum alloy used to avoid corrosion processes. There are various types, different in mesh size, wire diameter and integrated structures. In figure 1.5 we can see a wire mesh combined with vertical cables woven directly into it, a common solution applied to connect various panels together.

Fig 1.5: Double twisted wire mesh

Rope panels

These panels are woven from a single continuous length of high tensile strength steel wire and linked together with clips or knots (Fig 1.6). Rope panels are used in “soil nailing” as a flexible structural facing where a low deformability upon punching is required and at the same time a strong resistance of the net. Thanks to its very high tensile strength this solution is applied for the consolidation of great rocky block and in combination with double twisted wire mesh in densely fragmented rock masses.

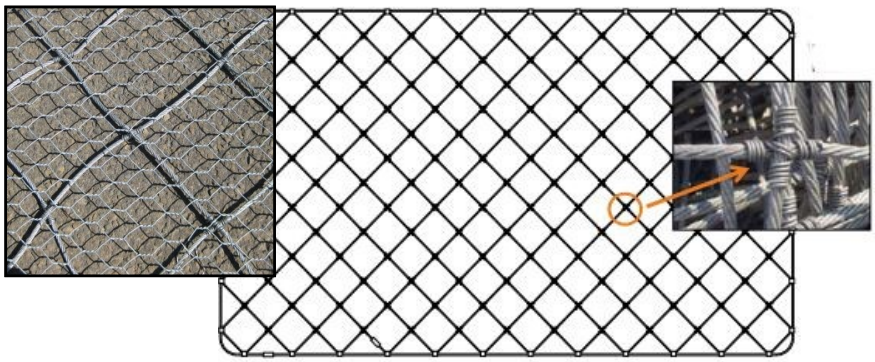

Fig 1.6: Rope panel in combination with DT wire mesh

1.3 Simple drapery mesh systems

Simple drapery mesh systems are designed to control the trajectory and the velocity of rock debris along slope without avoiding the detachment of the latter. The blocks and the rock debris are collected at the toe of the slope in a selected accumulation area that require an adequate maintenance. Simple drapery mesh systems are in turn subdivided in structures placed in adherence or not to the rocky wall.

- "In adherence system" is able to retain small block of rock or it at least prevents the fragments from gaining too high velocity (see Fig 1.7). The wire mesh needs a great flexibility and it's kept in adherence to the particular land morphology thanks to auxiliary anchors and steel ropes.

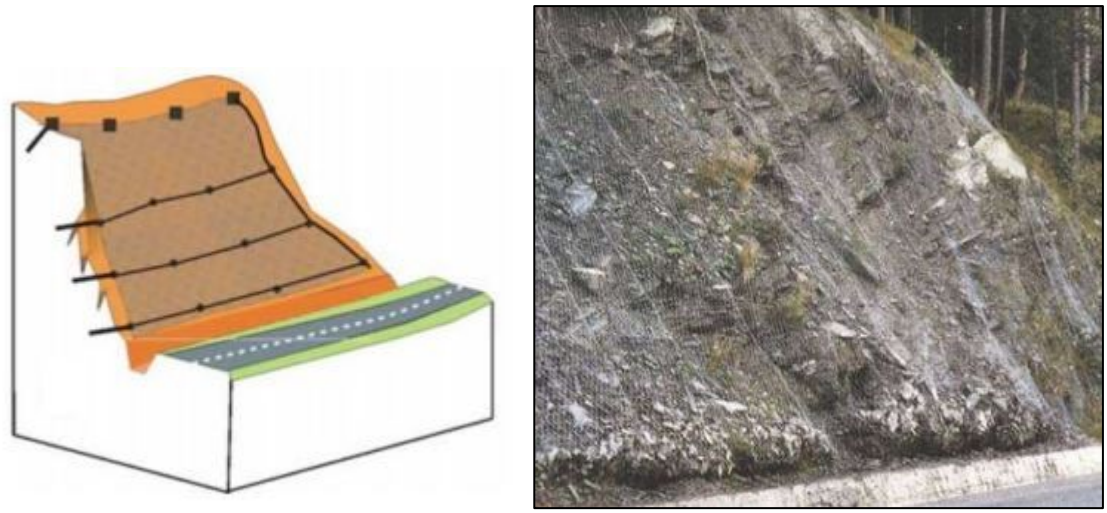

Fig 1.7: In adherence simple drapery mesh

- In "Not in adherence systems" the wire mesh is fixed only at the top of the rocky slope leaving it free to stretch under its weight. This technique is applied in vertical escarpments and it almost always requires the use of double twisted wire mesh. Figure 1.8 shows the application of a simple drapery system in an extraction quarry, where the only aim of the wire mesh structure is to control the trajectory of rock debris.

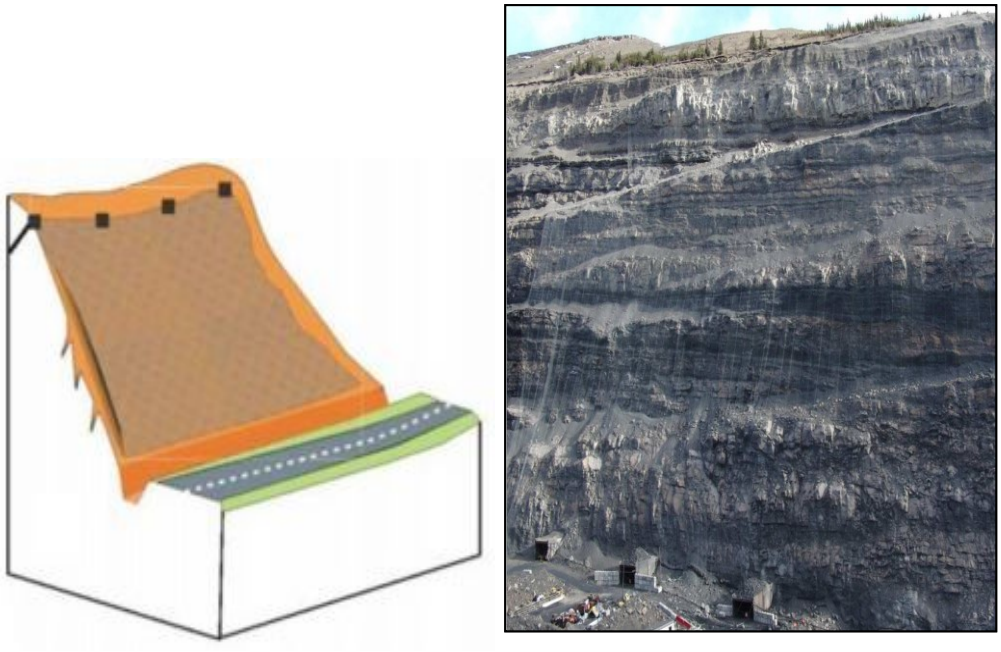

Fig 1.8: Not in adherence simple drapery mesh

In the installation phase the mesh is fixed on the slope crest and then unrolled on the slope escarpment, in simple drapery application it's fundamental look upon:

- Available space at the slope toe for maintenance and cleaning operations.
- Maximum permitted deformation and storage space at the slope toe.
- Morphology of the slope.
- Debris dimension.

1.4 Secured drapery mesh systems

These systems are aimed to avoid the detachment of instable rock blocks or debris strengthening the cortical rocky instabilities. In secured drapery applications the net is fixed to the instable surface through a uniform pattern of nails linked to the wire mesh through plates or rings, it can be accompanied with a system of steel ropes to increase rigidity and resistance (see Fig 1.9).

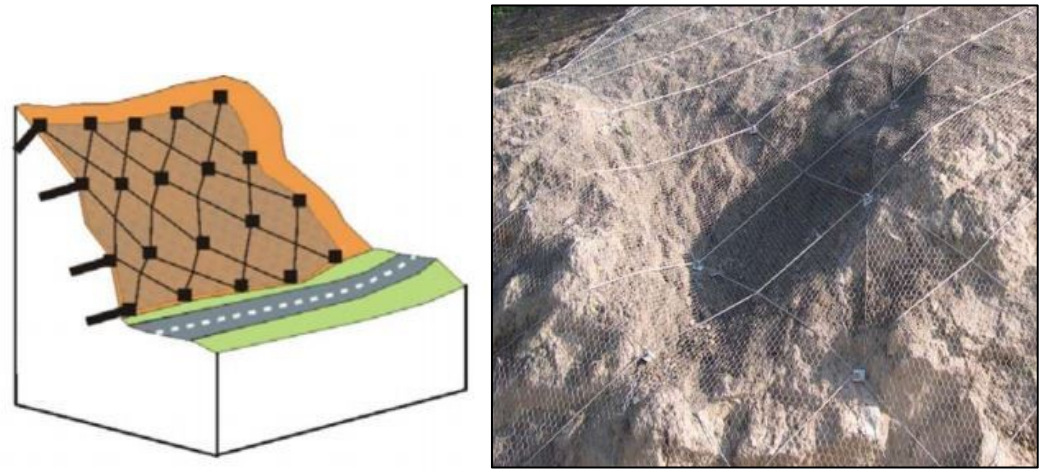

Fig 1.9: Secured drapery system

Cortical instabilities involve all micro-rockfall derived by the fragmentation of a superficial layer of a rocky slope that do not affect the global stability of the front. These are instabilities influencing the most fractured part of the rocky layer that is affected by degradation phenomena as thermal expansion, ice action, mineralogical alteration and hydration processes. Generally, the involved thickness is not more than 2-3m but due to random fragmentation is very difficult to describe these occurrences with simple kinematic schemes. For these reasons preliminary observation and analysis of the instable layer assume great importance, they allow us to have knowledge of the thickness and the size of the disjointed rock and the possible direction of the mass movement. In secured drapery system a correct proportion between the thickness of the cortical instability and the dimension of the anchors is required, the latter must be arranged with a suitable density able to guarantee that force exerted by the most dangerous rock mass doesn’t overcome the

permissible load of the anchor arrangement. Anchored systems perform a passive stabilizing activity, although the wire mesh can be tensioned, it is activated after a certain localized movement of the retained material. Depending on the level of fragmentation of the rock mass, the stabilizing activity is exerted more by the anchors or more by the wire-mesh; in case of a pseudo continuous block, bolts stabilize the layer while mesh is only responsible of contain small rocky elements, in case of a discontinuous mass the stabilizing effect exerted by bolts is very local while mesh stabilizes and contains the instable layer. The level of fragmentation affects the arrangement of the anchors, for a highly fragmented mass a diamond pattern is more effective, limiting the length of free-fall corridors between the mesh and slope, conversely for poorly weathered rock a square pattern is recommended (Fig 1.10).

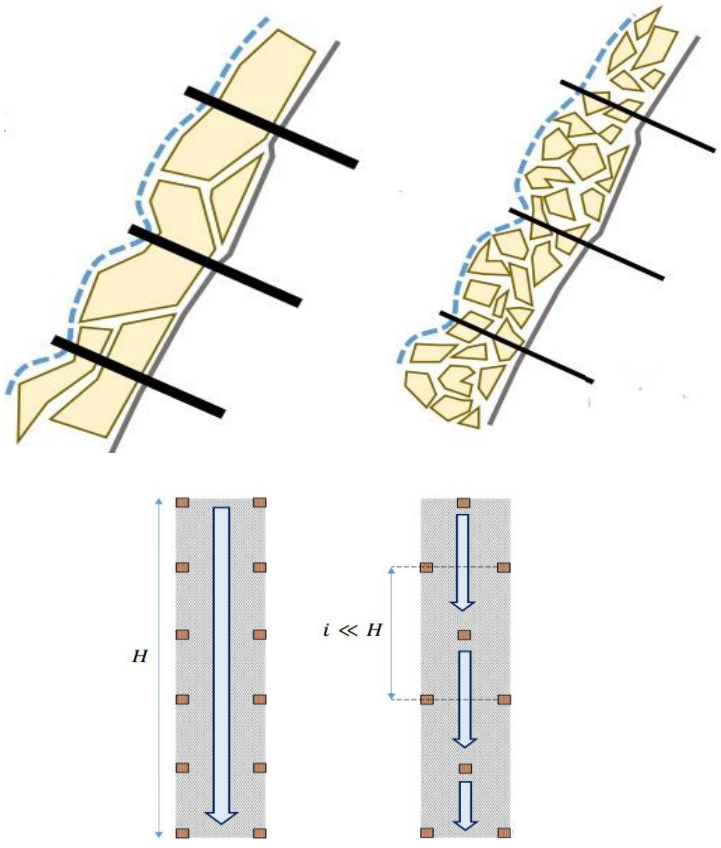

Fig 1.10: Anchors pattern for poorly and highly fragmented rock block

The length of the anchor rods must be sufficient to ensure that the tensile and shear stresses are discharged on the stable layer. It's useful to point out that all

the rocky penetration operations are carried out by hand-drilling machine, for this reason secured drapery activities are limited to an instable layer of 2-3m, for thickness greater than this limit a significant number of bars are needed to stabilize the slope. In this case, the mesh loses its functionality and the intervention becomes more similar to a soil or rock nailing (Fig 1.11).

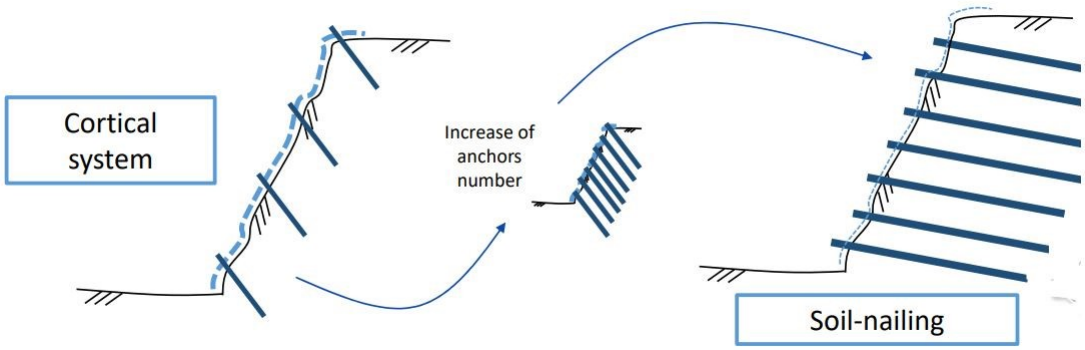

Fig 1.11: Reinforced cortical system vs soil nailing system

The knowledge of force displacement curve, obtained in laboratory tests is of fundamental importance to study the deformation response of our wire-mesh. Generally, as reported in figure 1.12 the mechanical behaviour of the panel is firstly characterized by a geometrical resistance followed by a phase where the material property can be exploited.

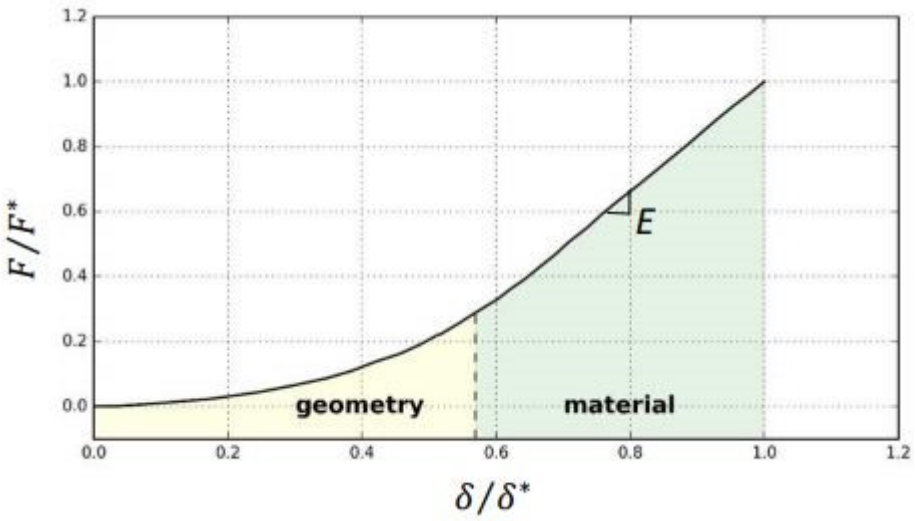

Fig 1.12: Force-Displacement curve

In these tests different types of meshes are tested against a punching element up to the breaking of some boundary bonds or tearing phenomena. The way in which the panel is woven influence the resistance and the deformability of the mesh. Double twisted wire meshes are characterized by an anisotropic response with a greater resistance in the DT wires direction, similarly single twisted ones have different tensile strengths and elongation in function of the considered direction. Other main factors to be evaluated in laboratory are: the tensile strength of the individual wires or cables, tensile strength of the junctions elements and the mesh flexibility.

In situ the situation profoundly changes, analysing for example an anchor element (see Fig 1.13a), the maximum allowable resistance has an order of magnitude related to that of the few wires blocked by the plate, this limit can be even much less than the laboratory breaking point where the mesh is completely fixed to a rigid frame. In the application field is worthy to apply a good stringing of the net, it allows to settle the slack and free movements in correspondence of anchors making the net ready to respond to strains with its strength capacities.

(a) *(b)*

Fig 1.13: (a) Anchor plate; (b) Laboratory test

Another aspect to evaluate is the morphology of slopes. In fact, the choice of the drapery mesh strongly depends on this factor. If we are in presence of an

escarpment characterized by great discontinuities it's convenient to apply a single twisted wire mesh due to its great deformability thus limiting the onerous costs deriving from the installation of a more rigid net.

In presence of a regular slope the installation of double twisted wire mesh and also of wire mesh panels does not involve additional complications.

The structure installation is divided in five main phases:

- Fixing of the mesh on the slope crest through anchor bolts
- Drilling operations and installation of anchor bars/bolts on the slope face by climbers
- Unrolling of the mesh on the slope face (Fig 1.14)
- Fixing of the mesh to the anchor bolts by means of special connections (plates, rings, clips)
- Application of additional devices for increasing the system resistance such as steel cables

Fig 1.14: Secured drapery system installation

Chapter 2

Pont Boset in situ test

In this chapter, after a brief introduction about laboratory tests, one of the few open accessible on-site tests regarding a secured drapery system will be introduced. This is the test carried out at Pont Boset in the Aosta Valley by the Maccaferri company in 2002.

2.1 Laboratory tests

Despite the worldwide application of secured drapery structures, their behaviour has been thoroughly analysed only in laboratory, where single wire mesh panels under quasi static or dynamic impacts and supporting components as clips, knots and cables had been tested. In these tests the punching and the tensile resistance of our wire mesh structure are investigated through particular testing machines (Fig 2.1, Fig 2.3).

In the tensile test a constant traction force is imposed to the panel until the point of failure is reached. This tensile strength is measured as a force per unit of length and it's fundamental to distinguish this value with the tensile resistance of the single wire. This resistance in fact does not depend only by the properties of the single wire but also by the shape and mesh weaving mode.

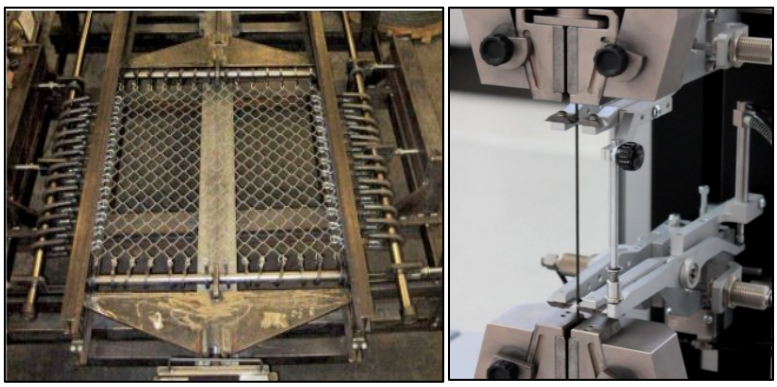

(a) *(b)*

Fig 2.1: (a) Wire mesh tensile test; (b) Single wire tensile test

In the punch test (see Fig 2.2) is measured the puncture resistance of a mesh through a force obtained pushing a plate or a punching element in perpendicular direction respect to the mesh plane. The mesh is usually fixed to a rigid external square frame. This constraint makes the panel much more rigid and this condition is responsible of the main differences between laboratory and in situ behaviour of drapery systems. There are several standards regarding the execution that differ for: size and form of the punching element, mesh panel dimension, number and kind of constraints on the panel edges, thrust velocity of the machine. The test interrupts when the punching machine reached the maximum load or some mesh breakage appears. From these tests the out of plane resistance of the mesh panel and the force-displacement curve are obtained.

Fig 2.2: Open-air puncture test

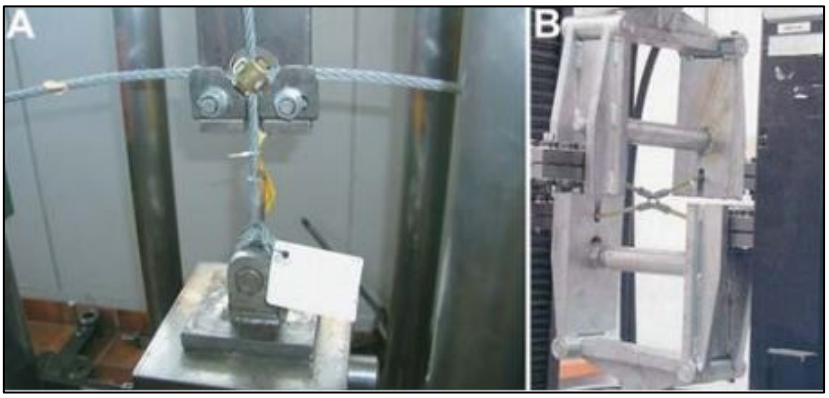

Fig 2.3: Test procedures for clips (a) and knots (b)

2.2 Pont Boset on site application

Regarding in situ applications no design guideline exists, and each manufacturer recommends his own standards and installation technique. Drapery application executed in Pont Boset in Aosta Valley is the only one full-scale test campaign developed on site that provide a good approximation of the real behaviour of secured mesh applications ("*Full scale testing on draped nets for rockfall protection*"; Paola Bertolo et al.; Canadian Geotechnical Journal, March 2009). In this site an almost 6m x 6m wire mesh drapery system with a square pattern of anchors of 3 meters of spacing in the central band was installed (Fig 2.4).

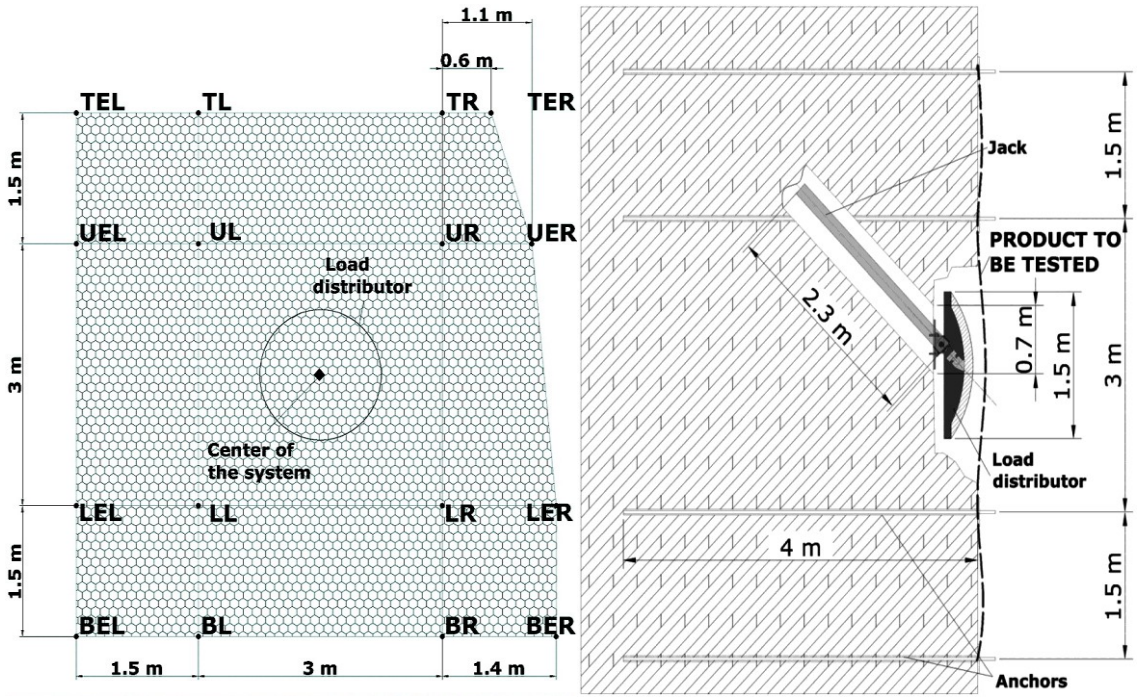

(a) *(b)*

Fig 2.4: (a) Front view of Pont Boset drapery system; (b) Detail on the punching device

The central panel was subjected to a puncture thrust where a spherical-cap-shape load distributor of 1.5m of diameter connected to the rock wall through an hydraulic arm was used as punching element. The hydraulic jack is 2.3m long and it's able to apply a maximum axial force of 200kN directed with an

inclination of 45° respect to the out of plane axis. This angle was selected because considered a common value of the dip of an hypothetical sliding joint. The jack was fixed to the rock wall through a collar and a cylindrical coupling pin to guarantee a movement of few degrees for force balancing and to avoid the bending of the piston. The jack is connected with the load device through a ball joint that allows it to rotate of some degrees respect to the vertical plane. This shape of the load distributor was chosen to guarantee a uniform loading process and to avoid lacerations resulting from possible pointed shapes. The test is carried out as following:

- Firstly, the mesh structure is installed on the slope through the pre-equipped anchor system.
- Then the jack is activated and the rod push the spherical load distributor against the mesh.
- The test is stopped when the jack is completely elongated (1500mm), when the mesh or the cables failed or when the jack arrive to its maximum force (200kN).

Tests were carried out considering various types of wire mesh, in this paper we focus only on those with double twisted wire mesh. The mesh is of double twisted steel woven wire of 3 mm manufactured to form a hexagonal shape, it's heavily galvanized with Galmac, a Zn-5%Al alloy and coated with Polyvinyl chloride.

In particular the mesh structure consists of an hexagon with two vertical sides of DT wires and the other four inclined sides with single wire. A specific DT mesh is described by 3 geometric length (see Fig 2.5):

Length "a": Length of the double twisted wire

Length "b": Vertical projection of the single wire length

MOS: Mesh opening size

The adopted system is characterized by a mesh with **a=4cm; b=4cm and MOS=8cm**

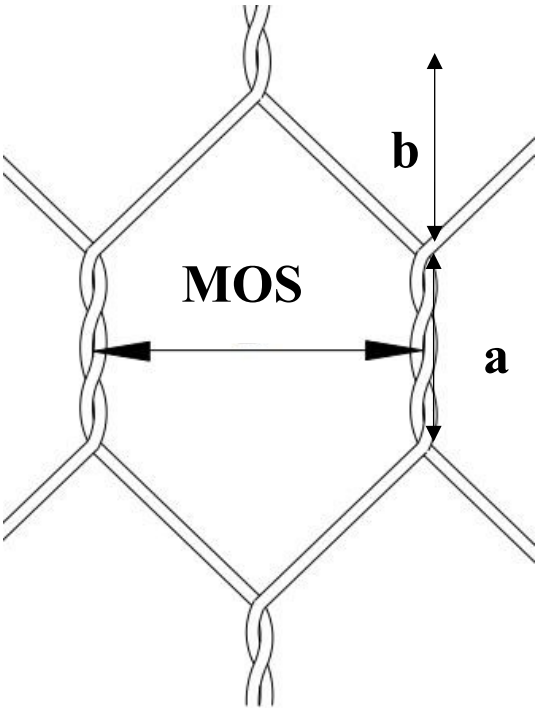

Fig 2.5: Double twisted mesh structure

The single wire of the mesh is characterized:

- **Tensile strength**: the wire used for the manufacture of rockfall protection have a tensile strength between 380-550 N/mm^2
- **Elongation:** strain shall not be less than 10%, according to EN-10223-3. Test must be carried out on a sample at least 25 cm long.
- **Galmac coating**: minimum quantities of 245gr/m^2 of Galmac according to EN10244
- **Adhesion of Galmac**: the adhesion of the Galmac coating to the wire shall be such that, when the wire is wrapped six turns around a mandrel having four times the diameter of the wire, it does not flake or crack when rubbing it with the bare fingers, in accordance with EN 10244.

2.3 Pont Boset testing phase

The fix drapery system was equipped with square anchor plates of 15 cm and with 10mm diameter cables pretensioned up to 3kN directly connected to the bolt pattern. During the testing activity 3 layouts of the system were analysed:

- ***Layout 1***: Cross cables in the central panel of the net system (Test 7)

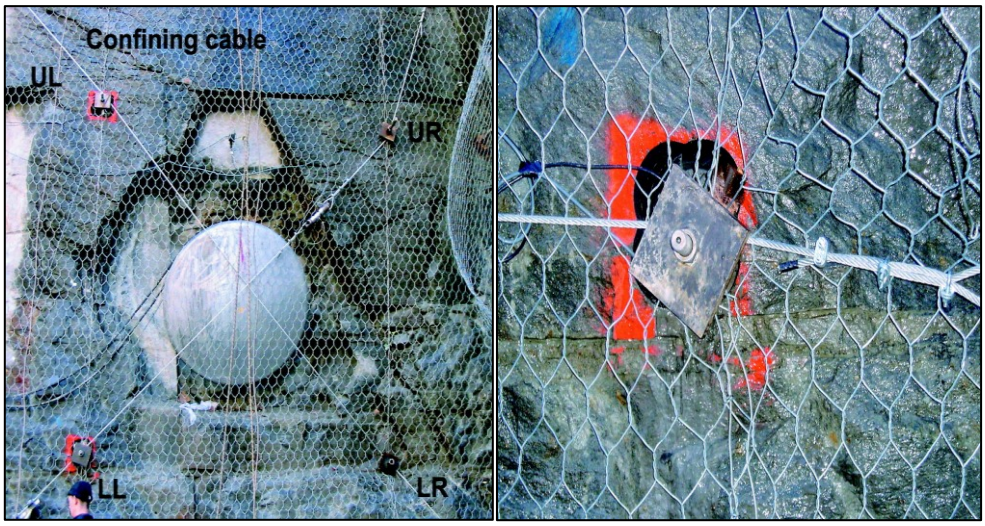

(a) *(b)*

Fig 2.6: (a) Front view of Pont Boset Test 7; (b) Detail on anchor plate

- ***Layout 2***: Secured Drapery reinforced with horizontal cables (Test8)

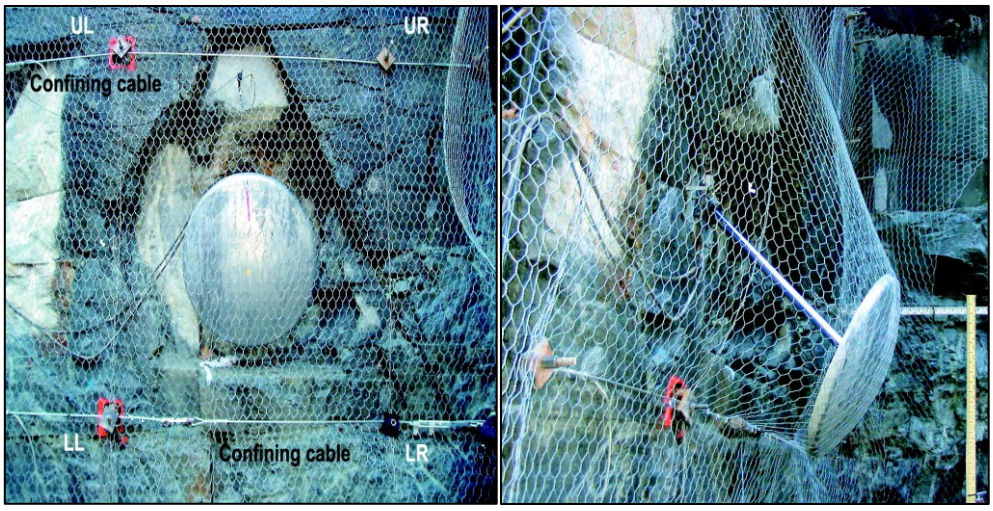

(a) *(b)*

Fig 2.7: (a) Front view of Pont Boset Test 8; (b) Detail on final punching element position

- ***Layout 3***: Simple drapery system supported only by 16 anchor plates (Test 9)

(a) *(b)*

Fig 2.8: (a)Front view of Pont Boset Test 9; (b) Detail on deformed wire mesh

In all the three configurations horizontal boundary cables located at the top and bottom of the panel were present.

Through motion-dynamic sensors and special dynamometers the following parameter were monitored: the total force acting on the upper left (UL) and the lower left (LL) anchors, the displacement normal to the slope of the central point between the upper left (UL) and the upper right (UR) anchors, the normal displacement of the hydraulic jack rod and the load applied by the distributor.

Thanks to these measurements the engineers were able to reconstruct the force-displacement curve of the mesh. Nowadays this is one of very few tests able to describe the real behaviour of a drapery system under real boundary conditions. If we focus on the force-displacement curve reported in figure 2.9 we can notice a first stage where the mesh deforms under low loads followed by a steeper phase where the panel is fully activated and able to contain the instable mass. The activation point and the slope of the final steeper section of each curve depend obviously by the rigidity of the system, going from a very deformable structure of Test 9 to a more rigid one of Test 7. It's clear also that

in these tests was clearly impossible to reach the jack's maximum force because the mesh is too deformable reaching in this way maximum rod displacement. An exception occurs in test 7, in fact it was stopped after a displacement of 200mm to avoid damages of the device because the load distributor was deflected by the cables, showing the possibility of a block slipping below the cables. Comparing the in-situ results with laboratory curves obtained by Bonati and Galimberti (2004) where the mesh was linked to a rigid square frame with 30 constraints and subjected to a punching action of concrete round shaped element of 1500mm in diameter, it's important to notice as the real boundary condition gives us more deformable curves. Globally during the tests the force exerted by the load distributor was almost uniformly distributed over the anchors points and few breaks of the wire were observed in particular with local ruptures near the plates position.

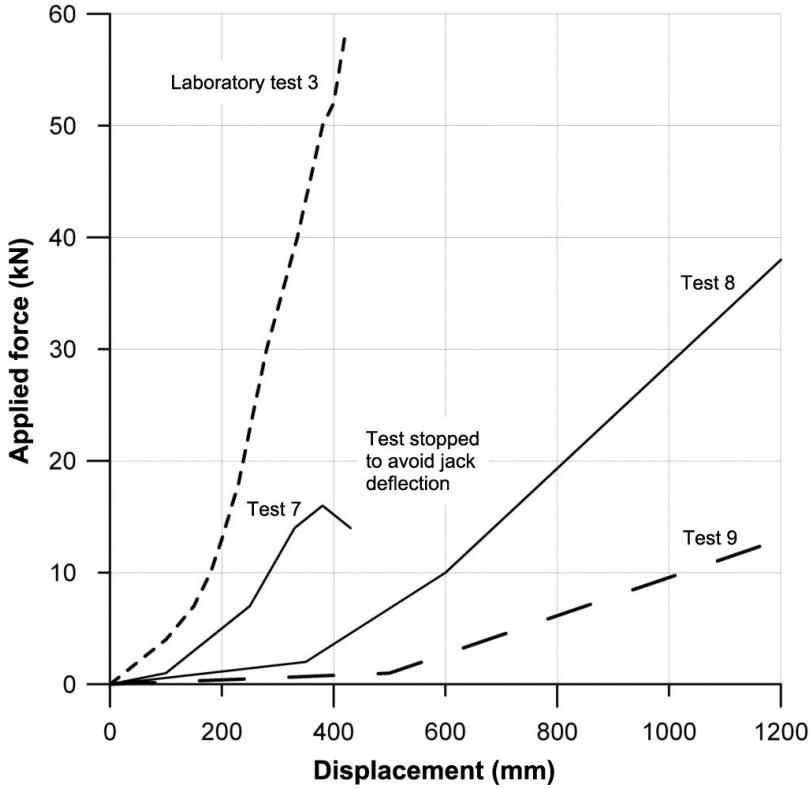

Fig 2.9: Test force-displacement curves

Chapter 3

Discrete Element Model

Numerical modelling is a mathematical representation of a physical (or other) behaviour, based on relevant hypothesis and simplifying assumptions (Sirois and Grilli, 2015). Numerical modelling methods are tools capable of representing, with high precision, the geometry and the mechanical response of a system subject to external forces considering its stress-strain behaviour and making the necessary calculations in a reasonable time. Numerical simulation reduces the number of expensive projects, prototypes and molds, improves equipment design, reduces material waste, reduces product development time and improves product quality. It is possible to classify numerical methods into two large groups: continuous methods and discrete methods, this thesis is focused on the last ones.

The discrete element method describes the evolution of a particle system in which the movement of individual bodies is computed in specific time steps. These methods permit access to micromechanical information that are hardly obtainable experimentally, such as contact forces amplitude and distribution in space/time. The method of discrete elements is based on the contact of elements: these bodies are independent from each other but capable of exchanging information. These conditions imply that there are no problems in the treatment of large deformations and there are no problems related to the detached elements. Three families of DE methodologies exist: the event-driven method, the contact-dynamics method and the molecular dynamics method, in this discussion we'll deal with the last-mentioned method.

3.1 The Discrete Element Method

The Discrete Element Method was developed by Peter A.Cundall and Otto D. L. Strack in 1979 at Minnesota University, US. It is based on the integration of the Newton's equations in time and space assuming that the particles are not deformable but can interpenetrate at the contact, relating the contact force with the interpenetration level between bodies. DEM describes the evolution of a particle system starting from the description of the motion of single particles allowing to know the macroscopic behaviour of the system. For a proper functioning DEM need to discretize the Newton's laws in time for each "discrete element" of the system. To compute all the forces that act on a specific body it's fundamental that method is able to detect all contacts between particles and to describe what happens, namely to define contact laws. The search for contacts is of fundamental importance, the correct development of a "detection algorithm" will in fact allow to limit computational times and ensure good efficiency to the numerical simulation.

3.1.1 DEM Cycle

Starting with a known configuration of our system at time t, we use a time integration in order to find what happens at time t_n. This integration scheme will be characterized by a specific time step Δt and should have some desirable properties such as:

- Good stability with large time-step Δt
- Good accuracy (orders of errors)
- Good conservation of energy and momentum

A lot of integration scheme exist, in this thesis we deal with the so-called **Leap-Frog Algorithm** (Fig 3.1)**.** Given a time step $\Delta \mathbf{t}$, the position and acceleration of particles are known at time $\mathbf{t+\Delta t}$ while velocities are known at time $\mathbf{t+\Delta t/2.}$ Starting from the initial position of our particle we compute acceleration thanks to 2nd Newton's Law (eq 2.1), from this acceleration considering it constant in the interval between $\mathbf{t-\Delta t/2}$ and $\mathbf{t+\Delta t/2}$ applying a time integration we are able

to obtain the velocity (eq 2.2) that allows us with another integration process to know the new position at time step **t**+Δ**t** (eq 2.3) (see Fig 3.1).

$$m_i \ddot{x}_i = \sum_j F_{j \to i} + f_e \qquad \textit{eq 2.1}$$

$$\dot{x}_{t+1/2\Delta t} = \ddot{x}_t \cdot \Delta t + \dot{x}_{(t-1/2\Delta t)} \qquad \textit{eq 2.2}$$

$$x_{t+\Delta t} = x_t + \dot{x}_{(t+1/2\Delta t)} \cdot \Delta t \qquad \textit{eq 2.3}$$

$m_i \rightarrow mass\ of\ particle\ i$

$x, \dot{x}, \ddot{x}, \rightarrow position, velocity\ and\ acceleration\ of\ the\ particle$

$F_{j \to i} \rightarrow force\ applied\ by\ the\ particle\ j\ to\ particle\ i$

$f_e \rightarrow external\ forces \qquad \Delta t \rightarrow time\ step\ interval$

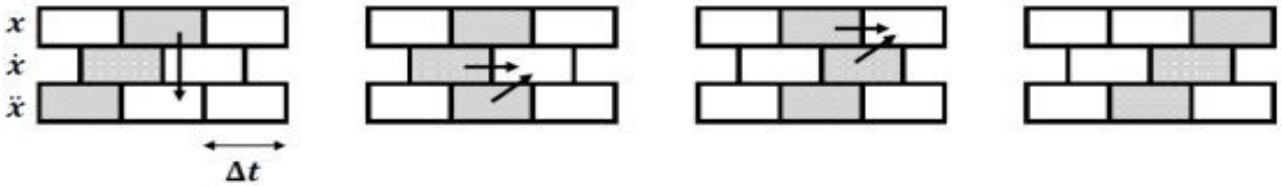

Fig 3.1: Leap Frog Algorithm schematization

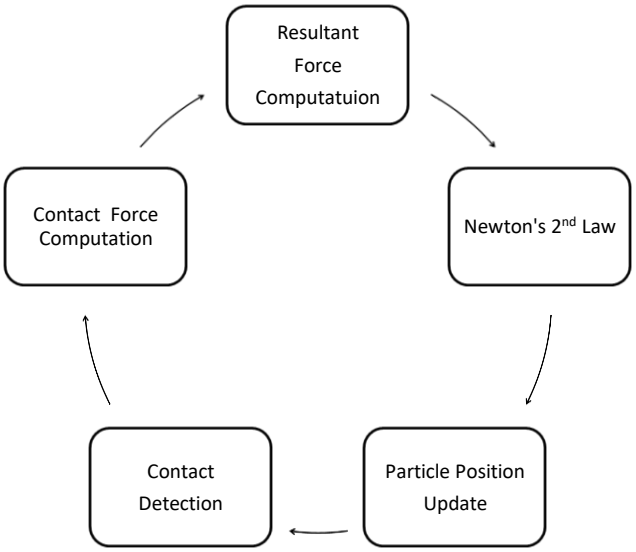

Fig 3.2: DEM cycle

3.1.2 DEM Contact Forces

Once defined the integration scheme of the system, it's worth talking about the micro-mechanism about interactions. As mentioned before the particles are treated as rigid bodies that can interpenetrate at the contact over a vanishingly small area related to the contact force via the force displacement curve. In DEM methodology 2 different contact forces can be identified:

- Normal contact forces
- Tangential contact forces

Normal Contact Forces

Basic contact law assumes a linear relationship (Fig 3.3) between the interpenetration length (δ) and the normal force through a constant k_n, function of the contact stiffness; the value of this constant must be entered as a fix parameter by the user before simulation, moreover it is possible to note that negative forces are not admitted from the model as cohesion is null in this type of phenomena.

More complex contact laws can be assumed, for instance a better representation of the normal contact force between two elastic bodies is given by Hertz theory where the normal force is computed in function of the elastic modulus(E), particle radius (R) and interpretation level (δ): $F_{n=}\frac{4}{3}ER^{\frac{1}{2}}d^{\frac{3}{2}}$

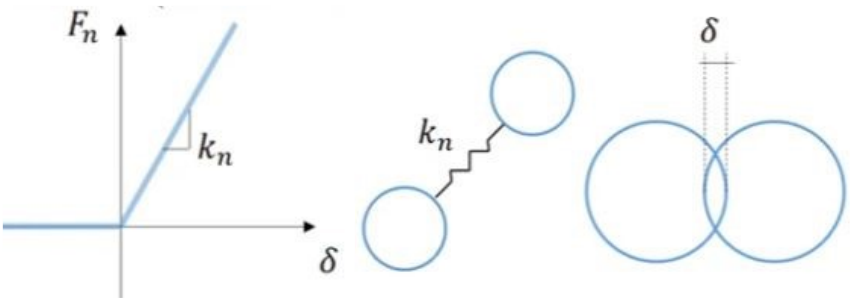

Fig 3.3: Normal contact force schematization

Tangential Contact Forces

Regarding the second component of contact force Cundall and Strack assume a friction plastic model (Fig 3.4) where the tangential force increases linearly in function of the relative shift between the two bodies through a constant k_s until the friction limit is reached and the bodies start to slide (see Fig 3.4).

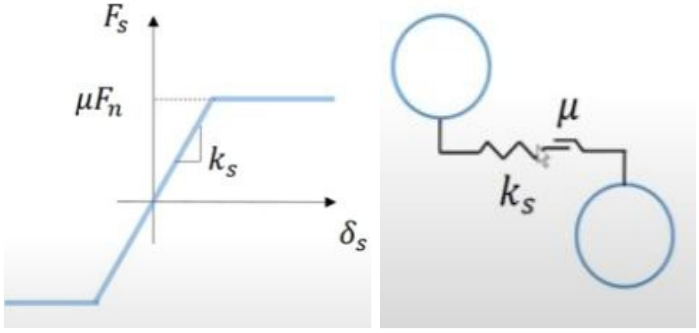

Fig 3.4: Tangential contact force schematization

3.1.3 DEM Integration time step

In order to avoid problems of convergence it is advisable to choose a correct time step of the numerical system. Given 3 particles arranged in a row, the core of the functioning is that the information between Body1 and Body2 cannot be transmitted to particle 3 in the same time step, but it will do it in the next one. This transmission velocity is directly proportional to the rigidity of the involved particles and inversely to their mass. It's fundamental to notice that the integration time step must be smaller than a critical one function of the eigen frequency of the system, if a greater time step is adopted our simulation is no longer representative. It's clear that as the integration step decreases, the computational effort required to the computing machine will be greater, obviously the computational time of a single timestep will depend on the total number of bodies of system. Generally, Δt_c can be computed in function of the mass *(m)* and stiffness (*k*) of the particle according to the following equation:

$$\Delta t_c = 2/w_{max} = 2\sqrt{m/k} \qquad \textit{eq 2.4}$$

$$w_{max} = highest\ eigen\ frequency$$

$$k = stiffness \quad m = mass$$

3.2 Wire mesh Modelling

DEM modelling of wire-meshes is based on the work of Hearn et al. (1995) and Nicot et al. (2001) where in these first approaches they analysed the behaviour of a steel net structure impacted by a boulder. Generally, a wire mesh in Discrete Element Methods is described through a regular pattern of spheres and/or cylinders linked together or connected through remote interactions. For a correct wire-mesh modelling it is necessary to have knowledge of the behaviour of the single wire of a wire mesh, its response to external forces is so obtained through the stress-strain curve acquired in laboratory subjecting it to a tensile test.

3.2.1 Interaction law

According to the **Elementary Wire Model (EWM)** developed by Thoeni et al. in 2011 the interaction law is directly defined by a linear piece-wise force-displacement curve which is derived from the stress-strain curve of a wire. This model describes an interaction between two particles which ends once the failure point is reached (max elongation). As shown in the figure 3.5, in the case of cessation of external forcing, the wire will keep a certain residual plastic deformation described by an unloading curve. It is useful to specify that a single particle of our mesh can present multiple interactions, to which we can assign different contact laws according to the internal characteristics of the single elements of the system.

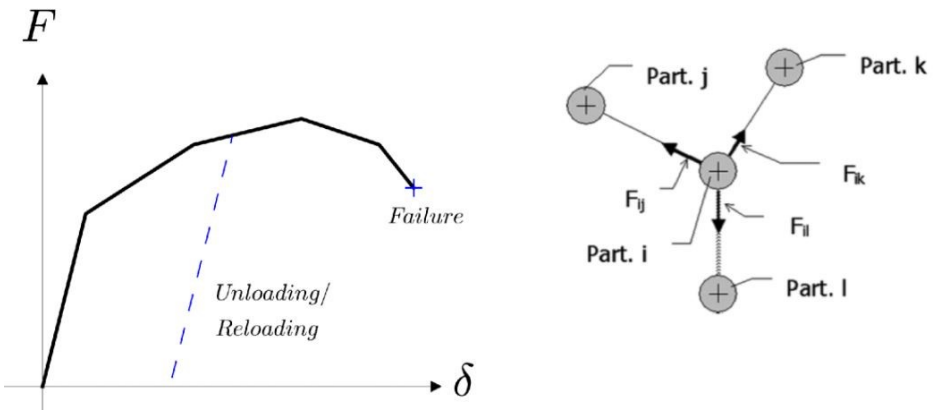

Fig 3.5: Single wire force-displacement curve according EWM

Stochastically Distorted Wire Model (SDWM) developed by Thoeni in 2013 introduce 2 new parameters:

- λ_u Determines a horizontal shift to the force displacement curve
- λ_f Determines the stiffness of the wire in the shifted area

This introduction allows to take into account deformations related to the production phase and differences of the single wires. Unlike EWM where all wires are identical in every property, this approach randomly inserts through parameters λ_u and λ_f internal irregularities at each single wire (see Fig 3.6).

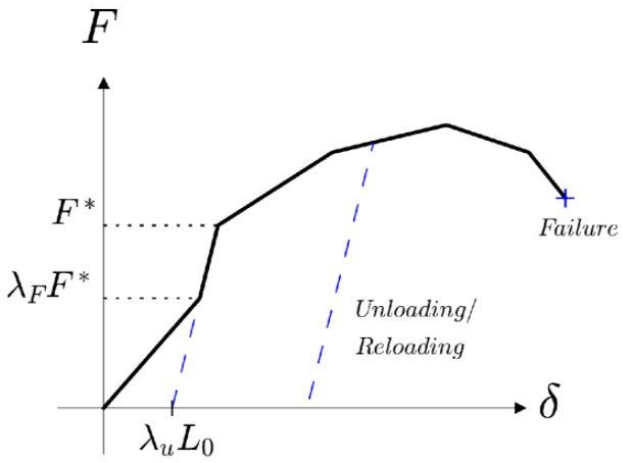

Fig 3.6: Single wire force-displacement curve according SDWM

3.2.2 Wire mesh discretization models

Nowadays various modelling methods have been developed and we can distinguish 3 main categories:

- Cell Based Approach
- Node-Wire Based Approach
- Cylinder-Wire Based Approach

Cell Based Approach

This method was introduced by Nicot et al. in 2001 and implemented by Coulibaly et al. in 2017, this approach guarantees a minimum discretization of the mesh structure by simulating the latter through spherical particles positioned in the center of each mesh. Particles are connected through remote interactions. As you can see in the figure 3.7 this method does not provide a correct reproduction of the network system, but in its favor it guarantees a good efficiency thank to its simplicity level. However, interaction laws require a specific calibration and some problems could emerge if our mesh system collides with external bodies characterized by a smaller dimension than the distance between 2 spheres, in fact in this case some contacts may be unrecognized and the final simulation loses precision

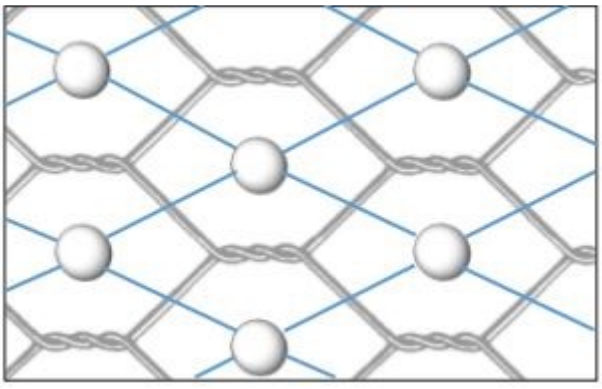

Fig 3.7: Cell Based Approach structure discretization

Node-Wire Based Approach

Developed by Bertrand et al. in 2005 this method provides a more precise reproduction of the mesh system. Starting from a periodic element of our structure, that in drapery application simulation could be the hexagonal double twisted mesh, a given pattern of spherical bodies each of which represent a node of the mesh is defined. Therefore, remote interactions between the particles are inserted according to the specific geometric characteristics of the considered element (see Fig 3.8). In this approach the wires actually do not exist but are replaced by the just described remote interactions, their weight is instead transferred to the spherical particles. What has just been described implies that a process of interaction between an external body and our system happens only when there is a contact between the external element and a sphere of the pattern. This fact puts in evidence that if we use an external granular element smaller than the mesh of our net we will have some losses of information and a wrong simulation of the process. For its part, this method provides a much simpler description of the network than CWB and is computationally much more efficient.

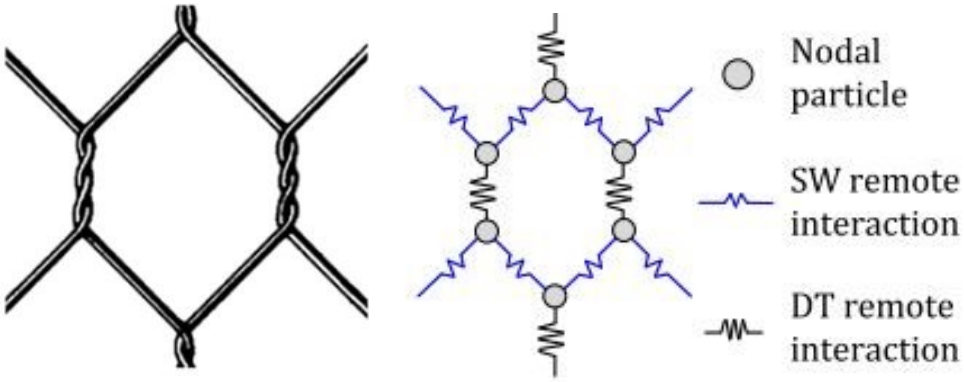

Fig 3.8: Reproduction of wires characteristics through remote interactions

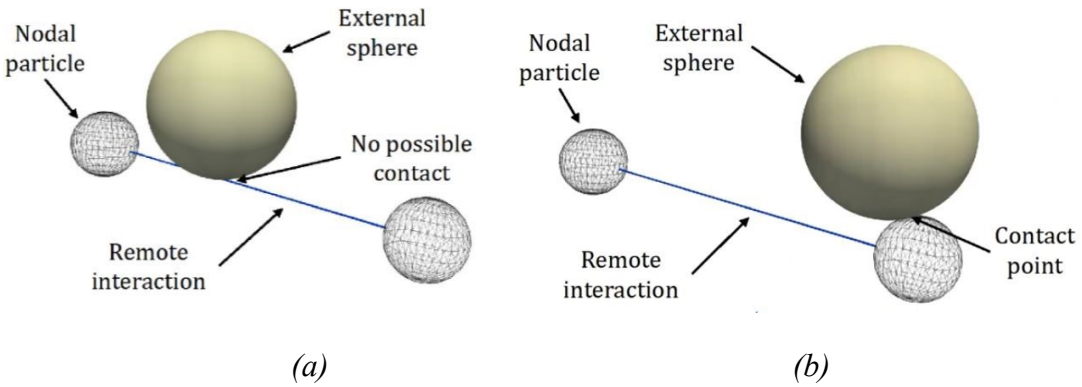

Fig 3.9:(a) No contact detection; (b)correct contact detection in NWB approach

Cylinder-Wire Based Approach

This method is built on the basis of the previous one but it introduces cylindrical bodies between node and node in order to avoid the lack of contacts between the external body and the mesh system (Fig 3.10). These cylinders are not dynamic bodies like spheres, in fact they are not considered in the motion integration processes, no force will act on them. They are only used to detect more contacts, all mechanical information will remain at nodes level, so the deformation of the cylinder follows the movement of spherical particles.

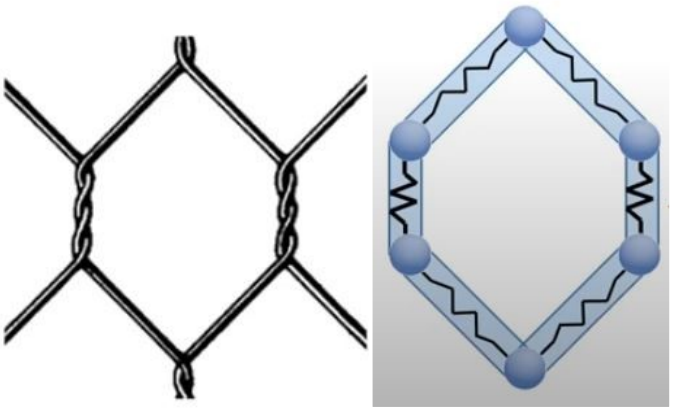

Fig 3.10: Mesh schematization according to CWB approach

According to this methodology three kinds of contacts between an external sphere and the mesh system can be individuated:

- Sphere-Sphere contact ► Same of the CB and NWB approaches
- Sphere-Cylinder contact ► When an external body touches the external surface of the cylinder, one virtual sphere of the same dimensions of nodal ones is created. This new virtual element is designed only to transfer the contact information's to the nodes (see Fig 3.11a).
- Cylinder-Cylinder contact ► Following the same reasoning above in case of cylinder-cylinder contact 2 virtual spheres are created to transfer the information to the nodes (see Fig 3.11b).

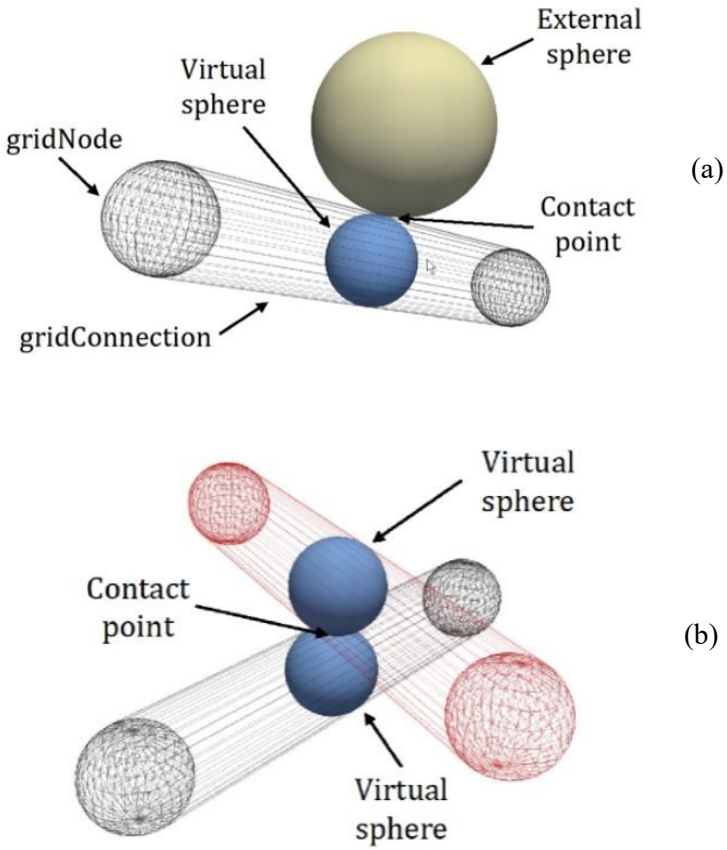

Fig 3.11:(a) Sphere-cylinder contact; (b) cylinder-cylinder contact

Chapter 4

Numerical Simulation

Numerical simulations were performed using Yade (https://yade-dem.org), an extensible open-source framework for discrete numerical models, focused on Discrete Element Method. The computation parts are written in c++ using flexible object model, allowing independent implementation of new algorithms and interfaces. Python is used for rapid and concise scene construction, simulation control, postprocessing and debugging.

This chapter will be divided into 3 parts:

- An initial part dedicated to the description of the wire-mesh creation method in YADE.
- A second phase of validation of the numerical model.
- A third one in which we will try to reproduce the tests carried out at Pont Boset.

4.1 Wire-mesh creation

For the mechanical simulation of the wire-mesh system the Node Wire Based approach has been chosen. Since that in the numerical reproduction a much larger punching element than the single mesh size is considered, this approach guarantees shorter computation times and a similar mechanical response respect to the CWB approach.

In this analysis an hexagonal mesh with wire diameter equal to 3mm was considered. The hexagonal periodic cell is characterized by 2 double twist wires in vertical position and 4 single wires inclined at 45° respect to the horizontal. Each mesh of the net is described by 3 parameters: length of the double twisted wire, vertical projection of the single wire and opening of the mesh. The first 2 characteristic lengths are each equal to 4cm while the last is 8 cm. According to the NWB approach the threads of the mesh are not

reproduced and the weight is carried by the 6 spherical particles corresponding to the nodes of the hexagon.

The interplays between nodes are simulated through remote interactions that reproduce the presence of the wires. These simulative interactions are created from the experimental data concerning the stress-strain curves of the single and double twisted wire according to the Elementary Wire Model. It is important to underline that compression forces are not considered and that the breaking of a wire occurs after that a maximum level of elongation has been reached. From the figure 4.1 it is possible to see how both wires are characterized by an elastoplastic behaviour, the single wire manifests a greater rigidity with the achievement of the plastic condition after an elongation of around 5%, the double twist one is instead less rigid with a plastic limit around 10%.

In the relative numerical modelling, each spherical particle is characterized by a diameter equal to 8 times the one of wires and by a mass of 4.5g. For each square meter 315 nodes are created, this spatial concentration guarantees a correct reproduction of the weight per square meter of the wire mesh equal to 1.4kg/m^2.

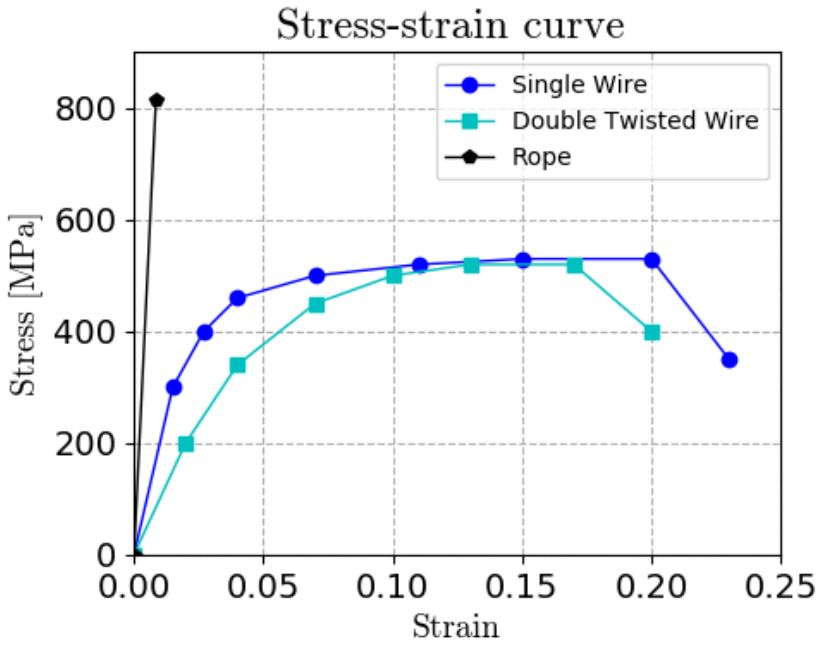

Fig 4.1: Wires stress-strain curves

The punching element is reproduced in the simulation using the so-called facets elements, these are triangular elements with 3 nodes and 2 facets (Fig 4.2). Their structure is very simple and allows a rapid calculation of displacement and forces.

Fig 4.2: facet element

Concerning this work the punch structure is composed by 694 facet elements fixed together in a way to create a solid-unique body, initially it has a diameter of 1 meter but this dimension can be varied in the software thanks to a scale factor that affects the facet length. Usually, the punching element is positioned parallel to the mesh with the top point of the dome at an infinitesimal distance from the mesh. During the simulation it can move on the z-x plane, i.e. in the outgoing direction from the panel's plane and in the vertical direction in the plane of the wire mesh. Furthermore, its rotation in the plane of the network is allowed thanks to a particular function able to compute the motion of the punch when subjected to mesh reaction forces and torque.

In some tests, as specified in the previous chapter, ropes are present to increase the stiffness and resistance of the drapery system. In the numerical model they are implemented through a particular function that provides to the nodes under consideration the properties of the rope. It is therefore not as in reality an external element but woven inside the wire mesh. In particular, steel ropes with a diameter of 10mm are used, implemented as for the wires thanks to the knowledge of their laboratory force displacement curve. These ropes are characterized by a tensile strength of 64kN and a young modulus of 96GPa.

Single wire mesh panels are then connected by means of vertical connection wires with a diameter of 3mm.

Regarding the contact between bodies, it is described by the Elementary Wire Model, implemented in Yade by Thoeni et al. in 2013. As mentioned in the previous chapter, the normal and tangential contact forces are related to the level of interpenetration between bodies and their intrinsic properties are related to 3 contact parameters:

Normal Contact Stiffness (k_n) ⟶ In simulation its value depends by the considered interaction, generally it's in the order of 10^6 N/m.

Tangential Contact Stiffness (k_t) ⟶ In the simulation is set as a fraction of k_n through the Poisson ratio.

$$\upsilon = 0.4 \quad k_t = \upsilon \cdot k_n \qquad \textit{eq 4.1}$$

Mesh-Punch Friction angle (Φ_u) ⟶ It's set equal to zero, this means that we have a frictionless contact.

From previous studies carried out by A.Pol et al. in 2020 it emerges that the variation of the contact parameters just described has a negligible influence on the mechanical response of the network, in fact it strongly depends on the mesh tensile behaviour introduced through the laboratory force-displacement curves. During simulation time step is not fixed, it varies in function of the particular eigen frequency of the system, generally it's in the order of 10^{-5} s. Data regarding for example force and displacement of the punching element are collected every 500 system iterations while graphical outputs (VTK files) are generated every 0.05 s.

Subsequently there is a set of tables that summarizes the parameters introduced in YADE regarding wire-mesh, ropes and punch creation input.

Nodes Property	
Diameter [mm]	24
Weight[g]	4.5
Poisson Modulus	0.3
Reproduced mesh density [kg/m^2]	1.4
Spatial density[n/m^2]	315

Tab 4.1

Wires Property	
Diameter [mm]	3
Young Modulus [GPa]	20
Poisson Modulus	0.3
Reproduced density [kg/m^3]	7500
Friction Angle [°]	30

Tab 4.2

Cables Property	
Diameter [mm]	10
Young Modulus [GPa]	96
Poisson Modulus	0.3
Reproduced density [kg/m^3]	7500
Friction Angle [°]	30

Tab 4.3

Load Distributor Property	
Diameter [m]	1.5
Young Modulus [GPa]	0.015
Poisson Modulus	0.3
Reproduced density [kg/m^3]	7500
Friction Angle [°]	0

Tab 4.4

4.2 Validation of the numerical model

The numerical model is initially validated through a comparison between the stress-strain curves obtained in the laboratory and those simulated through the software. The concerned test (Fig 4.3) responds to the standard UNI-11437 and states that a square mesh panel, suitably constrained at the edges to a rigid frame is subjected to an out of plane thrust exerted by a particular load distributor. This punching element is characterized by a spherical dome with diameter equal to 1 meter, a curvature radius of the shell of 1.2m and a curvature radius in proximity of the border equal to 0. 05m.It moves in a direction perpendicular to the panel at a constant velocity of 0.01m/s until the complete failure of the mesh or the reaching of the maximum applicable load. The tested portion is a 3x3m panel of an 8x10 hexagonal double twisted wire-mesh with a nominal diameter of 2.7mm and a weight of 1.4kg/m^2. The main output of these kind of test are stress-strain relationship obtained through load cells connected to the load distributor able to measure the force acting on it.

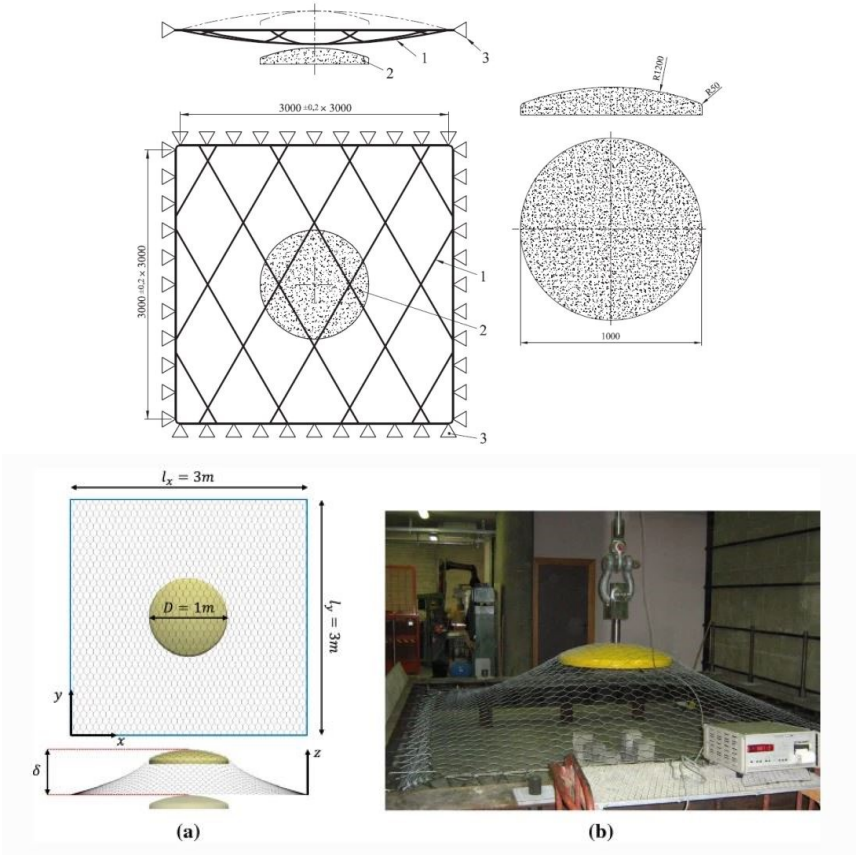

Fig 4.3: UNI-11437 Laboratory punch test

The numerical simulation is performed by reproducing at best the boundary conditions of the laboratory test by blocking the degrees of freedom of the nodes on the 4 sides of the panel. As regards all the other numerical parameters, they are not changed respect to the description done in the previous sub-chapter. It deserves attention to emphasize that the velocity of movement of the punch in the simulation is set to 1m/s hundred times greater regarding the laboratory one. This choice has been carried out to diminish the computational effort of the simulator machine. Although this compromise, substantial differences due to the variation of velocity didn't emerge. Comparing force-displacement curves shown in the figure 4.4 we conclude that the numerical method and the parameters chosen provide a good approximation of the mechanical behaviour of a wire-mesh subjected to an out of plane force. By matching the two curves it can be seen that once the system is activated the simulated response is the same as the one in the laboratory.

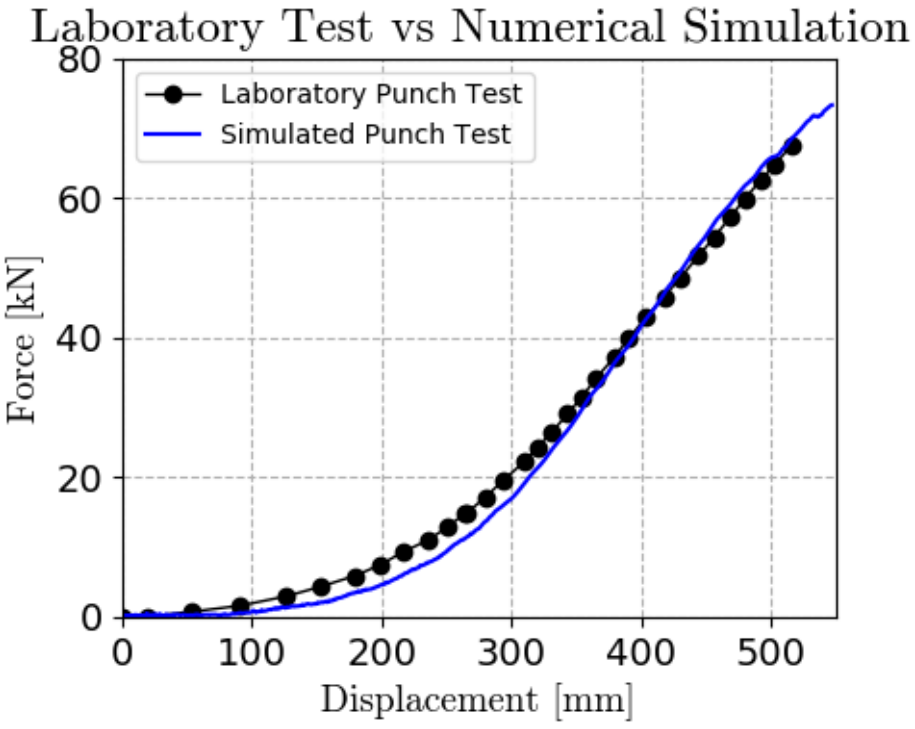

Fig 4.4: Laboratory punch test

4.3 Pont Boset Numerical Simulation

In this part of the thesis we will try to simulate the on-site test carried out at Pont Boset by Maccaferri company, in particular we will focus on test number 9, that is the one concerning a 6x6 m drapery system with a double twist mesh supported by the application of 2 horizontal cables of 10mm in diameter at the base and top of the rocky wall. The mesh is of double twisted steel woven wire of 3 mm manufactured to form a hexagonal shape with a MOS of 8 cm. Fix drapery system was equipped with sixteen square anchor plates of 15 cm that divide the mesh in 9 rectangular panels divided in 3 vertical bands by 2 connection wires of 3mm in diameter (see Fig 4.5). In the simulation phase the anchor plates are simulated by blocking the degrees of freedom of the knots of the locked meshes. The central panel was subjected to a puncture test where a spherical-cap-shape load distributor of 1.5m of diameter connected to the rock wall through an hydraulic arm was used as punching element. The hydraulic jack is 2.3m long and it's able to apply a maximum force of 200kN directed with an inclination of 45° respect to the out of plane axis. This angle was selected because considered an average value between the dip of the sliding joint. Further and detailed information about the Pont Boset site test is reported in chapter 2.

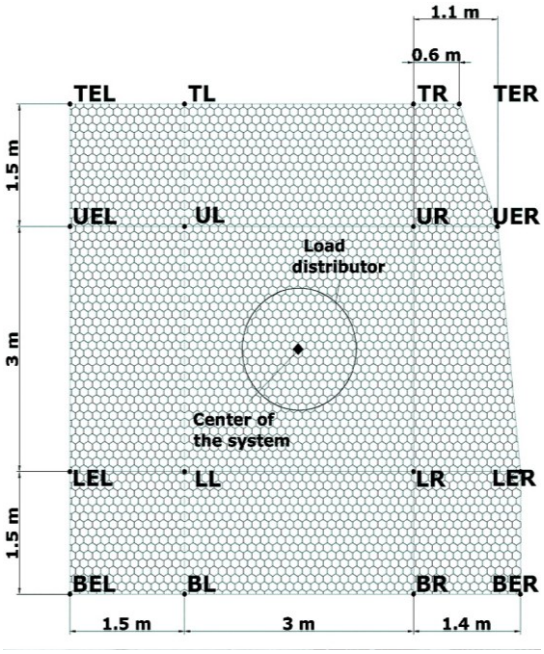

Fig 4.5: Geometric scheme of Pont Boset drapery mesh system

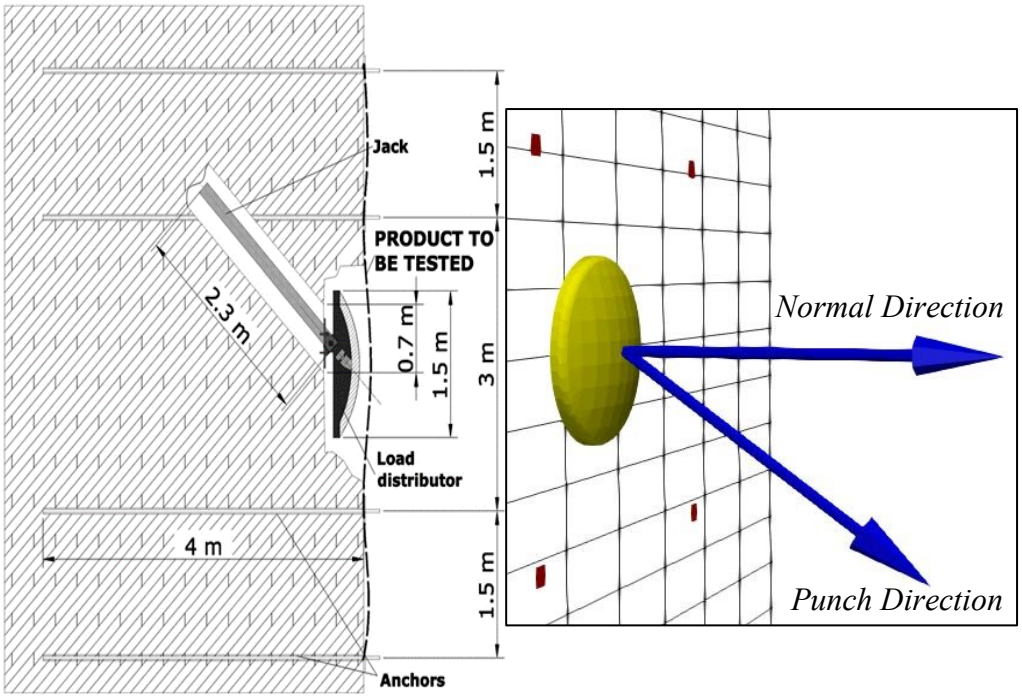

Fig 4.6: Detail on the punching device

4.3.1 Force-Displacement curve analysis

The purpose is to reconstruct a force displacement curve as close as possible to the one representing the on-site test. The force reported in the data collected is the one having a direction concordant with the thrust of the punch, while the displacement is orthogonal to the drapery system plane. As we can see in tab 4.5, the data provided are not exhaustive, therefore the interpolating curve of these data does not represent with certainty the mechanical behaviour of the mesh. Observing figure 4.7 it is possible to notice how the panel begins to oppose resistance around a displacement of the punch equal to 800mm, from that moment the curve takes an exponential trend up to the moment of tearing of the net in correspondence of the most loaded plates. It is important to note a small discontinuity of the curve around a displacement of 1100mm, it is due to the breakage of some wires, a phenomenon which however does not cause the collapse of the system.

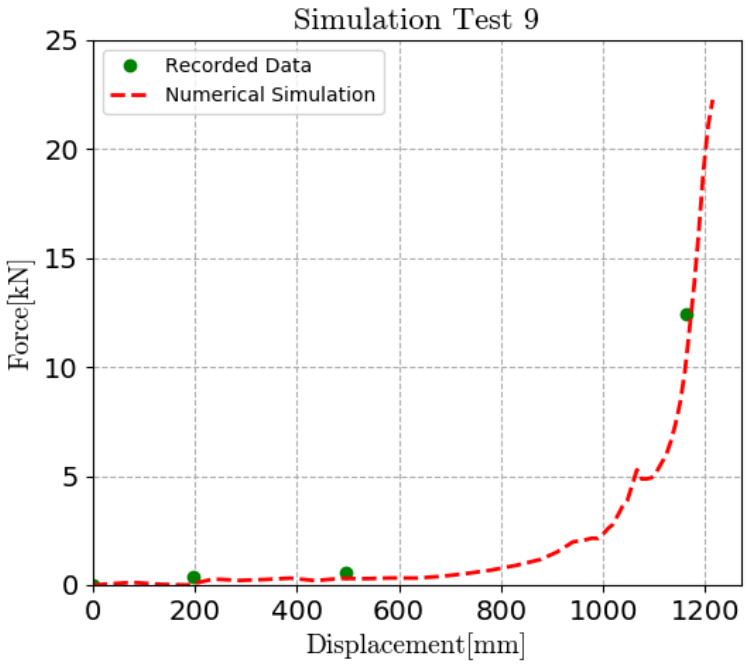

Fig 4.7: Force-Displacement curves comparison

Recorded points	δ(mm)	F (kN)
1	*0*	0
2	*196.57*	0.46
3	*497.08*	0.98
4	*1161.92*	12.42

Tab 4.5

In order to obtain a numerical simulation curve that could represent the collected data in an acceptable way, the mesh panel was loosened in initial tensile stress by moving each node of the net towards the center of the panel through 2 coefficients (see eq 4.2). These coefficients refer one to the vertical displacement of the node and the other to the horizontal one; both have a value equal to 0.05. The manipulation of the structure just described does not affect the shape of the force-displacement curve but only translates it, simulating a delay in the mechanical response of the mesh to an external stress. In figure 4.8 it is possible to see the influence of the variation of these coefficients on the simulated drapery system curves.

$$x_{new} = x_o + \alpha(x_c - x_0)\ ;\ y_{new} = y_o + \beta(y_c - y_0)\ ;\ z_{new} = z_0 \quad \textit{eq (4.2)}$$

$$a = horizontal\ coeff\ ;\ \beta = vetical\ coeff$$

$$(x_0, y_0, z_0) = intial\ position$$

$$(x_{new}, y_{new}, z_{new}) = new\ final\ position$$

$$(x_c, y_c, z_c) = (3,3,0) = center\ position$$

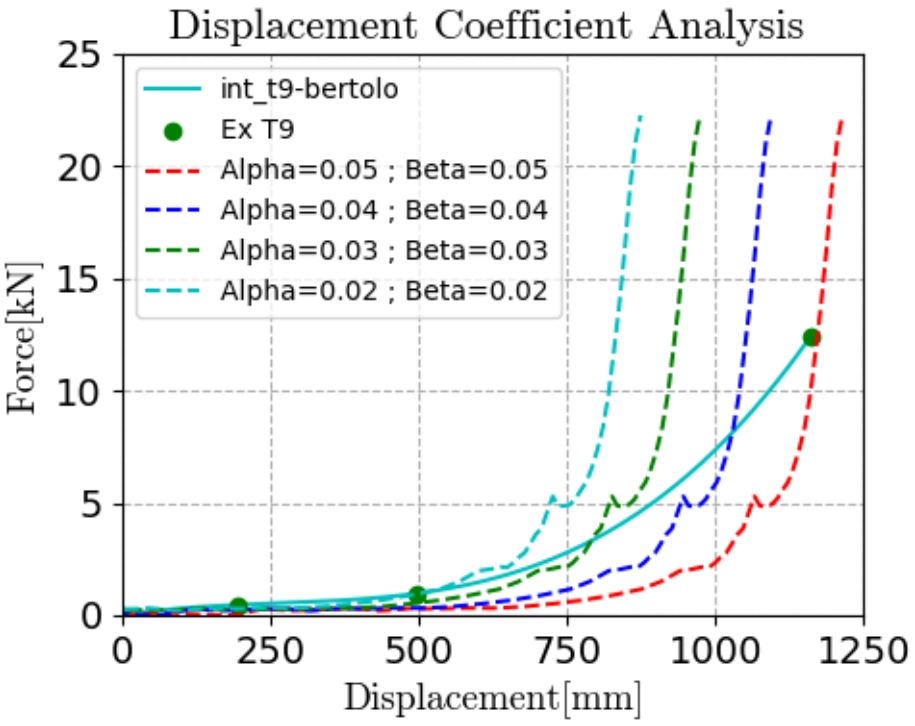

Fig 4.8: Alpha and Beta influence on force-displacement curves

4.3.2 Failure and loading condition analysis

In accordance with what happened in the experimental test, no significative laceration or failure occurs up to the last recorded measurement point, after this moment we start to see important wire breaks in correspondence of the LL and LR plates. Obviously, since the punch moves in a direction of 45° towards the base of the slope respect to the direction orthogonal to the plane of the drapery system, these plates are the most loaded. Analysing the loading process on the 4 plates placed in abscissa x = 1.5m (BL, LL, UL and TL), it can be noted that at the moment of failure, for a displacement of 1200mm the plates BL and LL are the most subjected to receive load from the punch. Obviously, since the system is symmetrical, the same effort will be distributed to the BR and LR plates. Proceeding vertically, the load stress on the anchoring systems decreases substantially, with the UL plate subjected to about half the stress carried by LL and with the TL plate not loaded (see Fig 4.9).

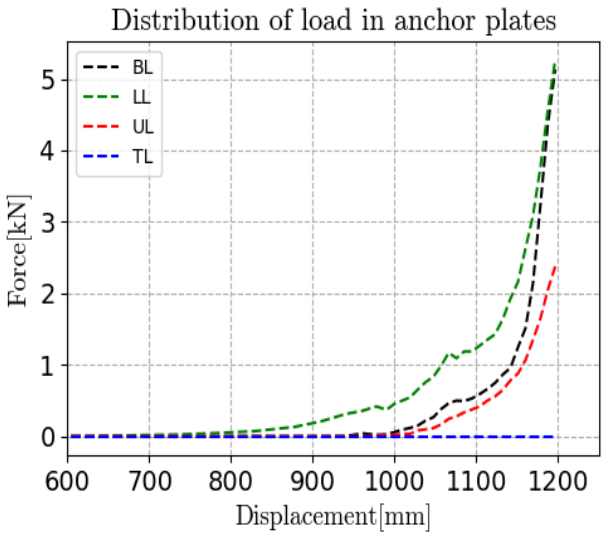

Fig 4.9: Loading process on plates

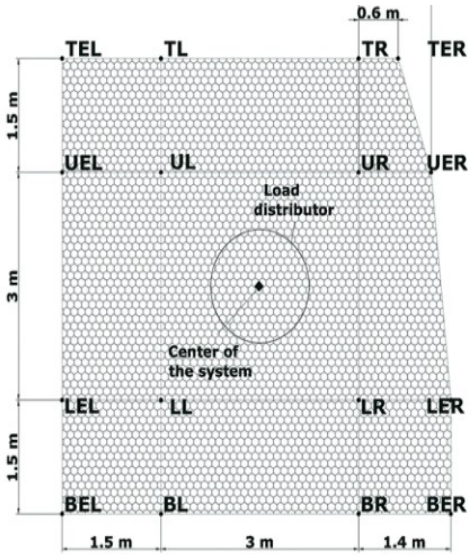

Fig 4.10: Anchor pattern

Loading Process	
Plate	**F (kN)**
BL	5.05
LL	5.18
UL	2.34
TL	0

Tab 4.6

The following three figures show the progressive mechanical response of the drapery system to the pushing action of the punch. From the images appears as the punch transfers to the network a strong energy in its impact with the possibility of generating elastic-waves of small amplitude within the system.This problem has been avoided by the intrinsc dissipative properties of the system and introducing a damping coefficient that reduces the effect of elastic waves produced in the collision between punch and mesh panel.

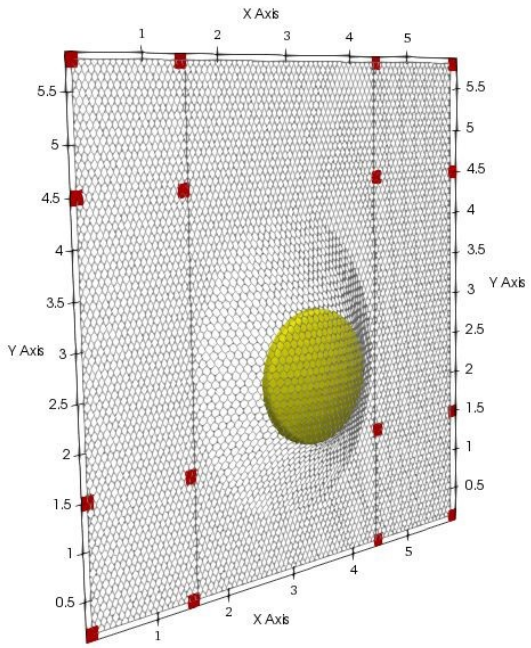

Fig 4.11

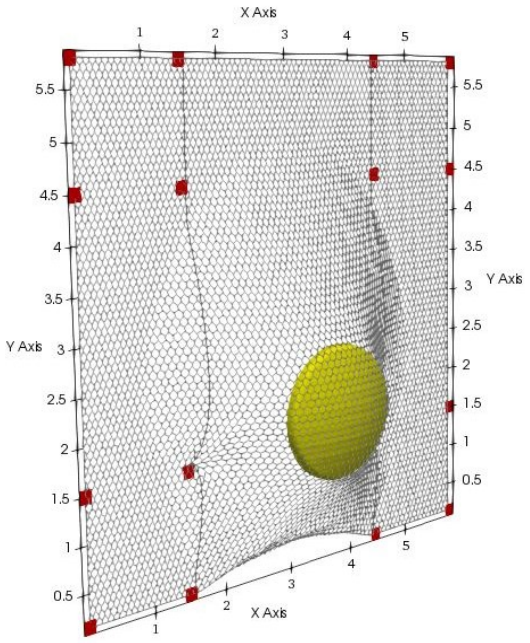

Fig 4.12

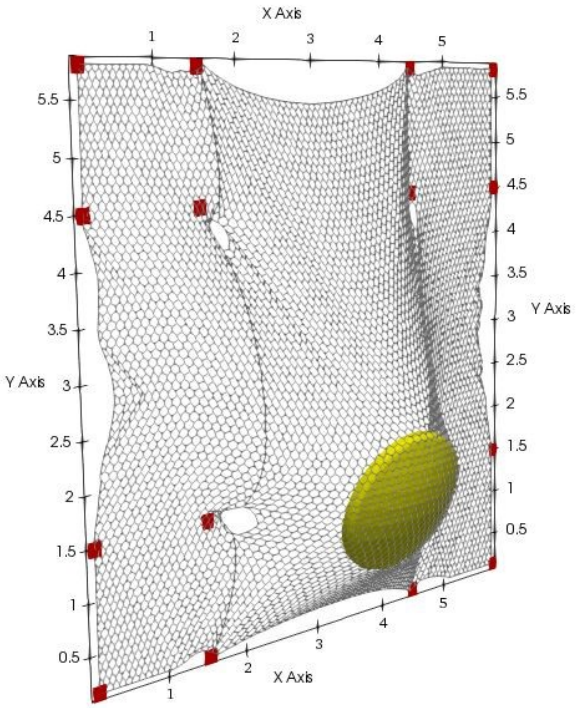

Fig 4.13

If we consider the distribution of the force exerted by the load distributor on the anchor plates, it can be observed that a large part of it is conveyed in normal force (see Fig 4.14), i.e. force exiting orthogonally out of mesh plane. The sum of horizontal tangential forces is negligible, remaining almost always zero during the simulation.In the vertical direction the sum of forces is almost always balanced for the entire simulation until a final increase due to the tensioning of the BL and LL plates.

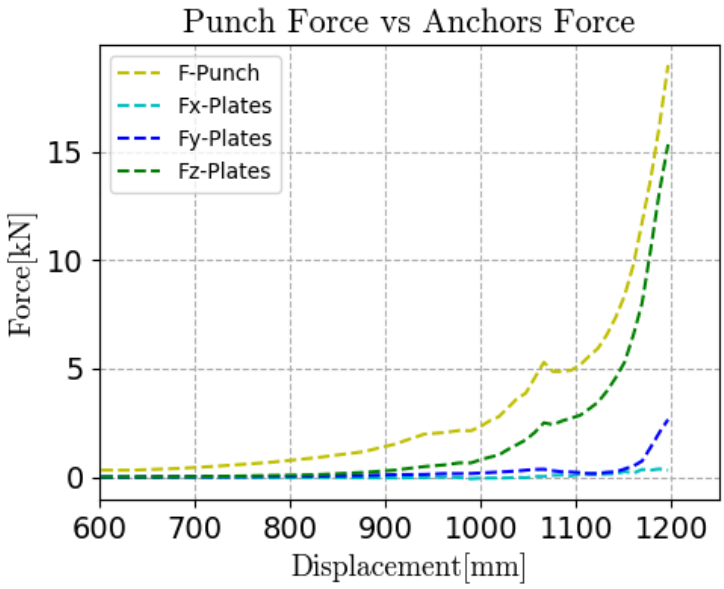

Fig 4.14: Load distribution in anchor system

We can now focus on the normal and tangential forces distributed on the anchor plates BL, LL, UL and TL. In particular is worth nothing the plate TL placed at the top of panel is not affected by the punching-load action.Regarding tangential forces in X direction plates LL and BL are the most stressed ones with a value approximately 3 times larger than the one recorded in UL plate (see Fig 4.15 and Tab 4.7). These forces, as pointed out in the previous paragraph, are however totally counterbalanced by the forces discharged in the plates placed at abscissa equal to 4.5m, the same happens between the plates placed at x = 0 and and x = 6, thus making the system as a whole balanced.

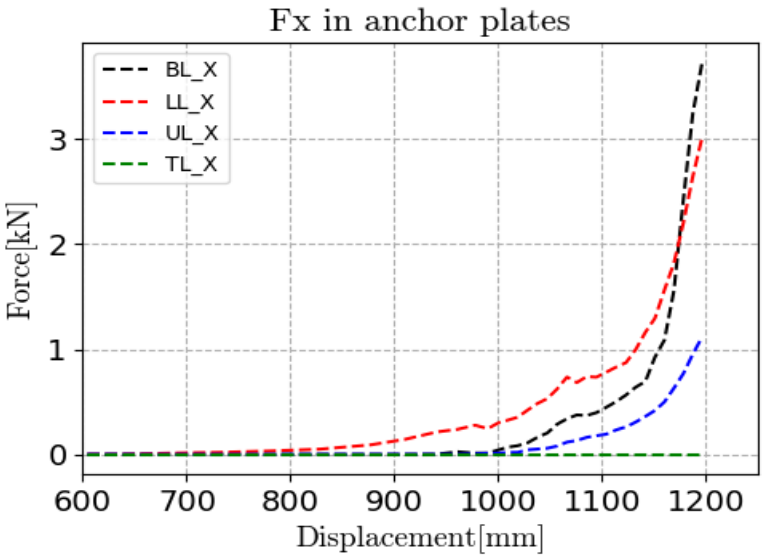

Max load in x direction	
Plate	***F(kN)***
BL	3.67
LL	2.97
UL	1.06
TL	0

Tab 4.7

Fig 4.15: Horizontal tangential forces analysis

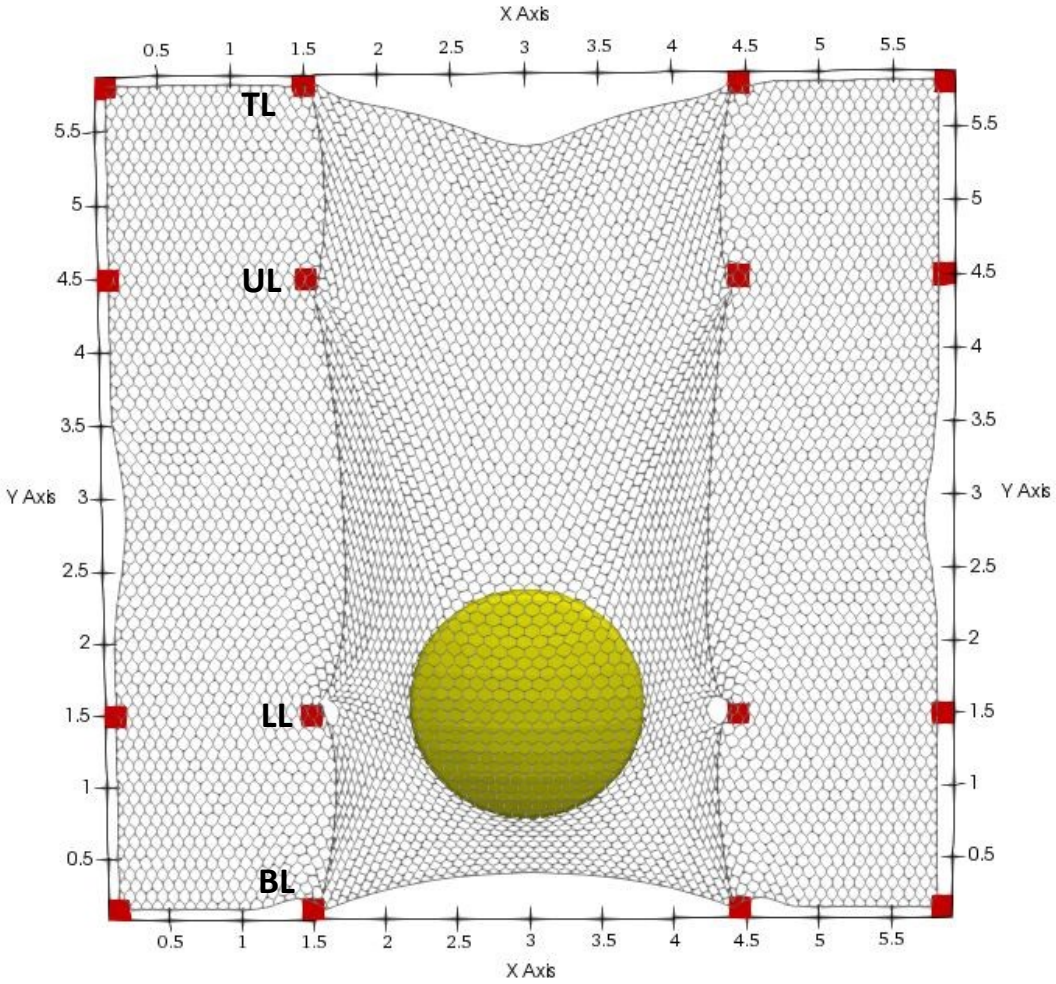

Fig 4.16: System failure condition

Analyzing the tangential force in the vertical direction the most stressed plates are BL and UL, with a fairly comparable value around 2kN, these two plates at the moment of yielding are respectively 1.5m and 3m from the center of thrust of the punch. The plate LL, on the other hand, being at the height of the thrust point is not stressed too much by the shear force (see Fig 4.17, Tab4.8)

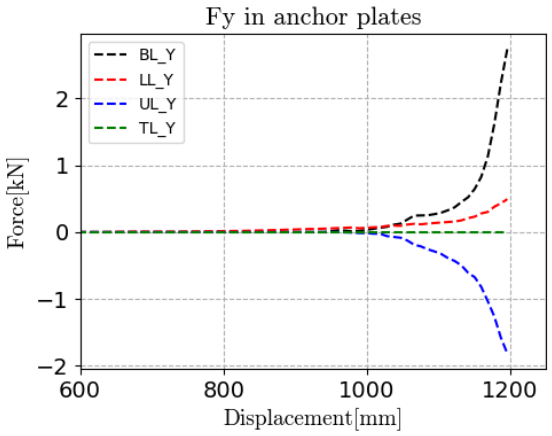

Max load in y direction	
Plate	***F(kN)***
BL	*2.73*
LL	*0.49*
UL	*-1.73*
TL	*0*

Tab 4.8

Fig 4.17: Vertical tangential forces analysis

The normal force is instead conveyed more to the plates near the load distributor, where the greatest displacement of the nodes in the direction outgoing from the mesh plane occurs (see Fig 4.18 and Tab 4.9).

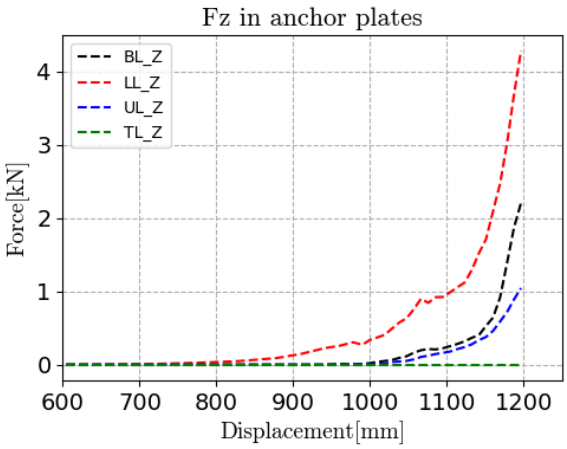

Max load in z direction	
Plate	***F(kN)***
BL	*2.15*
LL	*4.25*
UL	*1.07*
TL	*0*

Tab 4.9

Fig 4.18: Normal forces analysis

It is important to note that as shown in the table 4.6, the BL and LL plates are subjected to a very similar total force, respectively of 5.05kN and 5.18 kN,but only the latter manifests breaking phenomena. This detail makes us pay attention to the single forces acting on the plates, in particular by observing the figures (4.19, 4.20 and 4.21) and tables (4.10, 4.11 and 4.12) on the current and next page we can observe how the plate LL is subjected to lower tangential forces than BL but instead it is subjected to a normal one about the double of the plate below it. It can thus be highlighted that despite the tangential stresses influence the mechanical behavior of the mesh, what leads to the breaking of the net in correspondace of an anchor plate is largely due to an excessive normal effort and the consequent mesh deflection in the out of plane direction.

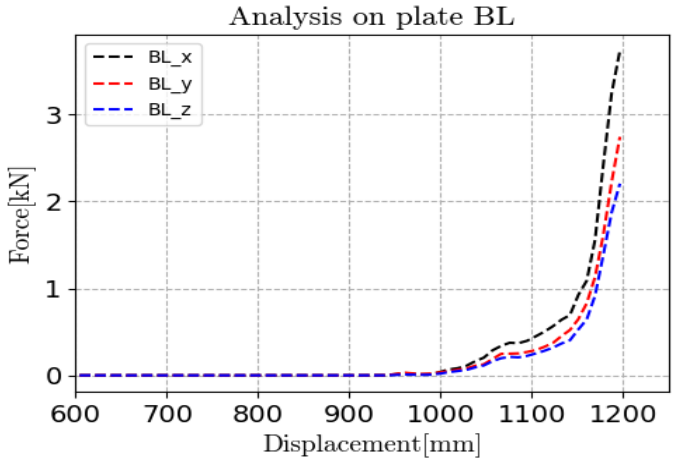

Fig 4.19: BL plate analysis

Load Analysis	
Plate BL	***Fmax (kN)***
Fx	*3.67*
Fy	*2.73*
Fz	*2.15*

Tab 4.10

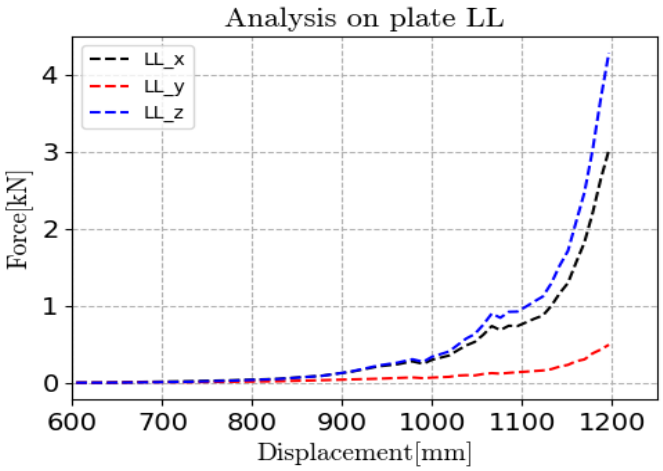

Fig 4.20: LL plate analysis

Load Analysis	
Plate LL	***Fmax (kN)***
Fx	2.97
Fy	*0.49*
Fz	*4.25*

Tab 4.11

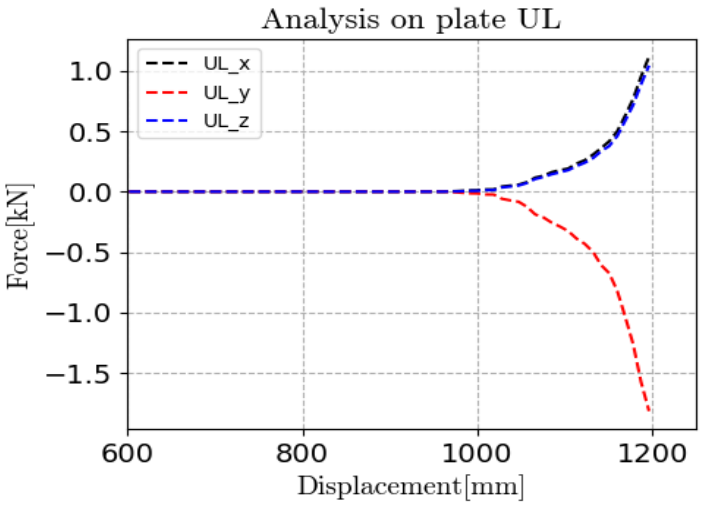

Fig 4.21: UL plate analysis

Load Analysis	
Plate UL	***Fmax (kN)***
Fx	*1.06*
Fy	*-1.73*
Fz	*1.07*

Tab 4.12

Chapter 5

Parametric analysis

In this chapter two sensitivity analysis will be performed in order to extend the previous described results to more general field conditions. A first parametric analysis will focus on the Pont Boset on-site test, while a second one will be dedicated to an in-depth comparison analysis of the laboratory test performed according to the UNI 11437 standard. The influence of some elements of the drapery system on the force displacement curve will be discussed. In particular the following geometric and material parameters will be analyzed: anchor plate dimension and spacing, panel aspect-ratio, mesh wire diameter, dimension and positon of the punching element in the panel.

5.1 Pont Boset Parametric Analysis

This first set of parametric analysis aims to study the influence of the parameters described above on a drapery application similar to the Pont Boset test. As reference test (see Tab 5.0) a simulation of a 9x9m anchored drapery system with 16 anchor plates of 15cm placed in a way to form nine square panels is considered (Fig 5.1).

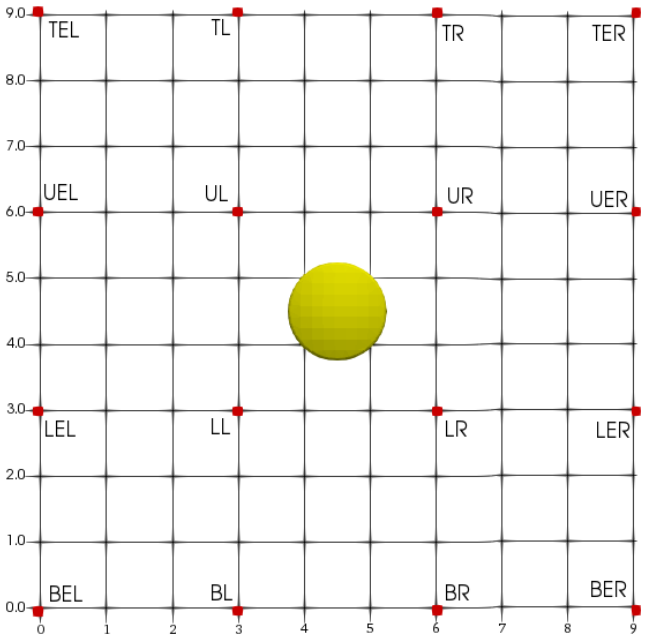

Fig 5.1: System geometric schematization

The loading distributor, characterized by a diameter of 1.5m, is positioned in the center of the central panel and moves at an angle of 45° respect to the normal direction to the mesh plane. What has just been described does not coincide with the Pont Boset test, which consists of a 6x6m wire mesh with a a 3x3m central panel, but guarantees an extension of the results to larger and more uniform drapery systems and not only to the specific case developed by Maccaferri. Despite this geometric difference between the two systems, the rupture occurs practically at the same instant and also the developed resistance almost coincides (Fig 5.2), highlighting that the boundary conditions of the central panel in the two considered cases do not influence its mechanical response. This allows us to compare the results of this analysis both to Pont Boset and to most common drapery-systems. In the following paragraphs concerning the influence of the single parameters on the wire mesh performance all the results are normalized on the failure values of 9x9m test, in particular on a force value F_r= 23.2kN and a deflection value of δ_r=1.265m.

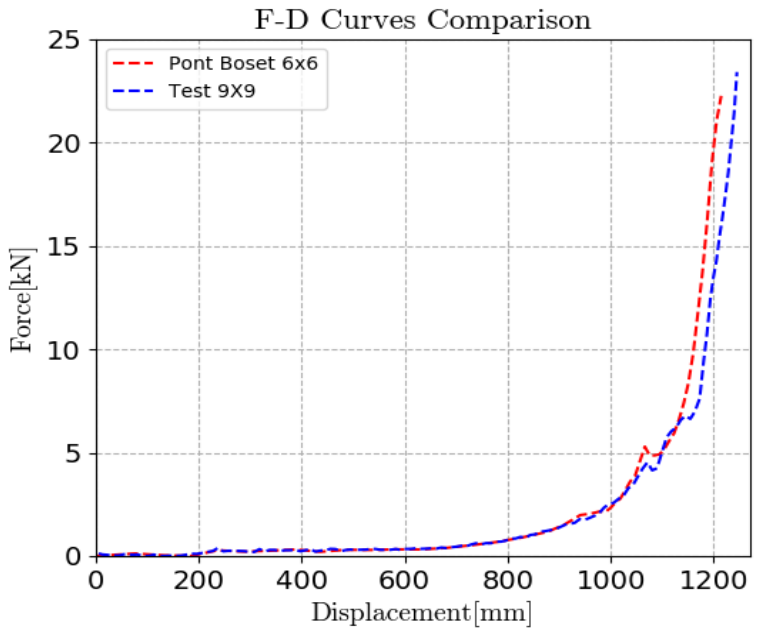

Fig 5.2: Pont Boset vs 9x9 test comparison

Reference Test	
Parameters	***Value***
Anchor Plate Size[cm]	*15*
Panle Aspect Ratio[L_x/L_y]	*1*
Anchor Plate spacing[m]	*3*
Punch Thrust Direction [°]	*45*
Punch Size[m]	*1.5*
Punch position [-]	*Center of the panel*
Wire diameter[mm]	*3*

Tab 5.0

5.1.1 Anchor plate size influence

The size of the anchoring plates is one of the most relevant elements regarding the resistance of a drapery system. In fact, by increasing the size of the plates, the number of locked nodes and wires of the wire mesh increases, thus making the panel stiffer and capable of bearing a greater punching stress. In this analysis the size of the plates is varied from a minimum of 8 cm to a maximum of 56cm with a step equal to the opening of the single mesh of the net (MOS = 8cm). Generally, in the practical field the anchor plates range from 15 to 40 cm, values outside this range have been analyzed to have a more accurate knowledge of their influence on the breaking point. In the analyzed cases, failures always occur in correspondence of the lower plates of the central panel (LL, LR), being the ones closest to the punching element. If on the other hand, a punching element characterized by smaller dimension than that of the plates had been used, the breakage would have instead occurred with a tear near the thrust point.

Plate Dimension Analysis			
Plate Dimension[m]	*Failure Force(kN)*	*Failure Displacement[m]*	*System Stiffness [kN/m]*
0.08	*19.1*	1.235	32.6
0.15	*23.2*	1.265	41.1
0.24	*30.5*	1.138	69.5
0.32	33.1	1.104	76.9
0.40	38.8	1.042	98.8
0.48	45.5	1.000	130.1
0.56	49.7	0.955	162.9

Tab 5.1

As it emerges by comparing the force-displacement curves of 4 different systems (Fig 5.3) the mechanical activation of the panel occurs at the same level of deflection but the curve becomes more rigid the larger the anchor plate used. Stiffness of the system is defined as the slope of the F-δ curve from the activation point. It is also clear that as the size of the plates increases, the maximum resistance force of the system increases while the failure

displacement decreases. It is interesting to observe from figures 5.4 and 5.5 how these dependences can be described by linear relations computed through linear least squares fit. The equations of the aforementioned relations are shown below where the failure strength and displacement are computed as function of the plate size d_p [m] normalized on the reference parameter (d_{pr} =0.15m) and the corresponding reference values F_r [kN] and δ_r [m].

$$F_{max} = \left(0.44\frac{d_p}{d_{pr}} + 0.58\right)F_r \quad d_p \geq 0.15m \quad (eq\ 5.1)$$

$$\delta_{max} = \left(-0.08\frac{d_p}{d_{pr}} + 1.04\right)\delta_r \quad d_p \geq 0.15m \quad (eq\ 5.2)$$

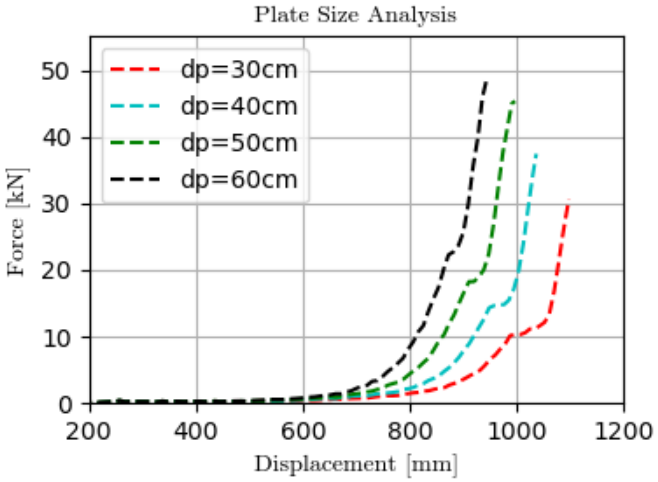

Fig 5.3: F-δ curves for different anchor systems

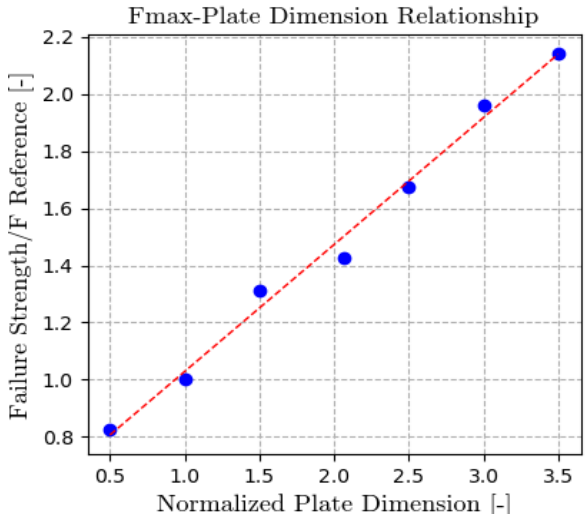

Fig 5.4: Force-d_p relation

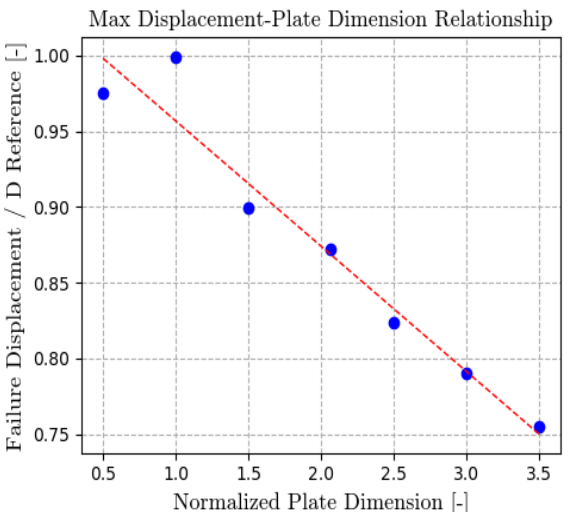

Fig 5.5: Displacement-d_p relation

5.1.2 Panel aspect ratio influence

Usually in drapery mesh systems applications square panels are used but in the case of particular morphological characteristics of the site, rectangular panels of different sizes can be taken into consideration. The panel size variation is given by a modification of anchor spacing along both vertical and horizontal direction. In this sub-chapter we will proceed to analyze the influence on panel mechanical strength of the ratio between the horizontal and vertical length of the panel, also called aspect ratio (AR) (see examples in Fig 5.6 and 5.7). The mechanical response of 7 different panels will be investigated going from an aspect ratio of 0.5 up to 2 with an incremental step of 0.25. It should be underlined that in this analysis the area has kept constant and equal to $9m^2$, furthermore all the force and displacement values are normalized with respect to the reference case, characterized by nine 3x3m panels.

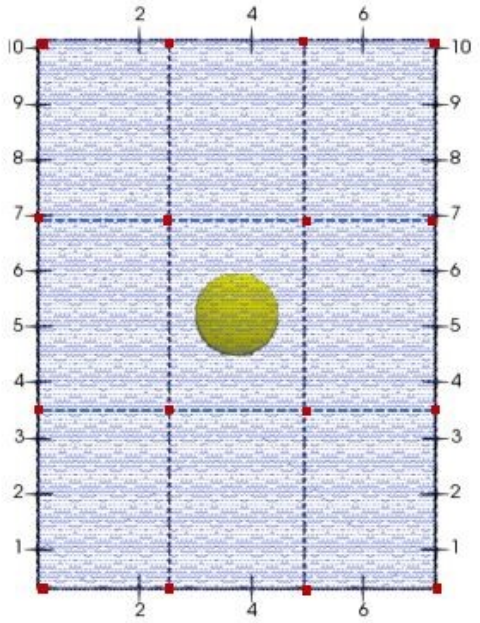

Fig 5.6: Panel Aspect Ratio 0.75

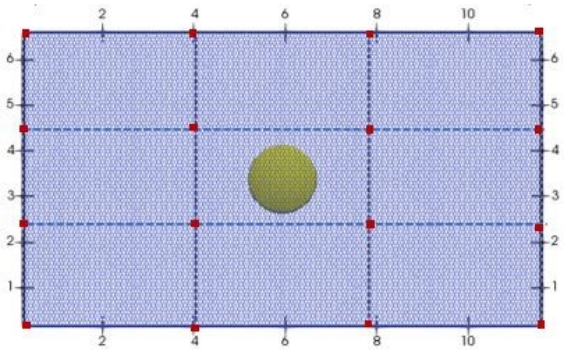

Fig 5.7: Panel Aspect Ratio 1.50

As reported in table 5.2 and in the following graphs, AR values lower than one lead to a faster activation of the panel, as regards the resistance instead, it is unaffected by this geometric variation. On the other hand, by increasing the horizontal width of the panel and decreasing the vertical height the load distributor is moved away from the most stressed plates, i.e. LL and LR, since

the punch does not move only in the out of the plane direction but also in the vertical one towards the base of the system. This leads to a greater deformability of the panel and at the same time also to a greater level of failure strength. By way of illustration, for an aspect ratio equal to 2 the failure strength exceeds the reference value by 3.5 times and failure displacement occurs at 2.2 times δ_r.

This anisotropy in the mechanical response of the wire mesh can therefore lead to think that more longitudinally extended panels are more reliable than square ones, on the contrary however, panels that are too deformable can lead to the formation of permanent distortion over time, thus decreasing the effectiveness and safety of the system.

Aspect Ratio Analysis						
Aspect Ratio[-]	***Panel Horizontal Width [m]***	***Panel Vertical Height[m]***	***System Horizontal Width[m]***	***System Vertical Height[m]***	***System Failure Force(kN)***	***System Failure Displacement[m]***
0.5	*2.12*	*4.24*	*6.36*	*12.72*	*18.6*	1.017
0.75	*2.68*	*3.35*	*8.04*	*10.05*	*17.3*	1.029
1	*3*	*3*	*9*	*9*	*23.2*	1.265
1.25	3.35	2.68	10.05	8.04	32.6	1.365
1.5	3.67	2.44	11.01	7.32	35.8	1.484
1.75	3.97	2.26	11.91	6.78	51.9	1.603
2	4.24	2.12	12.72	6.36	87.3	1.750

Tab 5.2

Relations between the failure force and the aspect ratio can be described by a third-degree polynomial curve (Fig 5.8), while the dependence of the max displacement on the AR value is linear (Fig 5.9).

$$F_{max} = (4.21AR - 4.35AR^2 + 1.65AR^3 - 0.50)F_r \quad (eq\ 5.3)$$

$$\delta_{max} = (0.4AR + 0.57)\delta_r \quad (eq\ 5.4)$$

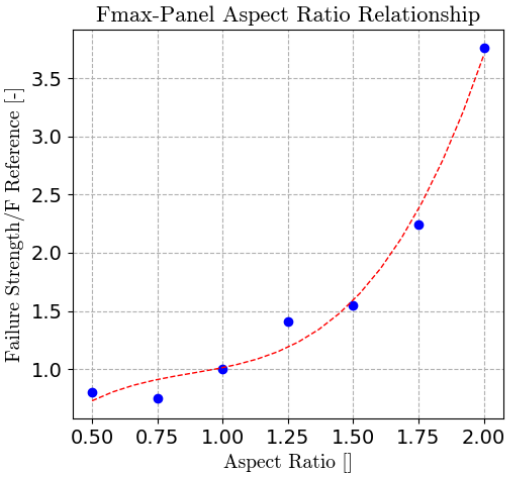

Fig 5.8: Force-AR relation

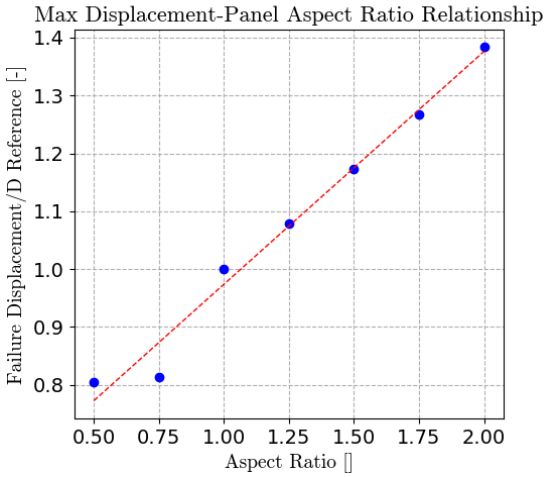

Fig 5.9: Displacement-AR relation

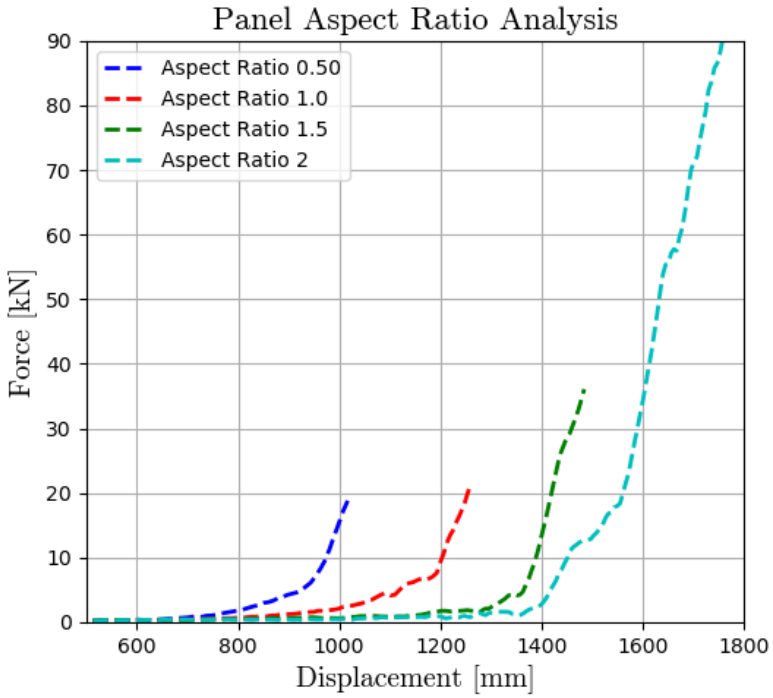

Fig 5.10: F-δ curves for different panels

5.1.3 Anchor spacing influence

The spacing between the anchors *i* determines the size of the panels that form the mesh drapery system, this geometric parameter has been varied by the same amount both vertically and horizontally compared to the reference test, thus maintaining a system consisting of 9 square panels of different sizes. The influence of different anchor spacing was therefore analyzed from a minimum value of 2m to a maximum of 4m with an incremental step of 0.25m, for a total of 8 further tests performed in addition to the reference one. Figure 5.11 shows 5 tests characterized by a progressive difference in the spacing of the anchors of 0.5m. By observing the force-displacement curves, it's clear how the maximum resistance of a panel is independent of the plates spacing. The variation of this parameter instead influences the mechanical activation of the panel, obviously panels characterized by a smaller size will have a faster response than larger panels. This variation is also associated with a deviation in the stiffness of the system, smaller panels exhibit a stiffer response than larger ones characterized by a more flexible behaviour.

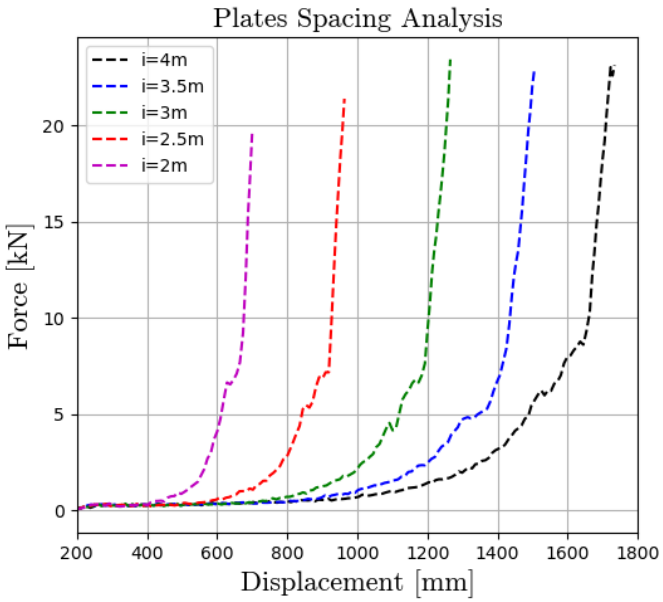

Fig 5.11: F- δ curves for different panels

Focusing on the results obtained in the 8 tests shown in table 5.3 and in the underlying graphs, as previously highlighted, the values of maximum force at failure are almost constant and all limited to a variation of less than 10%

compared to the reference test, with the exception of the test 1 where we observe a 17% lower value. This difference is due to the fact that the panel size differs little from punch dimension thus causing a more rigid mechanical response that leads to an early panel failure. As regards the relationship between the spacing of the plates and the out-of-plane deflection of the wire mesh, it is described by the following first-degree polynomial (Fig 5.13):

$$\delta_{max} = \left(1.23\frac{i}{i_r} - 0.26\right)\delta_r \quad (eq\ 5.5)$$

$$i_r = 3m\ \ refernce\ value\ for\ normalization$$

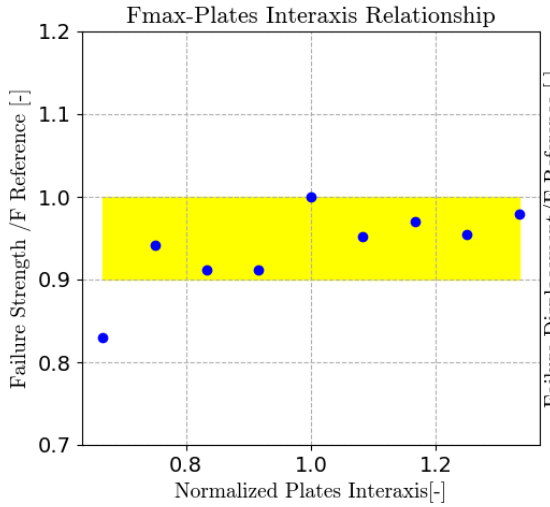

Fig 5.12: Force-i relation

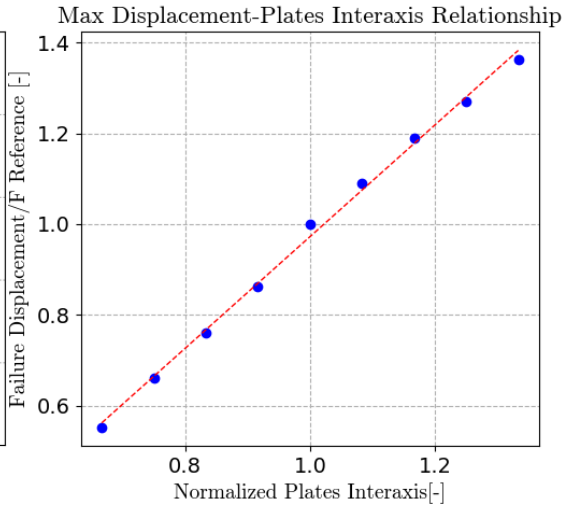

Fig 5.13: Displacement-i relation

Anchor Spacing Analysis			
Plate Spacing[m]	***Failure Force(kN)***	***Variation of F respect to F_r***	***Failure Displacement[m]***
2	*19.4*	-17%	0.700
2.25	*22.0*	-6%	0.838
2.5	*21.3*	-9%	0.963
2.75	21.3	-9%	1.091
3	23.2	/	1.265
3.25	22.3	-5%	1.381
3.5	22.7	-3%	1.506
3.75	22.3	-5%	1.609
4	22.8	-3%	1.725

Tab 5.3

5.1.4 Punch direction influence

In all the previous analysis the punching element moved with an inclination of 45° respect to the out of plane axis, as reported in chapter 2 this direction was selected because considered a common value of the sliding joint. Now it's time to study the influence of this thrust direction on the drapery mesh system mechanical response. 5 different thrust inclinations are analyzed with a progressive variation of 15 degrees. With the exception of the first case in which the punch moves in the out of plane direction, in the other tests the failure occurs simultaneously in correspondence with the LL and LR plates. In the case of zero inclination the 4 plates of the central panel are uniformly loaded and arrive at the same time at failure. Figure 5.14 shows the final position of the center of the load distributor with green placeholders, this highlights that an increase in the inclination degree leads to a greater stress condition on LL and LR plates.

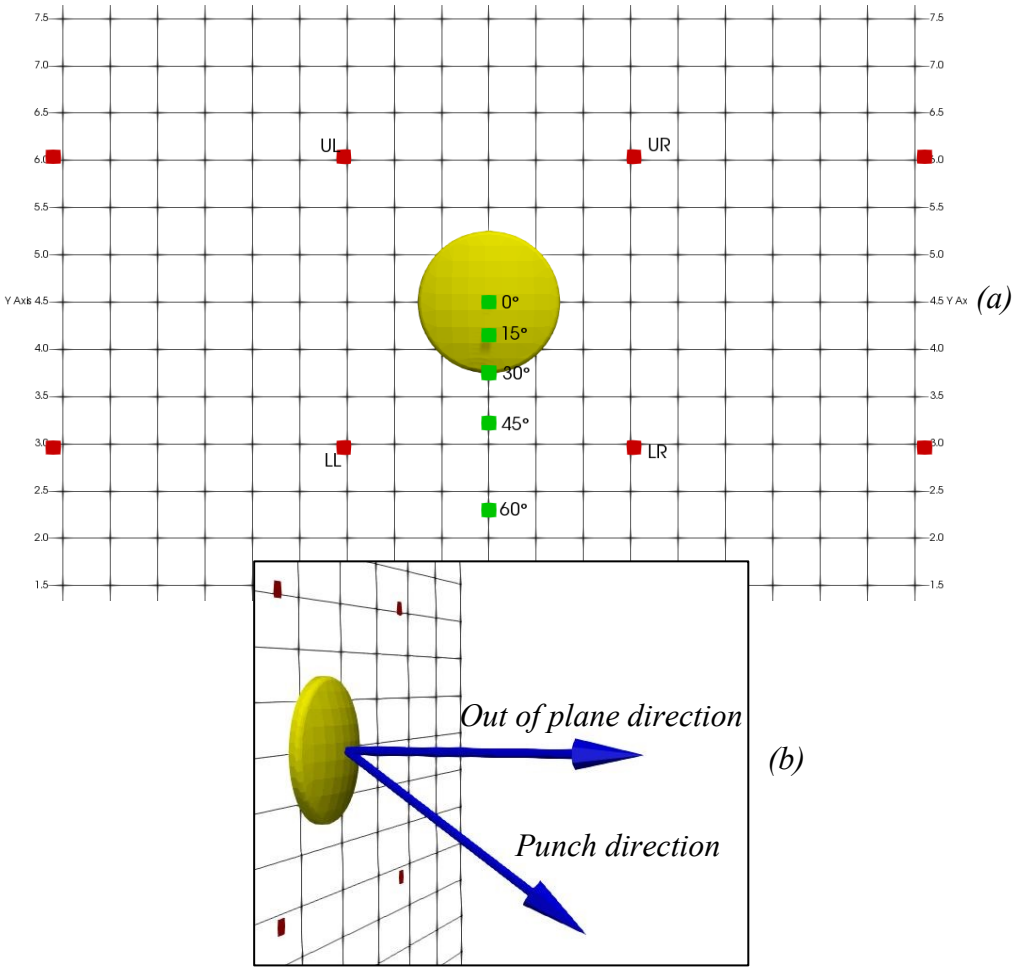

Fig 5.14:(a) Final punch position for each inclination; (b) General punch direction

From the comparison of the force-displacement curves (Fig5.15) it emerges that the break occurs more or less at the same level of deformation of the drapery system with a development of maximum resistant forces included within a range of 6kN . This fact highlights that in the possible detachment of a boulder from a rocky-wall, the direction of impact does not influence the resistance capacity of the cortical-reinforcement system. Some substantial differences, on the other hand, can be seen in the moment of activation of the panel and in the stiffness response. With the increase of the punch inclination there is a delay in the mechanical response in combination with a greater stiffness of the drapery system.

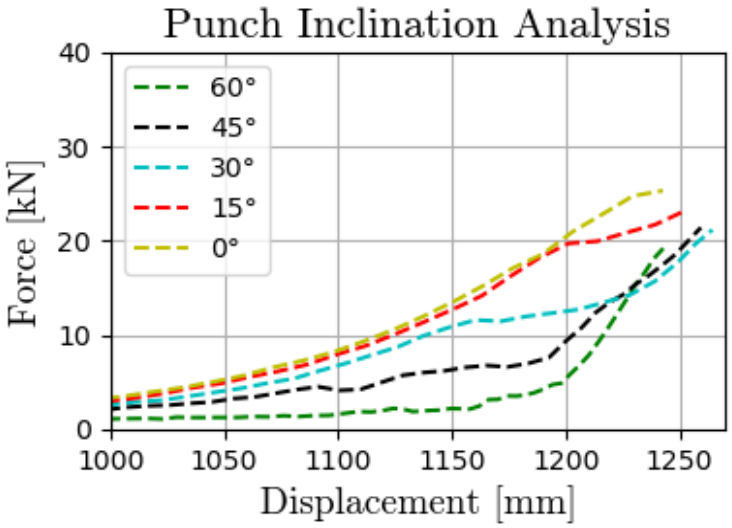

Fig 5.15: F-δ curves

Punch Inclination Analysis		
Inclination Angle [°]	***Failure Force[kN]***	***Failure Displacement [m]***
0°	*25.2*	1.242
15°	*24.1*	1.253
30°	*22.9*	1.270
45°	23.2	1.265
60°	19.0	1.243

Tab 5.4

It is now useful to analyze the behavior and the loads distributed on the plates which first show tearing phenomena, i.e. LL and LR. Since the system is symmetrical to the vertical axis, the two plates will show the same mechanical response, therefore only the LL plate will be analyzed. As it is possible to observe from the graphs 5.16, 5.18 and 5.20 each plate is stressed in a not negligible way in every direction. As regards the tangential force in the horizontal direction and the normal force recorded in the LL anchor, the variation of the thrust direction does not involve important differences. By analyzing the vertical tangential force instead, substantial differences emerge between the various cases, these are in fact due to the vertical distance of the punch from the anchors, this fact is easily understood by connecting the data of figure 5.19 with the illustration of fig 5.14. Table 5.5 shows all the force values recorded at the moment of failure in the plate LL.

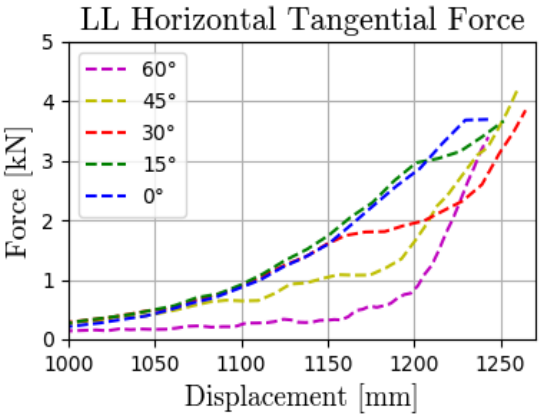

Fig 5.16 F- δ curves

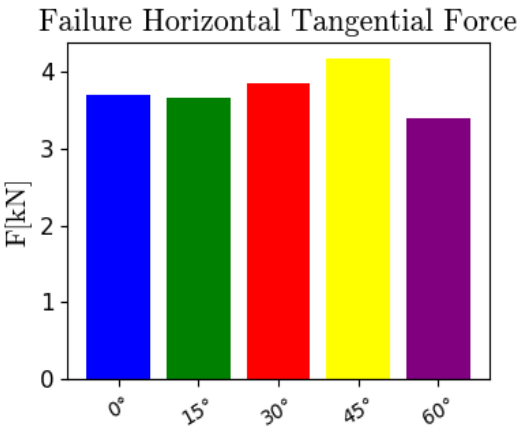

Fig 5.17

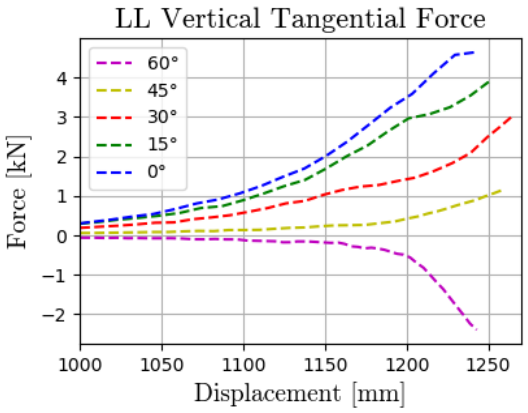

Fig 5.18: F- δ curves

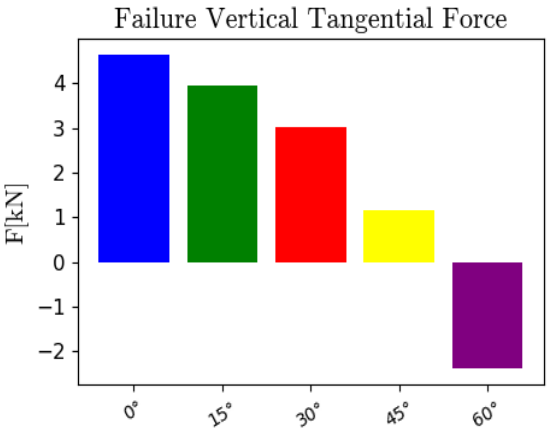

Fig 5.19

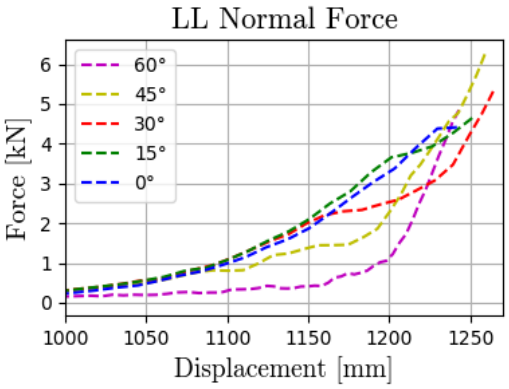

Fig 5.20: F- δ curves

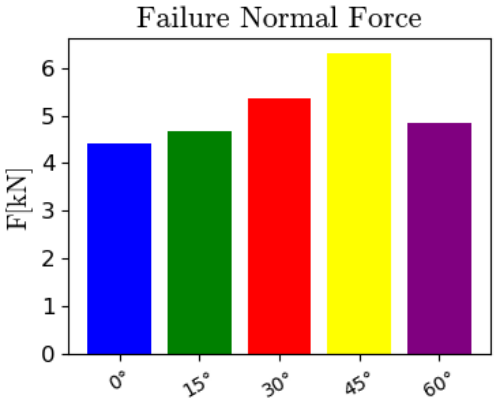

Fig 5.21

Plate LL Loading Analysis			
Inclination Degree [°]	***Hor.Shear Force (kN)***	***Vertical Shear Force (kN)***	***Normal Force (kN)***
0	*3.67*	4.62	4.41
15	*3.65*	3.86	4.64
30	*3.80*	2.95	5.33
45	4.15	1.15	6.26
60	3.40	-2.46	4.91

Tab 5.5

5.1.5 Punch dimension influence

In the impact of a rock against a drapery mesh system, the size and shape of the unstable block play a fundamental role. In all the analyzes carried out, the punch is characterized by a spherical shape in order to distribute the load over a greater surface. However, the case in which a block characterized by a sharp shape impacts the system should not be overlooked. This condition would in fact change the loading process leading to a preventive tearing of the drapery system. Without changing the shape of the thrust element, the sharpness of the block can in fact be simulated by reducing the contact surface and therefore decreasing the size of the punch. In this section we will analyze the effect of the size of the punching element maintaining its original shape. In order to perform this parametric analysis, the dimension of the load distributor is varied

ranging from 0.5m to 2.5m with incremental steps of 0.25m. 8 different configurations are then examined and compared with the reference one characterized by a 1.5m diameter punch, all forces and displacement values will then be normalized on this test. In all the analyzed cases since the load distributor is always wider than the plates, the break occurs close to the lower anchor plates of the central panel (i.e., LL LR), if instead we had used a punch smaller than the plate size the failure would probably have occurred at the center of thrust simulating a perforation of the mesh due to a very sharp rock block. Figure 5.22 shows 5 force-displacement curves for five different punch sizes. From a first observation it is clear that the size of the punch does not influence the maximum resistant force too much but acts above all in the maximum measured deflection level. This behavior is quite similar to what is obtained by varying the distance between the plates: an increase in the size of the punch provides a mechanical response similar to a decrease in the distance between the plates, resulting in a faster activation and a stiffer response of the panel to external forces. What has just been said is also highlighted in the graphs of figures 5.23 and 5.24. Concerning the failure values, they are all included between a value equal to 0.9 and 1 the reference value (F_r=23.2kN). Deformation and the punch size (D_{punch}) are instead linked by the following linear relationship where D_{punch_r}=1.5m and D_r=1.265m are the reference values.

$$\delta_{max} = \left(-0.27\frac{D_{punch}}{D_{punch\_r}} + 1.253\right)\delta_r \quad (eq\ 5.6)$$

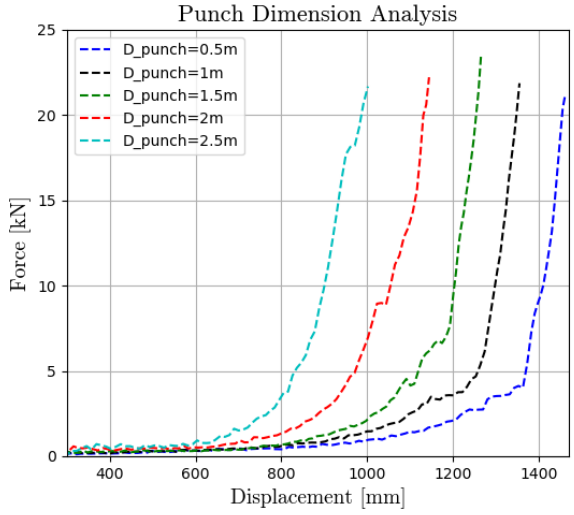

Fig:5.22: F- δ curves

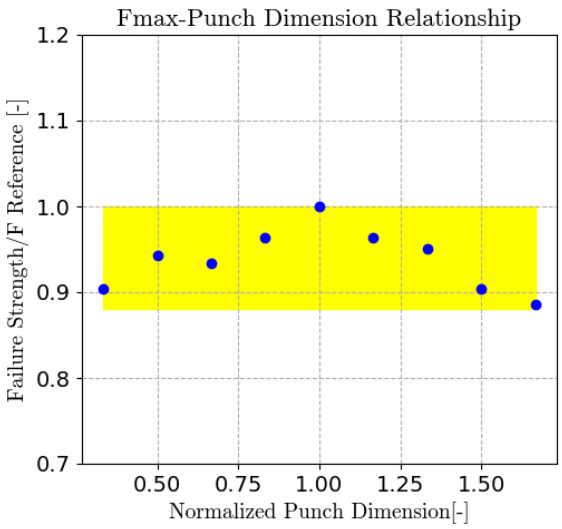

Fig 5.23: Force-D_{punh} relation

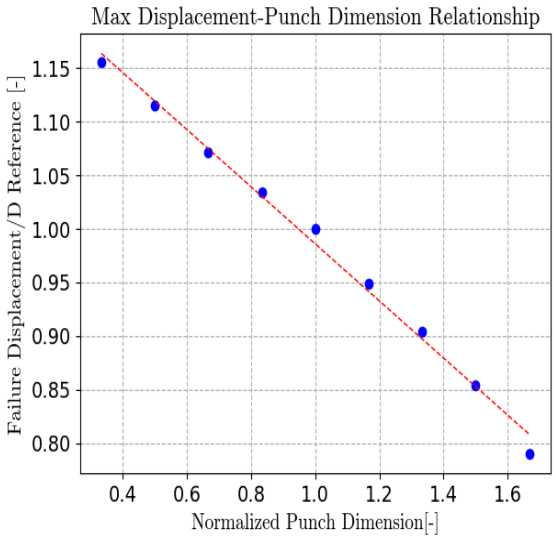

Fig 5.24: Displacement-D_{punch} relation

Punch Dimension Analysis		
Punch Dimension [m]	***Failure Force (kN)***	***Failure Displacement [m]***
0.5	*21.1*	1.462
0.75	*22.0*	1.411
1	*21.8*	1.356
1.25	22.5	1.308
1.5	23.2	1.265
1.75	22.5	1.203
2	22.2	1.144
2.25	21.1	1.080
2.5	20.1	1.003

Tab 5.6

5.1.6 Punch position influence

So far in the simulations the thrust of a rock block positioned in the center of the mesh panel has been analyzed. It seems interesting now to analyze what happens if the punch location is moved on the central panel. As shown in figure 5.25 seven different positions in addition to the initial one are taken into consideration by applying in 2 cases an eccentricity along x (P2, P3), in 4 cases along y (P4, P5, P6, P7) and in the P8 configuration a displacement both along the vertical and horizontal axis. In particular, the positions were varied by 2 quantities equal to a quarter and a half of the width of the mesh panel ($l_p/2$), i.e., 0.75m and 1.5m.

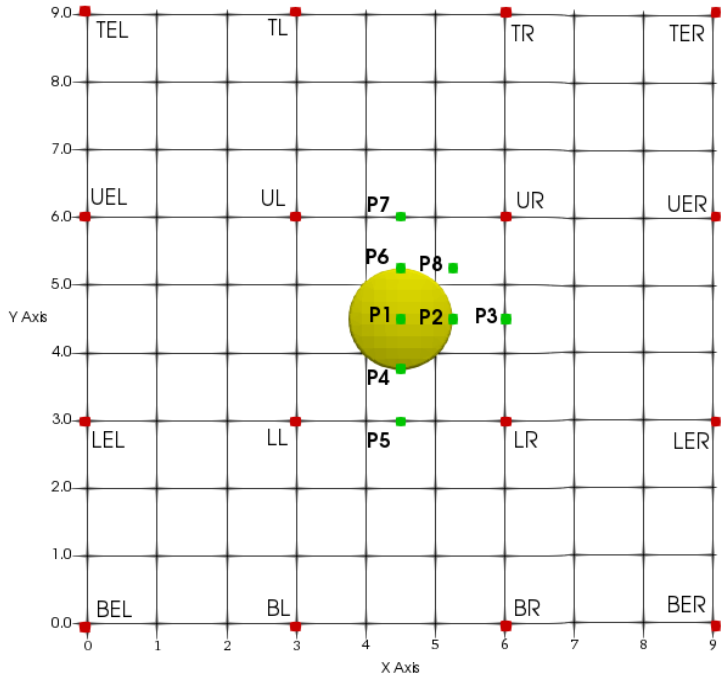

Fig 5.25: Geometrical scheme of analysed configurations

Observing the figure 5.26 it is possible to guess how by applying an eccentricity along the horizontal axis a progressive anticipation of the activation of the drapery system is manifested, also associated with a reduction of the punching resistance. The punch in fact in P2 and above all in P3 position is forced to push in a much more rigid area than the one in the reference case due to the presence of plate UR and LR above and below it.

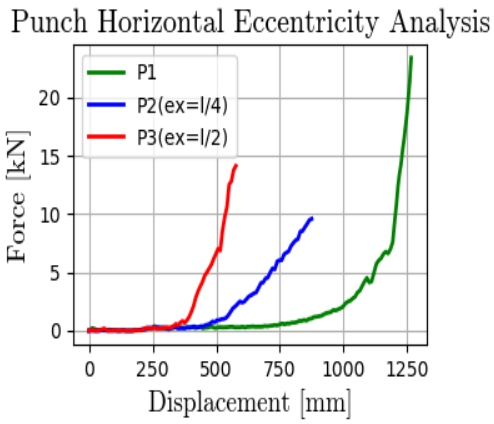

Fig 5.26: F- δ curves

The fact that the punch moves in the direction of 45° towards the bottom makes it necessary to test both positive and negative eccentricity with respect to the centre of the panel, as reported in Table5.7 for configurations P4-P5-P6 a failure in correspondence with the plates LL- LR is recorded, while P7 leads to a breakage in UL-UR plates. Despite this, there are no significant variations between these configurations with a failure that occurs at the same level of deflection of the panel, reaching a similar level of punching resistance.

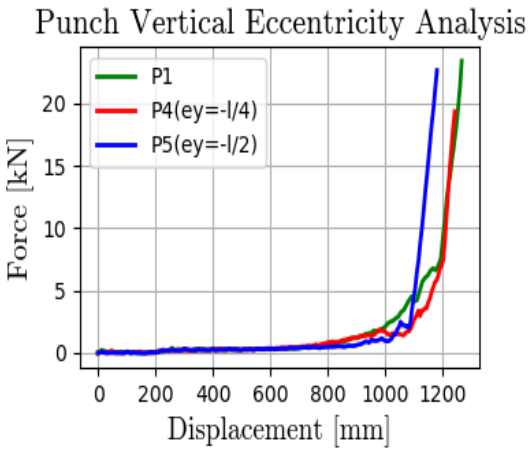

Fig 5.27: F- δ curves

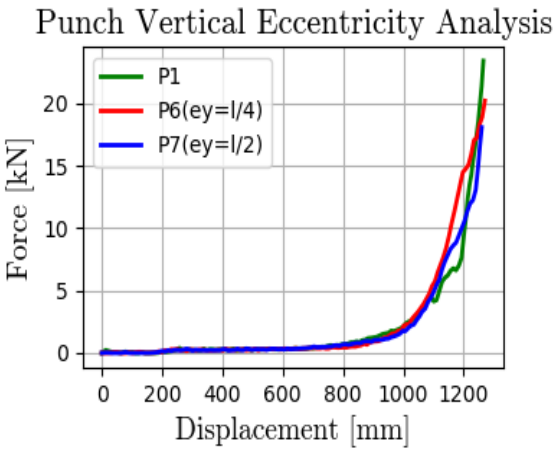

Fig 5.28: F- δ curves

In the case of P8 (Fig 5.29), on the other hand, where the punch is moved both along x and y by an amount equal to $l_p/2$, there is a slight decrease in the resistant force and a faster response of the system. Comparing this case with the P2 configuration characterized by the same horizontal eccentricity we notice a substantial difference mainly due to the fact that the punch moves in a vertical direction towards the LR plate thus making the P2 configuration

stiffer than the P8 one. It therefore emerges that the horizontal distance of the punch from the anchoring system influences the mechanical response of the system in a much more effective way than the vertical distance does.

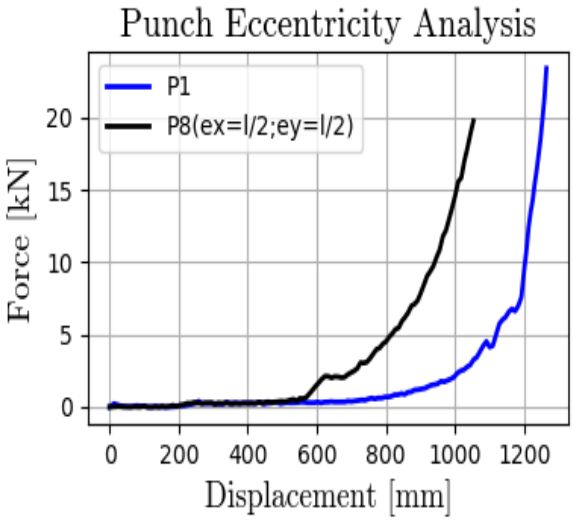

Fig 5.29: F- δ curves

Punch Position Analysis				
Conf. ID	***Punch Intitial Coordinates [m,m]***	***Failure Plates ID***	***System Failure Force(kN)***	***System Failure Displacement. [m]***
P1	*(4.5,4.5)*	*LL-LR*	*23.2*	*1.265*
P2	*(5.25,4.5)*	*LR*	*9.6*	*0.881*
P3	*(6,4.5)*	*LR*	*14.1*	*0.580*
P4	*(4.5,3.75)*	*LL-LR*	*19.3*	*1.243*
P5	*(4.5,3)*	*LL-LR*	*22.7*	*1.178*
P6	*(4.5,5.25)*	*LL-LR*	*20.2*	*1.273*
P7	*(4.5,6)*	*UL-UR*	*18.1*	*1.260*
P8	*(5.25,5.25)*	*LR*	*19.8*	*1.056*

Tab 5.7

5.1.7 Wire diameter influence

In the field of rockfall applications there are various types of wire meshes, different in shape and size of the mesh, diameter of the wires and their own coating against corrosion. As regards the double-twist systems, there are 2 types of hexagonal meshes, those 6x8cm and those 8x10cm, where the first number indicates the opening size and the second the vertical length. The standard diameters of steel wires used are: 2mm, 2.7mm, 3mm and 3.9mm. In this sub-chapter the influence of the wire diameter on the mechanical response of the system will be examined. In particular, in addition to the standard diameters listed above, some not on field applicable values of this parameter will be considered in order to have a more in-depth knowledge of their influence. Table 5.8 shows failure values regarding the punching resistance force and the final displacement for 6 different wire diameter configurations. The reference test is performed with a 8x10cm mesh equipped with a 3.0mm in diameter steel wire. Observing graph 5.30, an increase in resistance to punching following an increase in the diameter of the wires (d_w) of the mesh panel can be appreciated. The rupture resistance of the system is linked to the variation of this parameter through the following linear relationship (Fig 5.31):

$$F_{max} = \left(1.72\frac{d_w}{d_{wr}} - 0.6\right)F_r \quad (eq\ 5.7)$$

$$d_{wr} = 3mm\ \ refernce\ value\ for\ normalization$$

What has just been said may seem strange, in fact it seems normal to think that the resistance increases linearly with the area of the wire section and therefore quadratically with its own diameter, but this is what emerges by the performed tests. From comparing force-displacement curves of different configurations it is also very clear how a larger diameter of the wires leads to a stiffer mechanical response of the panel. Conversely this parameter does not influence the deformability at failure, with displacement values included in the interval of 9.8% of the reference value δ_r = 1.265m, as reported in figure 5.32.

Wire Diameter Analysis			
Wire Diameter [mm]	***Failure Force(kN)***	***Failure Displacement [m]***	***System Stiffness [kN/m]***
1.5	*10.0*	1.166	15
2	*14.4*	1.290	18.2
2.7	*18.6*	1.269	32.7
3	23.2	1.265	41.1
3.5	29.9	1.270	52.4
3.9	36.2	1.279	62.4
5	57.3	1.288	97.1

Tab 5.8

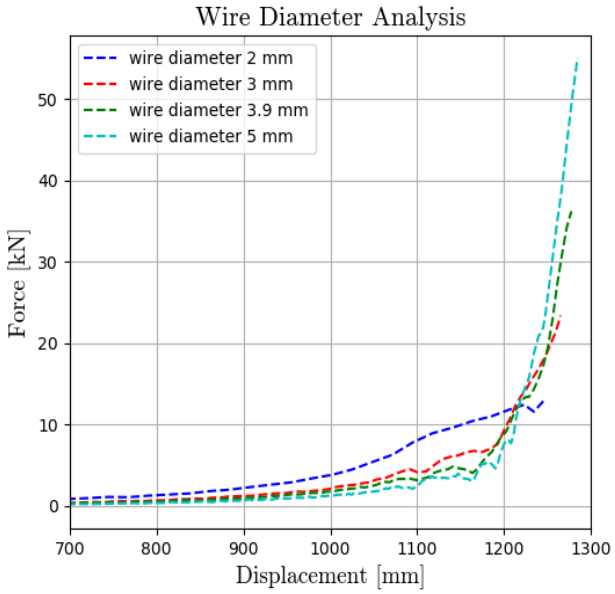

Fig 5.30: F- δ curves

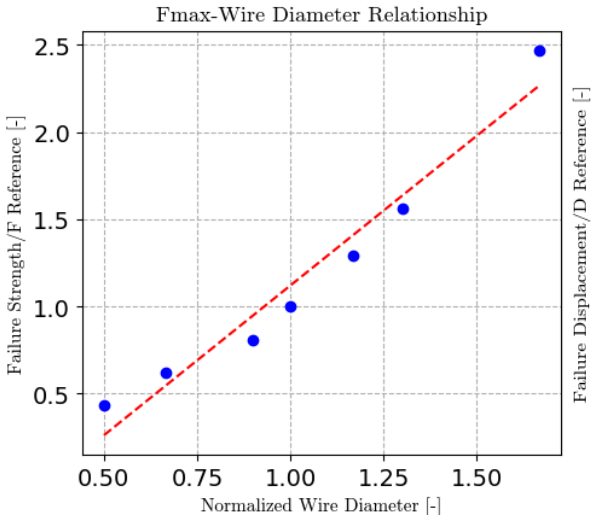

Fig 5.31: Force-d_w relation

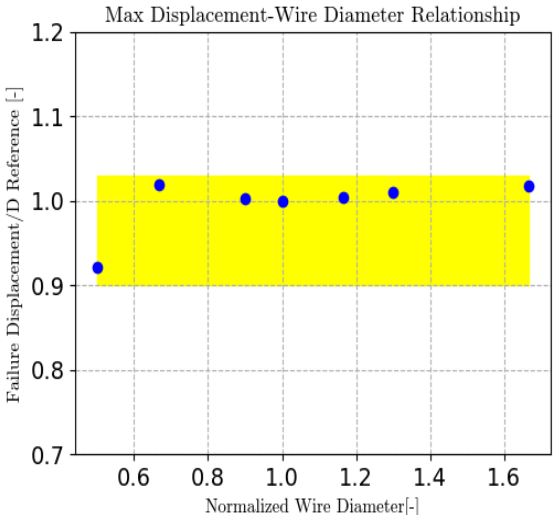

Fig 5.32: Displacement-d_w relation

5.1.8 Parametric analysis considerations

Summarizing what was carried out in these 7 sensitivities analyzes, we can divide the parameters according to their influence on the mechanical response of the drapery system. It should be remembered that the following conclusions are applicable to the particular case under consideration where each parameter has been varied while maintaining unchanged the others one. Table 5.9 summarizes the effects of a change in parameters by showing whether an increase in the value of the considered parameter affects with an increase (↑) or decrease (↓) or not (-) the point of failure and stiffness of the system.

PARAMETER'S FIELD OF INFLUENCE			
Analyzed Parameters	***Punching Resistance***	***Failure Displacement***	***System Stiffness***
Anchor Plate Size	↑	↓	↑
Panle Aspect Ratio for AR>1	↑	↑	↑
Anchor Plate Spacing	-	↑	↓
Punch Thrust Direction	-	-	↑
Punch Size	-	↓	↑
Wire Diameter	↑	-	↑

Tab 5.9

By breaking them down, there are parameters that affect the punching resistance level of the system, parameters that affect only the deflection level, others are irrelevant and others that affect both the strength and deformability.

Punching resistance influence parameters

Only a variation in the *diameter of the wires* leads to a variation in the resistance of the system without affecting the final deformation level. In particular, an increase in this parameter leads to a greater stiffness and maximum sustainable force of the panel, thus able to bear a greater load.

Failure deflection influence parameters

The parameters that lead to a single variation in the maximum level of deformation of the panel are: the *size of the punch* and the *anchor plates spacing*. In fact, an increase in the dimension of the load distributor has the same effect as a decrease in the plates spacing. These variations in fact cause the panel to respond in a faster and stiffer way to the external force, thus decreasing the maximum deformability level of the mesh. On the other hand, these parameters have a negligible effect on the maximum force that can be sustained by the mesh panel

Failure strength and deflection influence parameters

The parameters that influence both the maximum force and the level of deformation at break are: the *anchor plate size* and the *panel aspect ratio.* An increase in the size of the plates causes a linear increase in the failure strength and a linear decrease in the failure deflection level. Panels with different anchoring plates are activated in a narrow displacement interval but respond more rigidly the larger the plate size. As regards the aspect ratio, it has been observed that more elongated panels in the horizontal direction (Aspect ratio >1) allow to carry a greater load by associating this with a greater final deformability.

Exception case

A particular case is that of the *positioning of the punch*, as analyzed by applying a vertical eccentricity, there are no significant effects on the mechanical response of the system, vice versa moving the punch in a horizontal direction leads to a variation in the level of deformability and maximum force. In particular when the load distributor is located between two anchor rows and vertically aligned with them there is a substantial decrease in the maximum deflection and a slight decrease in the punching resistance.

No influence parameters

The analysis of the *punch thrust direction* conducts to the conclusion that this parameter can only lead to a variation of the force-displacement curve conformation, highlighting a more or less rigid behaviour of the system but not affecting the breaking load nor the final deflection level.

5.2 2nd Parametric Analysis

In this second phase of simulations the objective is to study the influence of the parameters previously analyzed on a configuration that is close to the conditions of the laboratory test, executed according to UNI 11437 (see Tab 5.10 for comparison). Going into detail, a 9x9m drapery mesh system equipped with 32 cm plates is used. The sixteen anchor plates are arranged with a distance of 3 m both vertically and horizontally and form 9 square panels. A load distributor with a spherical dome of 1m in diameter, positioned at the center of the central panel, moves in a perfectly orthogonal direction out of the drapery system consisting of double-twisted hexagonal meshes of 3mm wire in diameter. The main difference between this configuration and the laboratory one lies in the anchoring system, if in the first case plates are used in the second the meshes on the edges of the 3x3m panel are fixed to a rigid external frame strongly influencing the stiffness and the failure point values of the system (see Fig 5.33).

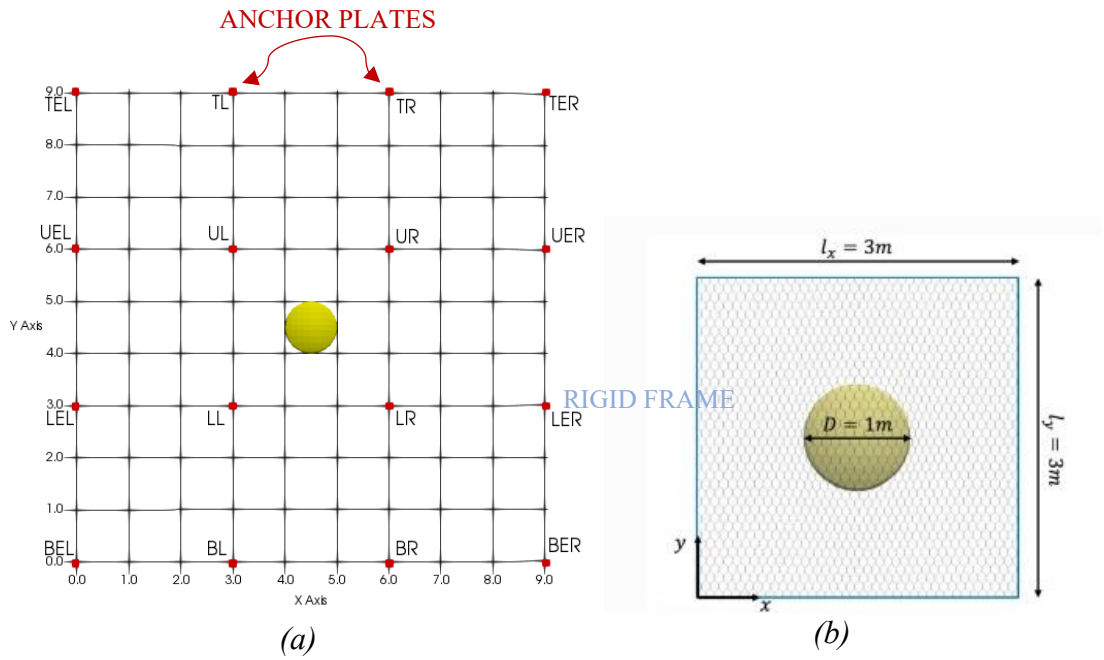

Fig 5.33:9x9 in situ configuration (a) vs Laboratory test (b)

Parameters	On field	Laboratory
System Dimension[m]	*9x9*	*3x3*
Tested Panel Dimensions[m]	*3x3*	*3x3*
Anchoring System Central Panel	*4 anchor plates of 32cm*	*Fixed square outer frame*
Panle Aspect Ratio[L_x/L_y]	*1*	*1*
Punch Thrust Direction [°]	*0*	*0*
Punch Size[m]	*1*	*1*
Punch position	*Center of the panel*	*Center of the panel*
Wire diameter[mm]	*3*	*2.7*

Tab 5.10

As can be appreciated from the graph of figure 5.34 the laboratory test leads to a high development of the punching resistance with a value of 73kN associated with a deflection of 0.6m. The simulation of the on-site test shows a substantial delay in the activation of the panel with an increase of final deformation, the maximum force value stops around 40kN. Focusing on the stiffness of the systems, defined as the slope of the curve once the system begins to resist,the laboratory test, undoubtedly due to the presence of the external frame, has a stiffness almost twice than the in field application. All the just mentioned values are stored in tab 5.11.

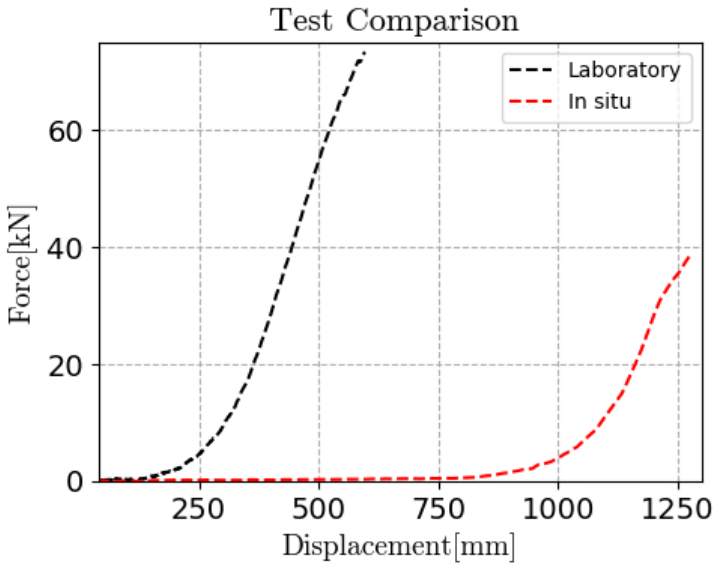

Fig 5.34: Force-displacement curves comparison

System Failure Values	On field	Lab
Punching Resistance[kN]	*38.5*	*73*
Failure Displacment[m]	*1.280*	*0.600*
Stiffness[kN/m]	*80.2*	*149.0*
System Activation [m]	*0.800*	*0.110*

Tab 5.11

From the configuration of the in situ test previously described one parameter at a time will be changed to study its influence on the mechanical response of the system. The force and deflection values will then be normalized to the laboratory breaking point values to facilitate a comparison process. Focusing on the initial test of parametric analysis the main differences from the sensitivity analyses performed before are about the size and direction of the punch. In fact, moving in the out of plane direction, the load distributor generates a uniform stress on all 4 plates of the central panel, leading simultanously to a tearing of the nodes around them. The system is therefore symmetric both along the horizontal and the vertical direction. Compared to previous analysis the plate BL is not stressed and UL and LL are affected in the same way in all directions as appreciable from figures 5.35-5.36 and tables 5.12 and 5.13.

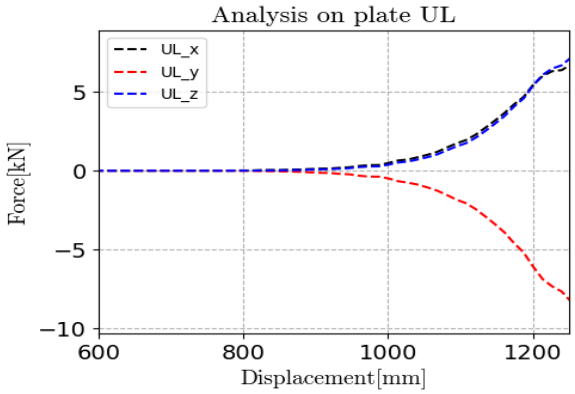

Fig 5.35: UL loading process

Load Analysis	
Plate UL	***F max (kN)***
Fx	*6.50*
Fy	*-8.15*
Fz	*7.02*

Tab 5.12

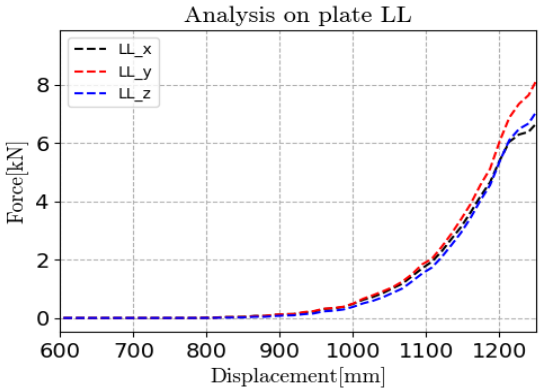

Fig 5.36: LL loading process

Load Analysis	
Plate LL	***F max (kN)***
Fx	*6.53*
Fy	*6.96*
Fz	*8.10*

Tab 5.13

5.2.1 Anchor plate size influence

As first parameter of this second analysis, the influence of the size of the anchor plates (d_p [m]) on the performance of the draping system is studied. Similarly to the corresponding analysis in paragraph 5.1.1, 7 different anchorage configurations are investigated from a size limit of 16cm to a maximum of 64cm with an incremental step of 8cm, equivalent to the mesh opening size. Comparing the force displacement curves as shown in figure 5.39 it's confirmed that an increase in the size of the anchorages leads to greater strength and stiffness of the panel. Considering the failure force (F_{max}) a linear increasing of the force is related to a d_p increase (eq 5.8), while at the same time a linear decreasing of the failure displacement (δ_{max}) is manifested (eq 5.9). In graphs 5.37-5.38 these relationships are reported; in particular the values of force and displacement are normalized on the final values of the laboratory test: F_r=73kN and δ_r=0.6m.

$$F_{max} = (0.7d_p + 0{,}27)F_r \quad (eq\ 5.8)$$

$$\delta_{max} = (-0.82d_p + 2.37)\delta_r \quad (eq\ 5.9)$$

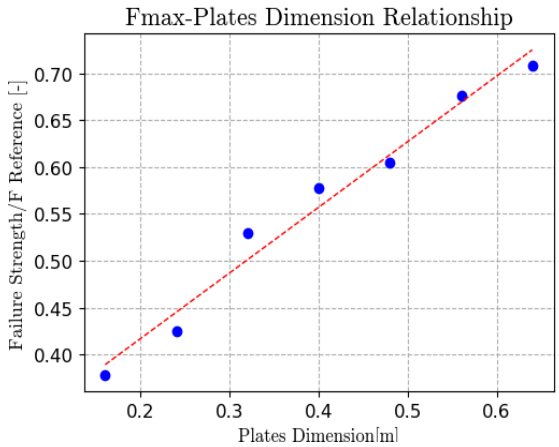

Fig 5.37: Force-d_p relation

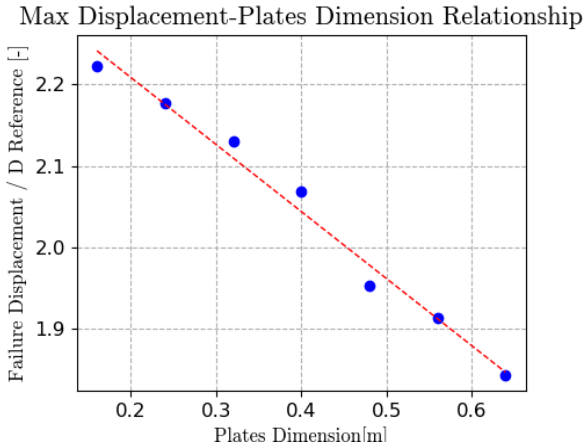

Fig 5.38: Displacement-d_p relation

Returning to the analysis of the force-displacement curves it emerges that the variation of the d_p parameter does not affect the level of deflection to which the panel begins to withstand, always around a displacement of 800mm. Focusing on the developed stiffness values, observing table 5.14, it is possible to note that in the last simulated case a higher value (169kN/m) than in the laboratory test is obtained. The difference in terms of maximum resistance with the laboratory configuration is always marked, never going below 20kN. Moreover, the mode and location of rupture is not affected by this variation with a simultaneous break in correspondence of the 4 central plates (LL, UL, LR, UR).

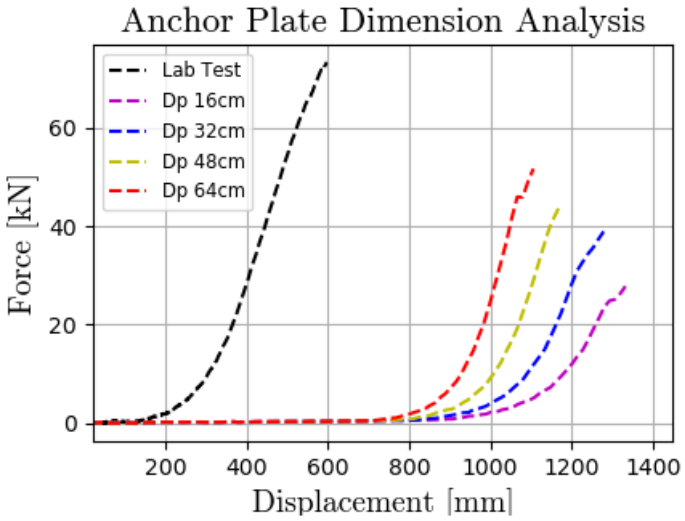

Fig 5.39: F- δ curves

Plate Dimension Analysis			
Plate Dimension [m]	***Failure Force (kN)***	***Failure Displacement [m]***	***System Stiffness [kN/m]***
0.16	*27.6*	1.334	51.6
0.24	*31.0*	1.306	61.3
0.32	38.5	1.280	80.2
0.40	42.1	1.241	95.4
0.48	44.2	1.172	118.9
0.56	49.4	1.148	142.0
0.64	51.7	1.106	169.0
(Lab) Frame	73.0	0.600	149

Tab 5.14

5.2.2 Panel aspect ratio influence

The effect of a variation in the ratio between the horizontal and vertical length of the panel, also called aspect ratio, is now investigated. Ten different configurations with an AR value ranging between 0.25 and 2 have been investigated, in all these tests the area of the panels has been kept constant around a value of $9m^2$. As can be seen from the graphs showing the force displacement curves and more easily from graph 5.42 the relationship between maximum force and aspect ratio is described by a third degree polynomial fit (eq 5.10) which has a minimum for a value of AR=0.75. For AR values between 0.65 and 1.25 the maximum developed resistance is similar, outside this range there is a significant increase in the load capacity of the panel. The analysis shows that horizontally elongated systems have a better performance than those that are in the vertical direction; comparing for example the tests carried out with AR=0.5 and AR=2, which are characterized by the same lengths but placed in the opposite direction, it emerges how comparing the maximum failure forces (Tab 5.15) the second configuration provides a better performance than the first one. Returning to figures 5.40 and 5.41 it emerges as if moving away from the range of values of AR (0.5-0.75) the panel shows a delay in activation, thus developing a greater final deflection,the relation that links the final displacemtent with the panel aspect ratio is also in this case a cubic form with a minimun located for AR=0.65.As regards stiffness, a slight increase is manifested with values of AR that move away from value of AR = 0.75.

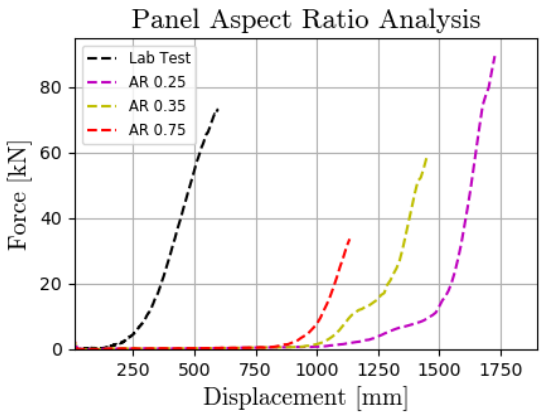

Fig 5.40: F- δ curves

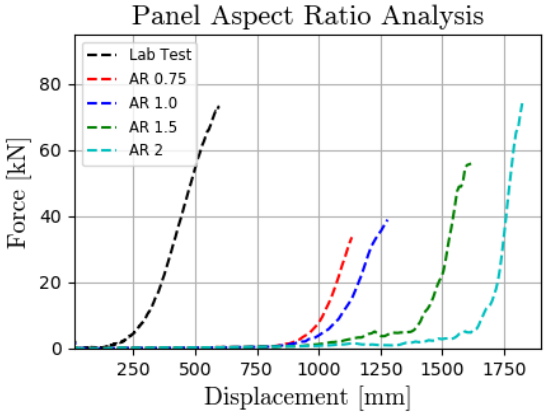

Fig 5.41: F- δ curves

$$F_{max} = (-3.59AR + 2.79AR^2 - 0.61AR^3 + 1.87)F_r \quad (eq\ 5.10)$$

$$\delta_{max} = (-6.41AR + 5.88AR^2 - 1.47AR^3 + 4.03)\delta_r \quad (eq\ 5.11)$$

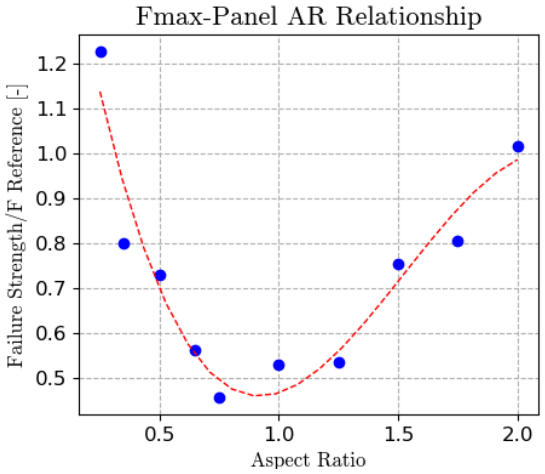

Fig 5.42: Force-AR relation

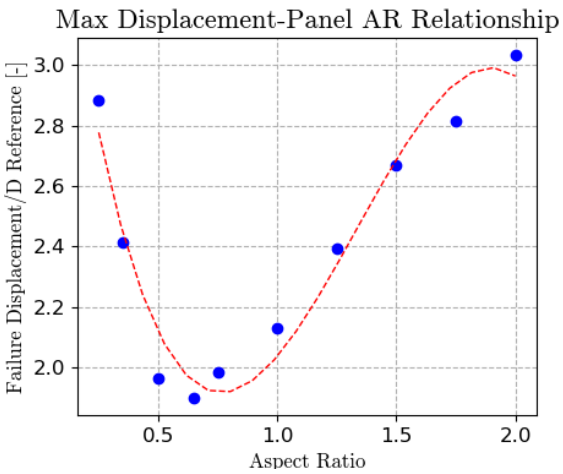

Fig 5.43: Displacement-AR relation

Aspect Ratio Analysis						
Aspect Ratio [-]	***Panel Horizontal Width [m]***	***Panel Vertical Height[m]***	***System Horizontal Width [m]***	***System Vertical Height[m]***	***System Failure Force (kN)***	***System Failure Displacement[m]***
0.25	*1.5*	*6*	*4.5*	*18*	*89.6*	1.729
0.35	*1.78*	*5.05*	*5.35*	*15.15*	*58.3*	1.448
0.5	*2.12*	*4.24*	*6.36*	*12.72*	*53.2*	1.179
0.65	*2.42*	*3.72*	*7.25*	*11.16*	*41.1*	1.139
0.75	*2.68*	*3.35*	*8.04*	*10.05*	*33.3*	1.189
1	*3*	*3*	*9*	*9*	*38.5*	1.280
1.25	3.35	2.68	10.05	8.04	39.1	1.435
1.5	3.67	2.44	11.01	7.32	55.0	1.601
1.75	3.97	2.26	11.91	6.78	58,9	1.668
2	4.24	2.12	12.72	6.36	74.2	1.820
(Lab) 1	3	3	3	3	73.0	0.600

Tab 5.15

5.2.3 Anchor spacing influence

As underlined in paragraph 5.1.3, enlarging or decreasing the size of the panel while maintaining its square shape influences the deformability and the activation moment of the drapery system while the maximum resistance to punching is unaffected. The influence of different anchor spacing (i) was therefore analyzed from a minimum value of 2m to a maximum of 4m with an incremental step of 0.25m. Figure 5.44 shows the mechanical response of 4 configurations.Increasing the size of the panels there is a delay in the opposition of the panel to the action of the load distributor, this variation is also associated with a linear decrease in stiffness . In particular analyzing the data of table 5.16 the stiffness varies from a maximum of 131.4 kN/m for i=2 to a minimum of 64.5kN/m for i=4m. The maximum resistance is not affected with values within an interval ranging from 48% to 57% the normalization value of laboratory (F_r=73kN). As the stiffness decreases the final deflection value of the system linearly increases with the size of the panel according to the folowing equation:

$$\delta_{max} = \left(2.72\frac{i}{i_r} - 0.48\right)\delta_r \qquad (eq\ 5.12)$$

$i_r = 3m\ \ refernce\ value\ for\ normalization$

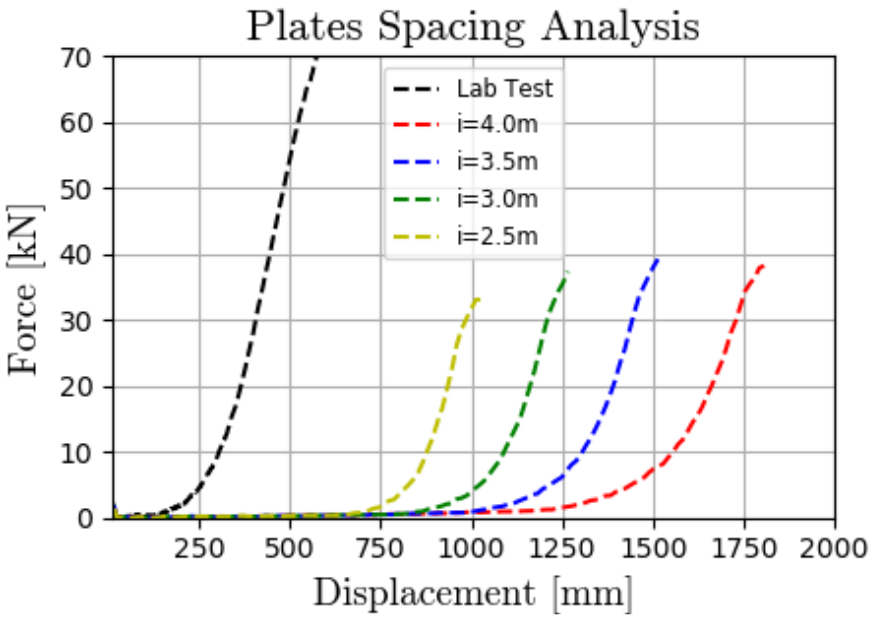

Fig 5.44: F- δ curves

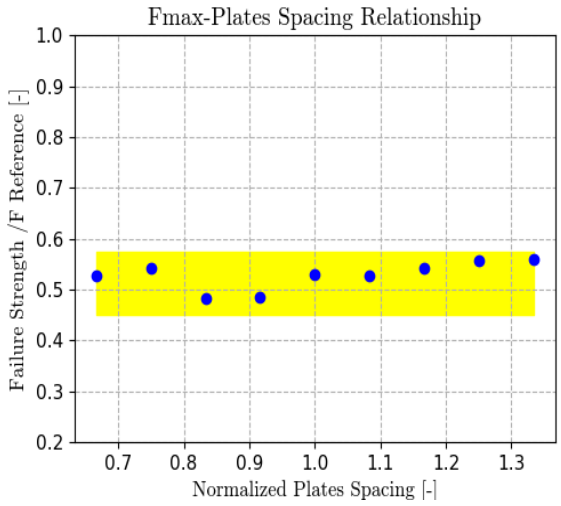

Fig 5.45: Force-i relation

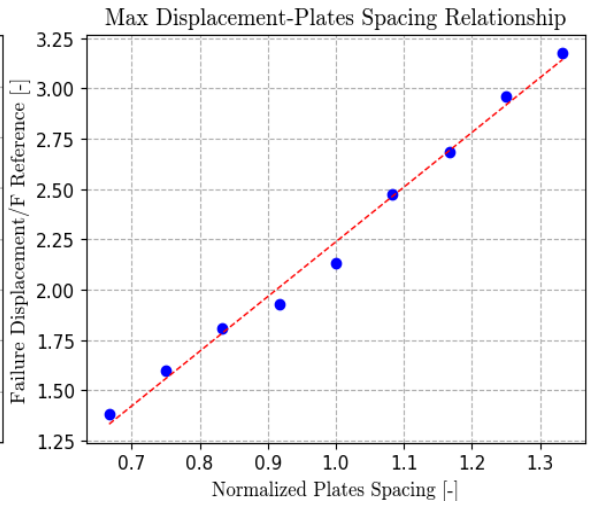

Fig 5.46: Displacement-i relation

The variation of the center distance of the plates does not affect the modality of failure since the system remains symmetrical along x and y directions, so the 4 plates of the central panel are stressed with the same intensity by the punch device.Comparing the obtained simulation results with the laboratory test, it is possible to appreciate a similar stiffness between the latter and the test performed with i=2, the difference in terms of maximum resistance is instead constant, around a value of 35kN.

Anchor Spacing Analysis			
Plate Interaxis[m]	***Failure Force(kN)***	***Failure Displacement[m]***	***System Stiffness [kN/m]***
2	*38.5*	0.827	131.4
2.25	*39.5*	0.957	121.5
2.5	*35.4*	1.086	96.2
2.75	35.5	1.155	85.3
3	38.5	1.280	80.2
3.25	38.4	1.485	77.5
3.5	39.5	1.611	72.8
3.75	40.5	1.778	70.1
4	40.7	1.906	64.5
(Lab) 3m	73	0.600	149

Tab 5.16

5.2.4 Punch direction influence

In the laboratory test the punch pushes in a perfectly orthogonal direction to the wire mesh plane. Now, as in the previous analysis we considered other 4 directions of thrust with a progressive increase in inclination of 15° up to an angle of 60° formed by the direction of movement of the punch and the normal to the plane of the panel. The variation of this angle involves substantial differences in the loading process of the plates. If in fact in the case of the punch that moves in the direction outside the plane the break occurs simultaneously in the 4 central plates in other cases as you can appreciate from fig 5.47 ,which shows the final position of the load distributor, the failure process occurs near LL and LR anchor plates. It's so clear that the most stressed plates are the ones closest to the center of thrust of the punch device.

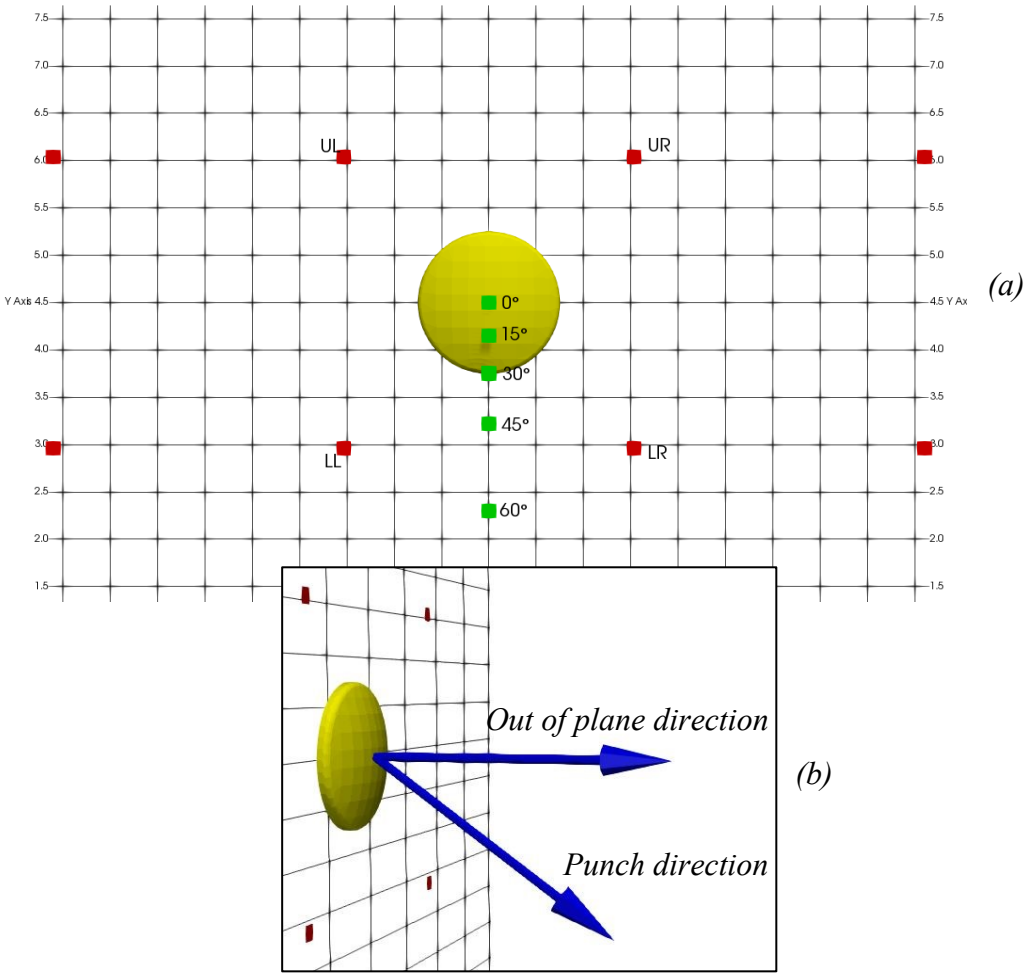

Fig 5.47:(a) Final punch position for each inclination; (b) General punch direction

Figure 5.48 shows the force-displacement curves for the 5 different configurations taken into consideration. Observing, it is easy to understand that this parameter is irrelevant to the breaking condition which occurs around 1.250m in displacement and for a maximum load around 35kN. In the various analysed cases some differences in the loading process are appreciable, in fact increasing the thrust inclination the draping system is activated later and has a more rigid response up to the breaking point. What has just been said is easy to understand by comparing, for example, the load curve with thrust at 15° and the one at 60°. All complete data regarding the failure conditions are reported in table 5.17.

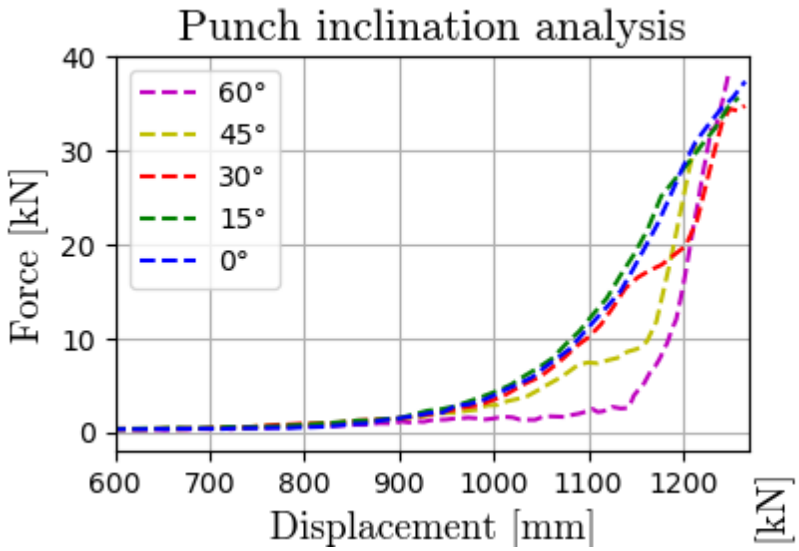

Fig 5.48: F-δ curves

Punch Inclination Analysis			
Inclination Angle [°]	***Failure Force[kN]***	***Failure Displacement.[m]***	***System Stiffness [kN/m***
0°	*38.5*	1.280	80.2
15°	*35.6*	1.260	77.4
30°	*34.8*	1.265	74.8
45°	31.2	1.218	98.5
60°	38.6	1.248	300.5
(Lab) 0°	73	0.600	149

Tab 5.17

It is time now to focus on the variations in the loading process due to the change in punch inclination, the graphs in the next page show the shear forces and the normal stress on the BL, LL and UL plates as the thrust direction varies (Fig 5.50, 5.51 and 5.52). It is clearly observable that as the inclination increases the load is transferred from the UL plate to the BL plate. Concentrating on the plate LL (see Fig 5.49) which in all cases undergoes phenomena of mesh breaking, it is clear that the horizontal tangential force is kept constantly within an interval [6-9.0kN], showing a slight increase after an inclination of 30°. Analyzing the vertical one instead LL undergoes a gradual decrease up to the inclination of 45° and then sustain a considerable force in the opposite direction for an inclination of 60 °. As regards the normal force in LL, it has a behavior similar to that of horizontal one with the maximum values obtained for inclinations of 45° and 60° .From this analysis it evidently emerges how important is the relative punch position in the panel to know which are the most tensioned anchors. For a correct understanding it is advisable to observe these bar graphs with the graphic illustration in figure 5.47(a).

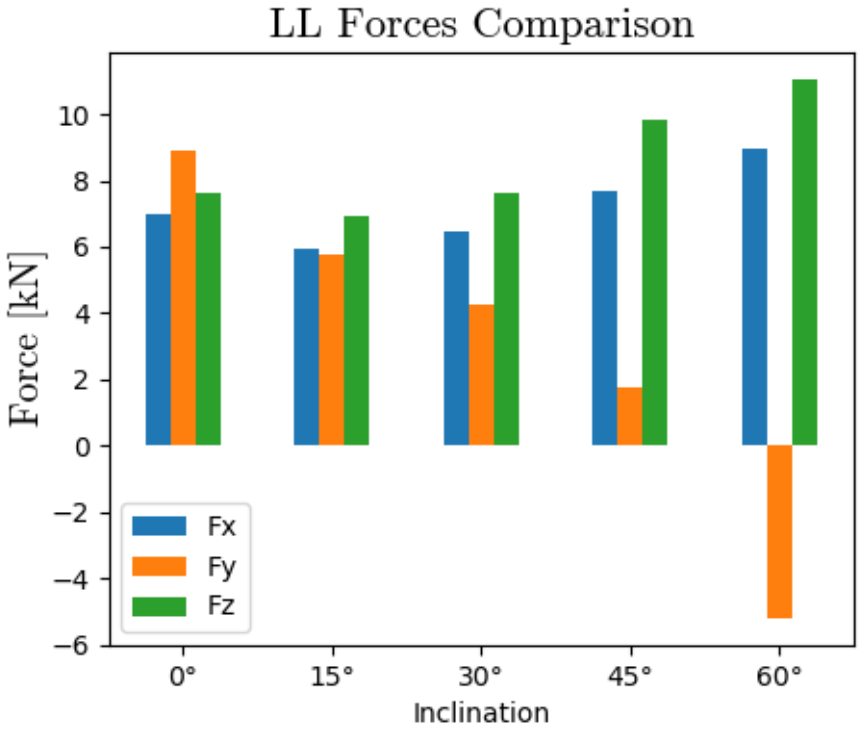

Fig 5.49: LL forces for different inclinations

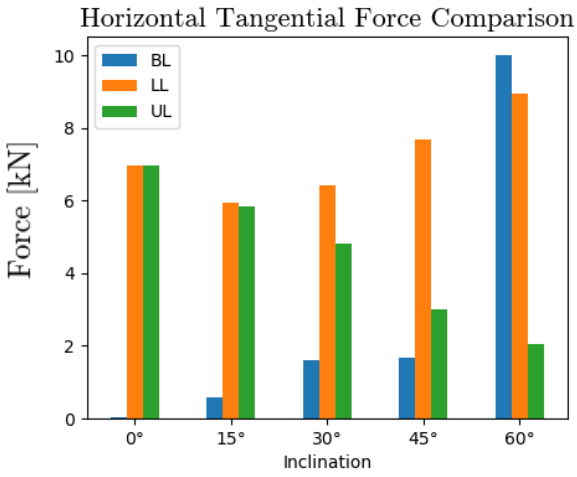

Fig 5.50: Plates horizontal tangential force

Max Horizontal Tangential Force(kN)			
Angle	**BL**	**LL**	**UL**
0°	0	6.9	6.93
15°	0.5	5.8	5.7
30°	1.5	6.4	4.8
45°	1.6	7.6	2.9
60°	9.9	8.9	2

Tab 5.18

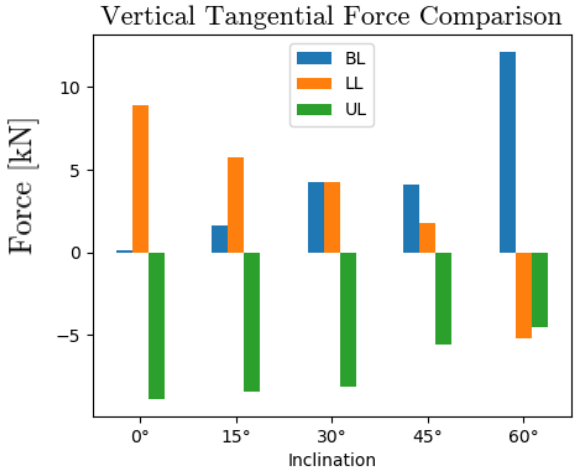

Fig 5.51: Plates vertical tangential force

Max Vertical Tangential Force(kN)			
Angle	**BL**	**LL**	**UL**
0°	0	8.7	-8.7
15°	1.6	5.7	-8.3
30°	4.1	4.1	-8.1
45°	4	1.5	-5.6
60°	22.1	-5.3	-5.1

Tab 5.19

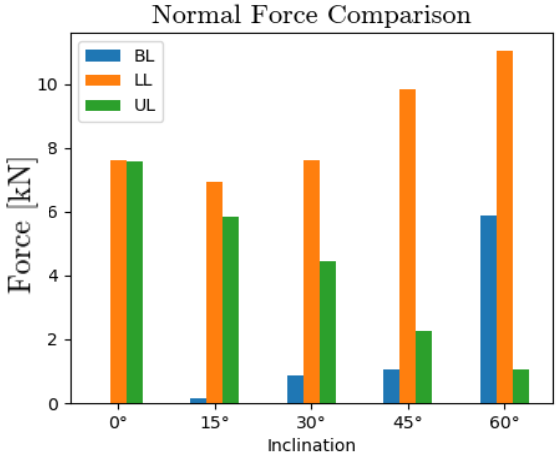

Fig 5.52: Plates normal force

Max Normal Force(kN)			
Angle	**BL**	**LL**	**UL**
0°	0	7.5	7.5
15°	0.1	6.9	5.8
30°	0.8	7.6	4.4
45°	1	9.8	2.3
60°	5.9	11.0	1.1

Tab 5.20

5.2.5 Punch dimension influence

In this section the effect of a change in the size of the punch (D_{punch}) device in 9 different configurations ranging from a minimum diameter of the distributor of 0.5m up to a maximum of 2.5m will be analyzed. Observing what is reported in figure 5.53 a first difference immediately emerges from the similar sensitivity analysis performed in paragraph 5.1.5; the variation of the parameter D_{punch} in fact not only affects the stiffness and the final deformation of the drapery system but also leads to an increase in the punching resistance;variation not found in the first set of analysis. This difference is mainly due to the different anchor plates that are equipped in the the two systems, respectively of 15cm in the first case and 32cm in the second. The mentioned discrepancy will be discussed in a more detail way in chapter 5.2.8. Returning to the current analysis is clearly visible from figures 5.54 and 5.55 as an increase in the size of the pucnh leads to a linear decrease in the final displacement and at the same time to a significant increase in resistance, relation described through a second degree equation. Figure 5.53 also shows that the activation point of the mechanical response of the panel undergoes a not excessive variation keeping within the range [600-900mm]. On the other hand, there is a considerable variation in the system stiffness, with a marked increase following a punch size increment,reaching in configuration with D_{punch} >2m comparable values of the laboratory one.

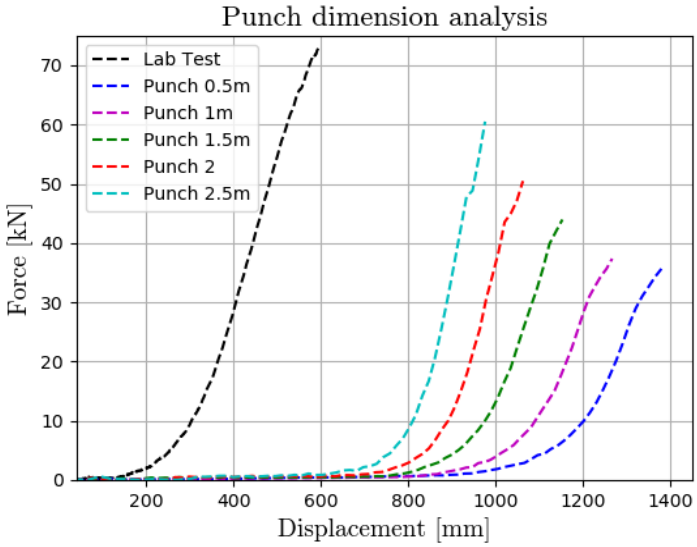

Fig:5.53: F- δ curves

$$\delta_{max} = \left(-0.33\frac{D_{punch}}{D_{punch_r}} + 2.45\right)\delta_r \quad (eq\ 5.13)$$

$$F_{max} = \left(-0.03\frac{D_{punch}}{D_{punch\_r}} + 0.07(\frac{D_{punch}}{D_{punch\_r}})^2 + 0.50\right)F_r \quad (eq\ 5.14)$$

$$D_{punch\_r} = 1m\ reference\ value\ for\ normalization$$

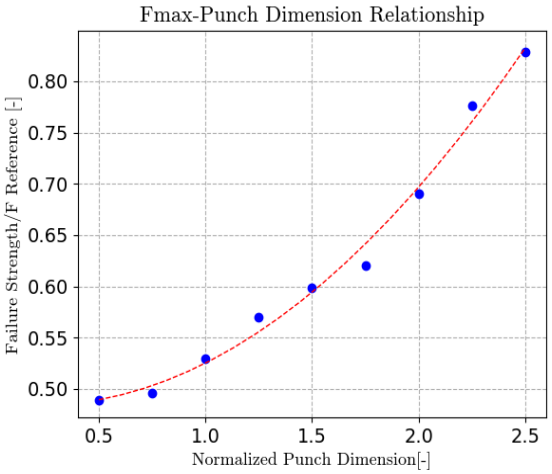

Fig 5.54: Force-D_p relation

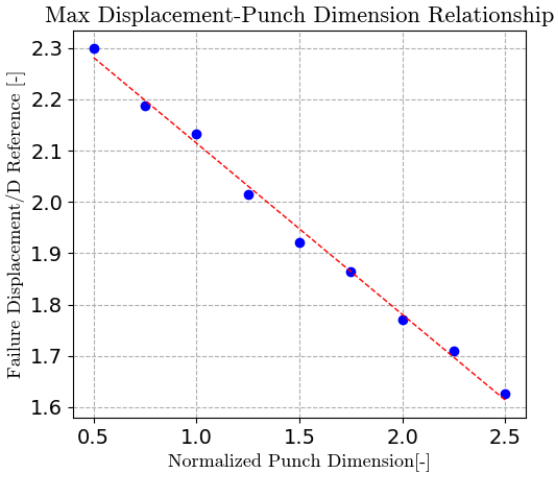

Fig 5.55: Displacement-D_p relation

Punch Dimension Analysis			
Punch Dimension [m]	***Failure Force (kN)***	***Failure Displacement [m]***	***System Stiffness [kN/m]***
0.5	*35.7*	1.380	67.3
0.75	*36.2*	1.313	73.4
1	*38.5*	1.280	80.2
1.25	41.5	1.209	90.4
1.5	43.7	1.153	108.4
1.75	45.3	1.118	115.3
2	50.3	1.062	123.8
2.25	56.7	1.026	142.1
2.5	60.5	0.976	161
(Lab) 1	73	0.6	149

Tab 5.21

5.2.6 Punch position influence

As it was understood from the previous analysis, the relative position between punch and anchor plates plays a fundamental role on the mechanical response of the drapery system. For this reason in this paragraph the influence of a variation of position of the punch in the panel is studied applying in 2 cases a horizontal eccentricity (P2-P3), in 4 configurations a vertical eccentricity (P4-P5-P6-P7) and in P8 a displacement in both axes (Fig 5.56). In particular, the positions were varied by 2 quantities equal to a quarter and a half of the length of the mesh panel ($l_p/2$), i.e. 0.75m and 1.5m. Configuration P1 refers to the standard case in which punch is positioned in the center of the panel.

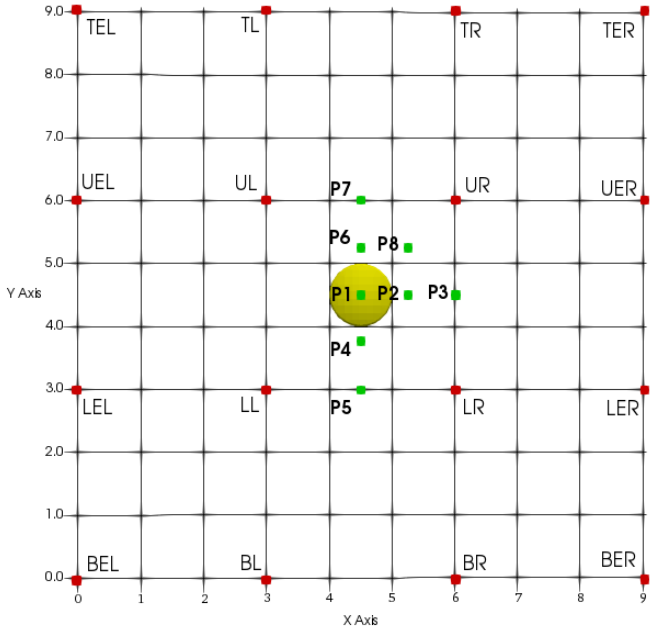

Fig 5.56: Punch position configurations

Starting from the P2-P3 cases it is clearly noted how the approach of the punch to the UR-LR plates up to arrange themselves in the same vertical axis involves a substantial pre-activation of the panel and a smaller final deflection level. As regards the stiffness, its value keeps similar in the 2 analyzed configurations, with a value close to that of P1 configuration (80.2kN/m). In the same way the punching strength remains unchanged with a value close to 40kN. The obtained results therefore remain far from the laboratory test both in terms of load capacity and in terms of system stiffness. The application of a vertical eccentricity on the other hand does not involve substantial differences

in the mechanical response of the drapery system keeping the maximum resistance and final displacement values unchanged (Fig 5.59). In the P8 configuration the punch is brought to a distance of about 1.05m from the UR , pouring on it most of its load. This condition leads to a preventive collapse of the wire-mesh in the UR plate around a maximum force value of 18.1 kN (Fig 5.58).

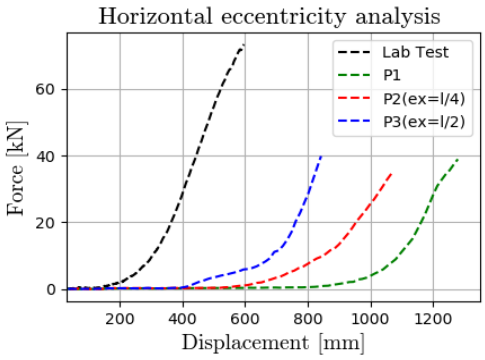

Fig 5.57: F- δ curves

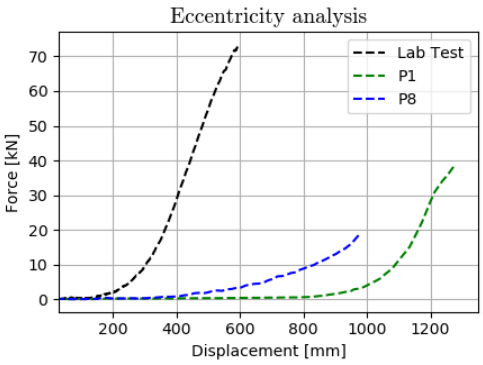

Fig 5.58: F- δ curves

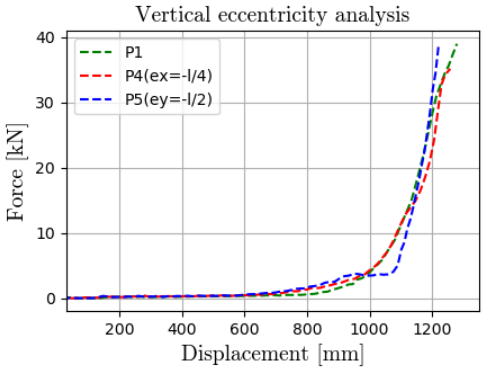

Fig 5.59: F- δ curves

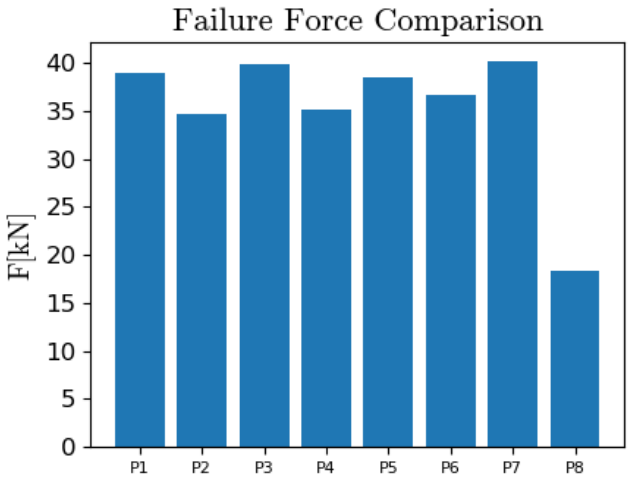

Fig 5.60: Comparison of failure forces with punch position

Punch Position Analysis				
Conf. ID	Punch Intitial Coordinates (X,Y)	Failure Plates ID	System Failure Force(kN)	System Failure Displacement. [m]
P1	(4.5,4.5)	UR-UL-LL-LR	38.5	1.280
P2	(5.25,4.5)	UR-LR	34.5	1.073
P3	(6,4.5)	UR-LR	40	0.843
P4	(4.5,3.75)	LL-LR	35.1	1.256
P5	(4.5,3)	LL-LR	38.2	1.224
P6	(4.5,5.25)	UL-LR	36.5	1.224
P7	(4.5,6)	UL-UR	40.3	1.270
P8	(5.25,5.25)	UR	18.1	0.975
Lab	Center	/	73.0	0.600

Tab 5.22

5.2.7 Wire diameter influence

The last parameter to be analyzed is the size of single that form the meshes of the panel. 8 different diameters d_w from a minimum of 1mm to a maximum of 5mm has been tested tested in as many configurations. From a first viewing of force-displacement curves reported in fig 5.61 what has been gained from the previous analysis emerges. A substantial increase in the resistance to punching associated with an increase in stiffness is clearly evident. As reported in table 5.23 the failure force varies from a minimum of 12.1kN for 1mm wires up to a maximum of 90.5kN for 5mm ones,in the same way the stiffness varies from a minimum of 26.4 kN /m to a maximum of 183kN/m. The final resistance of the system is linked to the variation of d_w parameter through the following linear relationship (Fig 5.62):

$$F_{max} = \left(0.71\frac{d_w}{d_{wr}} - 0.19\right)F_r \quad (eq\ 5.15)$$

$$d_{wr} = 2.7mm \ \ reference\ value\ for\ normalization$$

The variation of this parameter doesn't affect the deformability of the system with a final displacement which remains included in a range of 135mm in all the performed configurations.

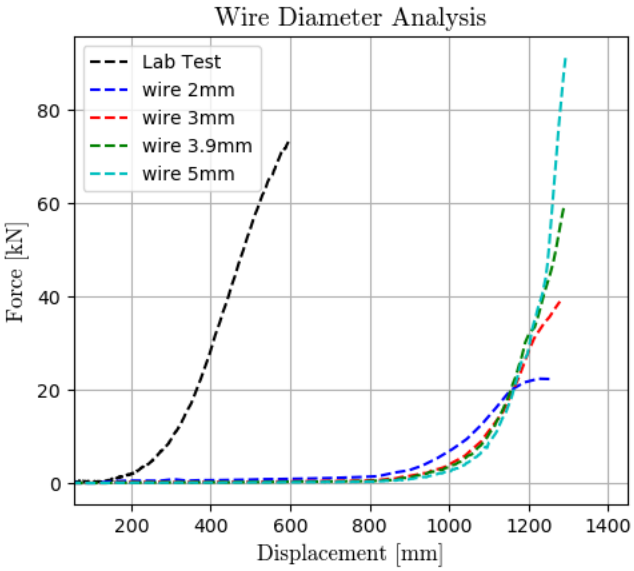

Fig 5.61: F-δ curves

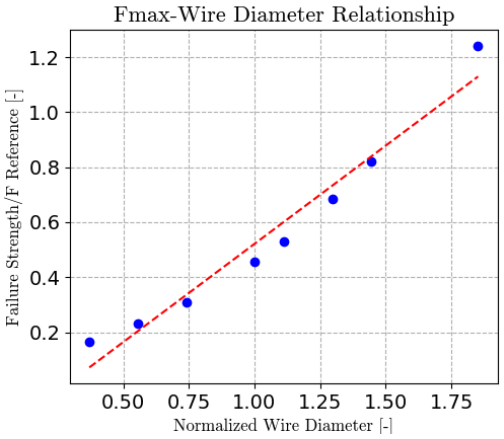

Fig 5.62: Force-d_w relation

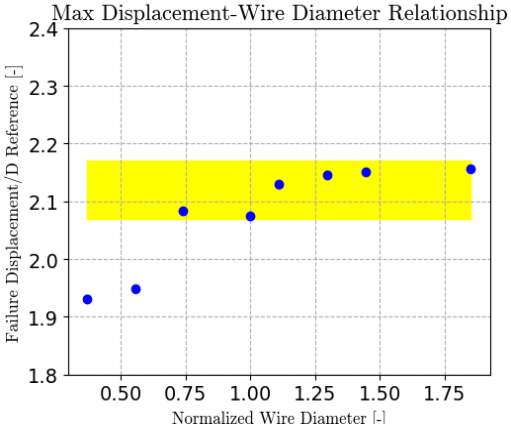

Fig 5.63: Displacement-d_w relation

Wire Diameter Analysis			
Wire Diameter [mm]	***Failure Force (kN)***	***Failure Displacement [m]***	***System Stiffness [kN/m]***
1	*12.1*	1.159	26.4
1.5	*17.2*	1.169	36.6
2	*22.5*	1.250	50.0
2.7	*33.4*	1.245	75.1
3	38.5	1.280	80.2
3.5	50.2	1.287	103.3
3.9	59.8	1.292	121.5
5	90.5	1.294	183.2
(Lab) 2.7	73	1.265	149

Tab 5.23

5.2.8 Parametric analysis considerations

From the second set of considered analysis it's appreciable a situation almost completely in agreement with what obtained from the first set of simulations. In this paragraph only one noticeable difference between the 2 groups of performed sensitivity analysis will be discussed. All other considerations and recapitulations are reported in the paragraph 5.1.8. A marked difference is obtained from the relationship between the size of the punch (D_{punch}) and the maximum punching resistance of the drapery system. If in the first analysis the failure force of the panel is not affected by the variation of the punch size, in the second study a linear increase in the load-bearing capacity of the panel emerges as a consequence of an increase in D_{punch}. This difference can be easily appreciated in the graphs of fig 5.64 and 5.65. The just mentioned discrepancy in the results can be explained by the fact that the two analysed systems are equipped with two different anchor plates. If in the first system the punch moves in a direction of 45° downwards, stressing the plates of 15cm at the base of the panel, in the second it moves in a perfectly orthogonal direction to the plane of the wire mesh, evenly stressing the four 32cm plates of panel. Larger plates lead the system to have a reserve of resistance, the mesh panel thus manages to develop a greater load capacity as the size of the punch increases. It is good to remember that the failure of the system is not only a consequence of the force exerted on it but also of the maximum obtained deformation.

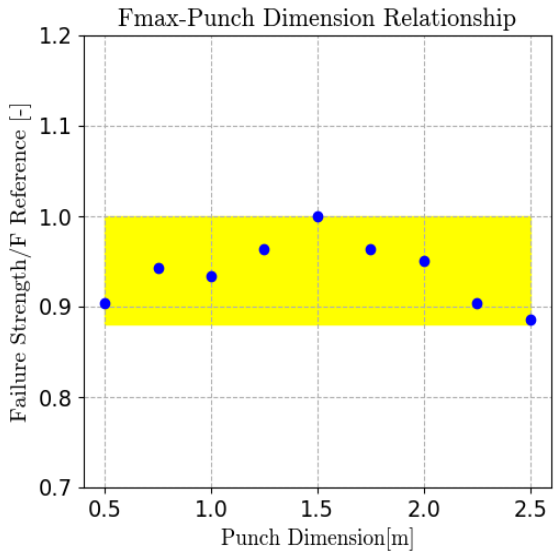

Fig 5.64: Force-D_{punch} relation-1st Analysis

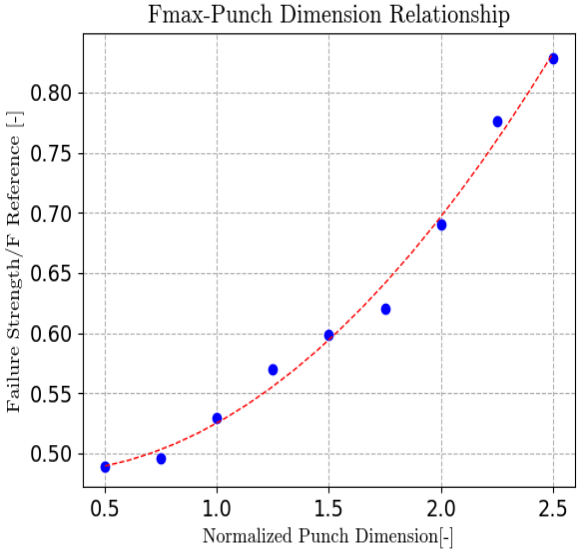

Fig 5.65: Force-D_{punch} relation-2nd Analysis

Conclusions

The field of drapery systems application is extremely varied and complex for the following reasons:

- The are **no clear guidelines** that allow an easy design and resolution of the problem entrusting great responsibilities and choices to designers.
- **Various geological conditions** strongly influence the type of required intervention. For this reason, geotechnical surveys play a fundamental role allowing us to have knowledge of the discontinuity plane and fragmentation level of the cortical instabilities, elements that affect the choice of the most suitable system according to its load capacity and maximum deformability.
- A point of extreme importance is also the **final purpose** of the application of a rockfall wire mesh, simple drapery systems are designed to control only the trajectory and the velocity of rock debris while secured wire-meshes aim mainly to avoid the detachment of the instable rock mass.

Passing to the simulation part of the Pont Boset drapery system test the main difficulty was to guess which of the multiple performed simulations was the most truthful. The recorded data in the force and displacement field were scarce and could not provide detailed information on the mechanical response of the system. Despite this problem thanks to the validation of the model with an already performed experimental test and the comparison of simulated conditions with real ones occurred in the infield application, the obtained simulated results can be considered reliable.

The Pont Boset test is the only on-site test that provides free access data, in the future it would be interesting to have available the mechanical response of other on-site tests characterized by different configurations in order to more easily relate experimental and simulated data. In the simulation field various aspects could be improved, for example by implementing the problem with the "*Cylinder Wire Based Approach*" or by introducing steel cables as external elements to the network. Solutions that would certainly improve the accuracy

of the simulation but at the same time would require much more computational time.

The performed sensitivity analyzes described in Chapter 5 allowed us to understand which and in what way are the most influential parameters on the performance of the drapery system. From the first set of parametric analyzes, based on Pont Boset configuration, and the second one, closer to the laboratory test according UNI11437, emerges a concordant conclusion that shows how there are parameters that affect the punching resistance level of the system, parameters that affect only the deflection level, others are irrelevant and others that affect both the maximum strength and deformability (see Tab C.1).

Parameters	***Field of influence***
Anchor Plate Size[cm]	*Panel deformability and resistance*
Panle Aspect Ratio[L_x/L_y]	*Panel deformability and resistance*
Anchor Plate spacing[m]	*Panel deformability*
Punch Thrust Direction [°]	*Neglibile influence*
Punch Size[m]	*Panel deformability and resistance*
Punch position	*Mainly panel deformability*
Wire diameter[mm]	*Panel resistance*

Tab C.1

Focusing on the second set of analysis, it is clear that the results obtained from the simulation of the on-site drapery system are very far from those in the laboratory. Few simulations have been able to develop a punching resistance and stiffness comparable to that of the UNI 11437 test and in those rare cases there was still a relevant discrepancy in the activation moment of the panel. What has just been said highlights how important the boundary conditions are in a drapery system and their influence on the performance of the panel. In conclusion we can say that this parametric analysis is therefore able to provide an important aid in the design phase of a drapery system. Provided a maximum force that can act on the system or established a maximum deformation level, the designer knowing the force displacement curves and the influence of each parameter on them is so able to choose the best configuration suitable for the specific application case.

Bibliography

-Antonio Pol, Fabio Gabrieli, Lorenzo Brezzi - *"Discrete element analysis of the punching behaviour of a secured dradpery system:from laboratory characterization to idealized in situ conditions"*; Acta Geotechnica, November 2020.

-Antonio Pol, Fabio Gabrieli - *"Discrete element simulation of wire-mesh retaining systems:An insight into the mechanical behaviour";*Computer and geotechnics.

-P. A. Cundall, O. D. L. Strack - "*A discrete numerical model for granular assemblies"*; Geotechnique, March 1979.

-F. Gabrieli, A. Pol, K. Thoeni and N. Mazzon - "*Particle-based modelling of cortical meshes for soil retaining applications"* in Numerical Methods in Geotechnical Engineering IX.

-Antonio Pol – "Discrete element modelling of wire meshes for secured drapery applications"; Phd thesis, Università di Padova.

-Alessandro Pellizzari ,"*Punch test analysis with DEM on secured drapery systems*"; Master degree thesis, Università di Padova, 2021.

-Blanco-Fernandez,Castro-Fresno,Coz-Diaz,Lopez-Quijada-*"Flexible systems anchored to the ground for slope stabilisation:Critical review of existing design methods*"; Engineering geology, 2011.

-Paola Bertolo, Claudio Oggeri, Daniele Peila - "*Full scale testing on draped nets for rockfall protection*"; Canadian Geotechnical Journal, March 2009.

-Francesco Ferraiolo, Giorgio Giacchetti - *"Rivestimenti corticali:alcune considerazioni sull'apllicazione delle reti di protezione"* in Atto del convegno Bonifica dei versanti rocciosi per la protezione del territorio, Trento 2004.

-Cala, Flum, Ruegger, Roduner - "*Tecco Slope Stabilization System and RUVOLUM Dimensioning Method"*; Switzerland 2020.

-Stefano Cardinali - "*Soluzioni per la mitigazione del rischio da caduta massi*"; Ufficio tecnico Officine Maccafferi Italia.

-D.K. Anderson, B.P Wham – "*Wire mesh tension testing"*; Laboratory report, University of Colorado Boulder,July 2019.

- K. Thoeni, A. Giacomini, C. Lambert, S. W. Sloan, and J. P. Carter, *"A 3D discrete element modelling approach for rockfall analysis with drapery systems";* International Journal of Rock Mechanics and Minning Sciences, 2014.